



UNIVERSITÀ
DEGLI STUDI
DI PADOVA



DIPARTIMENTO DI INGEGNERIA INDUSTRIALE

UNIVERSITÀ DEGLI STUDI DI PADOVA
DIPARTIMENTO DI INGEGNERIA INDUSTRIALE
CORSO DI DOTTORATO IN: INGEGNERIA INDUSTRIALE
CURRICOLO: INGEGNERIA CHIMICA, MECCANICA E DEI MATERIALI
XXIX CICLO

GOLD ALLOYS: STUDY OF THE MICROSTRUCTURAL, MECHANICAL CHARACTERISTICS AND FINAL OPTIMIZATION OF PRODUCTION PARAMETERS FOR THE REALIZATION OF FULL AND CABLE PIPE CHAINS

Direttore della Scuola : Ch.^{mo} Prof. Paolo Colombo

Coordinatore d'indirizzo : Ch.^{mo} Prof. Giovanni Meneghetti

Supervisore : Ch.^{mo} Prof. Manuele Dabalà

Tutor Aziendale : Ing. Fabrizio Furlan

Dottorando : Claudio Cason

A.A. 2016/2017

ABSTRACT

The gold market is one of the major world markets and the Italian companies place the country as one of the major players in this sector. However, the production in these companies is mostly based on the use of artisan skills, without investing in research and studies about the production processes of these materials. In fact, often the process depends on a "craft" way of working, in which the technical and scientific knowledge are dictated more by experience than by a systematic scientific approach. The international bibliography regarding the world of machining of gold alloys is not as developed as in the case of other metal alloys (steels and aluminum alloys), in which the aesthetic appearance is much less important than the functional aspect. The increase in the nationally and internationally competitiveness caused a growing interest to the study of these materials and their metallurgical properties, with the need to create more complex products that are able to maintaining their extremely high quality. Many of the metallurgical concepts of other materials (in particular face-centered cubic structure alloys) can be applied to gold alloys. However, the greatest variety in composition, the well-defined standards in form, the mechanical and aesthetic properties that they have to satisfy, made necessary the knowledge of mode and characteristics, with which the different constituents influencing the machining, heat treatments and the final quality of the semi-finished product.

In the first part of the thesis, the main properties of pure gold and gold alloys will be presented, with a particular attention to the main jewelry production technologies and the main usage of gold in the world market.

In first chapter the supply, demand and pricing of gold will be generally described to allow an easy collocation of the information contained and the results explained in this thesis, in a larger context such as the world gold market.

After, in chapter 2, will be described the main features of gold, which make its the most important metal used for the production of precious artifacts. The attention will be focused mainly on the electronic configuration of gold, and on the physical, optical, and crystallographic properties that result from this.

In chapter 3, the aim is to introduce the metallurgical principles of alloying for improve particular properties, such as strengthening, or for adjust other characteristics of gold alloys in order to meet certain requirements. Will be introduced the industrial operations of casting, deformation, heat treatment, and interesting using of innovative approaches to the goldsmith production.

Chapter 4 is an overview of the main technologies used in gold jewelry manufacture, the aim is to give a more complete idea of the means of the term "jewelry", and of the key role of a scientific

approach, or the scientific research, focused to improve and develop the industrial production system.

The second part of this thesis summarizes the work carried out during the three-year Ph.D in Industrial Engineering.

The objectives of the project are the determination of the relationships between the composition and different properties of the gold alloys (the caratage, the color, the mechanical properties,...) used by the goldsmith company in the different stage of the production cycle for the realization of full pipe and cable chain. In particular will be studied the effect of the various constituents and their quantity in the alloys, the mechanical properties and the weldability of these. The investigation will be performed from the melting process, through different plastic deformation and annealing steps, until the realization of the welded semi-finished product.

A further objective of the project is the study of the mechanisms of plastic deformation of the different alloys used in the company, in order to optimize the processes of deformation and heat treatments depending on the material used, the various alloying elements and the different production cycles.

In chapter 5, will be briefly described the experimental apparatus used for the characterization of the samples (taken from the whole production process in the goldsmith company FilK S.p.A.), in the laboratories of the Department of Industrial Engineering of the Padua University.

In chapter 6, will be described the production cycle of the gold welding wires used to solder the hollow gold chain produced. The effect of the microstructure and residual stresses on the corrosion and mechanical properties will be discussed. The study will focus on the control of production parameters in order to improve machinability of the gold wires and to increase their properties.

In chapter 7, a statistic analysis of some mechanical and compositional characteristics of gold alloy wires will be reported. The purpose is to individuate an approximation of the possible existing influences and relationships between these and the energy absorbed during deformation. The properties that will be investigated are elongation, Young modulus, ultimate strength and the concentration of gold.

In Chapter 8, the production processes of gold alloys plates will be described. The aim of this part of thesis is to optimize the microstructure and the mechanical properties of the products, which, successively, will be welded to an iron sheet to create the base for the final hollow chain products. The parameters of production cycles and the intrinsic properties of the different gold alloys will be studied, with particular attention to the stresses and the microstructures generated from the subsequent deformation and annealing steps.

Finally, in chapter 9 the plating process will be analyzed, in order to define the influence of the process parameters on the characteristics of the semi-finished products. Furthermore, different ageing treatments for various gold alloy compositions will be described, the results will allow to optimize time and temperature of the age-hardening treatments for the company's gold alloys.

The whole production tests were performed, in collaboration with Ing. Fabrizio Furlan, in Filk S.p.A., the goldsmith company partner of this collaboration and unique supplier of the material for this research. The main part of the characterization of the different gold samples was carried out at the metallurgy laboratories in the Department of Industrial Engineering, University of Padua, under the supervision of prof. Manuele Dabalà and in collaboration with Ing. Luca Pezzato.

Some analyzes, especially the chemical etching of the specimens with different solutions of cyanides, have been performed at other structure: in the laboratories of Progold S.p.A. in collaboration with Ing. Daniele Maggian, Dr. Patrizio Sbornicchia and Dr. Valerio Doppio.

The obtained results allowed improving the workability of the gold alloys used by the company with a reduction of the industrial wastes. The optimization of the production parameters, in the different processes, allowed to increase the microstructural quality of the semi-finished products with an improvement on the mechanical and metallurgical characteristics. A suitable control on the production processes and, the optimization of the gold alloy's compositions, allowed to increase the constancy, the reproducibility of the results and the quality in the production of hollow and cable pipe chains. The obtained results also have a scientific relevance that have allowed their presentation in numerous national and international conferences and publication in scientific journals as reported at the end of the thesis.

SOMMARIO

Il mercato orafa è uno dei principali mercati mondiali e l'insieme delle aziende italiane del settore pongono il paese come uno dei maggiori attori in questo mercato. Tuttavia la produzione delle aziende si è sempre avvalsa di conoscenze artigianali, senza investire nell'approfondimento scientifico sistematico dei fenomeni che coinvolgono i processi produttivi di tali materiali. Infatti, spesso le produzioni sono legate ad un modo di operare "artigianale" dove frequentemente le produzioni sono legate a lavorazioni tradizionali nelle quali le conoscenze tecnico-scientifiche sono dettate più dall'esperienza che da un approccio scientifico sistematico. Anche la bibliografia internazionale legata al mondo delle lavorazioni delle leghe d'oro non è così sviluppata come nel caso di altre leghe metalliche (ad esempio acciai e leghe di alluminio) in cui l'aspetto estetico, peculiare nelle produzioni di metalli preziosi, è di gran lunga meno importante dell'aspetto funzionale.

Si è riscontrata una necessità sempre maggiore di sviluppare un approccio scientifico allo studio sistematico dei materiali e delle loro proprietà, causata da una sempre maggiore concorrenzialità sia in ambito nazionale che soprattutto internazionale unita poi all'esigenza di creare manufatti sempre più complessi che riescano a mantenere inalterata la loro qualità estremamente elevata.

Sebbene molti concetti della metallurgia di altri materiali (in particolare delle leghe a base cubica a corpo centrato) possano essere applicati alle leghe d'oro, la grandissima varietà di composizione, la necessità che i manufatti verifichino dei precisi standard riguardanti forme, proprietà meccaniche, proprietà estetiche rendono necessario apprendere modalità e caratteristiche con le quali i diversi costituenti influenzano le lavorazioni, i trattamenti termici e la qualità finale del semilavorato.

Nella prima parte di questa tesi, verranno presentate le principali proprietà dell'oro puro e delle sue leghe, con particolare attenzione alle principali tecnologie di produzione per gioielleria e ai principali utilizzi dell'oro nel mercato mondiale.

Nel primo capitolo verranno descritti, in modo generale, i significati di offerta, domanda e prezzo dell'oro, al fine di permettere una semplice collocazione, delle informazioni e dei risultati contenuti in questa tesi, in un contesto più ampio quale è quello del mercato mondiale dell'oro.

Successivamente, nel capitolo 2, verranno descritte le principali caratteristiche dell'oro, che lo rendono il metallo più importante per la produzione di manufatti preziosi. L'attenzione sarà concentrata, principalmente, sulla configurazione elettronica dell'oro e sulle proprietà fisiche, ottiche e cristallografiche che ne derivano.

Nel capitolo 3, l'obiettivo è di introdurre i principi metallurgici dell'alligazione volta a migliorare particolari proprietà come la resistenza meccanica o per regolare altre caratteristiche delle leghe d'oro al fine di soddisfare particolari requisiti. Verranno introdotte le operazioni industriali di

fusione, deformazione, trattamento termico e interessanti utilizzi di innovativi approcci alla produzione orafa.

Il capitolo 4 è una panoramica delle più importanti tecnologie usate nel mondo della produzione di gioielli in oro, lo scopo è di dare un'idea più completa del termine "gioielleria", e del ruolo chiave di un approccio scientifico, o di una ricerca scientifica, focalizzato al miglioramento e lo sviluppo del sistema produttivo industriale.

La seconda parte di questa tesi riassume il lavoro svolto durante i tre anni di dottorato in Ingegneria Industriale.

Obiettivi del progetto sono la determinazione delle relazioni tra composizione e proprietà (titolo e colore) e caratteristiche meccaniche delle leghe utilizzate in azienda nelle diverse fasi del ciclo produttivo per la realizzazione di catene in tubo pieno e cavo. In particolare verrà studiato l'effetto dei diversi costituenti, e la loro quantità in lega, che provocano una modifica del colore delle leghe, delle caratteristiche meccaniche e della saldabilità di queste a partire dal processo di fusione fino alla realizzazione del semilavorato saldato. Ulteriore obiettivo del progetto è lo studio dei meccanismi di deformazione plastica delle diverse leghe utilizzate in azienda al fine di ottimizzare i processi di deformazione e di trattamento termico a seconda del materiale utilizzato, dei diversi elementi alliganti e dei diversi cicli di produzione.

Nel capitolo 5, verrà brevemente descritto l'apparato sperimentale usato per la caratterizzazione dei campioni (prelevati dall'intero processo produttivo nell'azienda orafa Filk S.p.A.), nei laboratori del Dipartimento di Ingegneria Industriale dell'Università di Padova.

Nel capitolo 6, verrà illustrato il ciclo di produzione dei fili d'oro per saldatura usati per saldare tra loro gli anelli delle catene d'oro vuote prodotte. Verrà descritto l'effetto della microstruttura e delle tensioni residue sulle proprietà di resistenza alla corrosione e meccaniche. Lo studio sarà focalizzato sul controllo dei parametri di produzione al fine di aumentare la lavorabilità dei fili d'oro e di incrementarne le proprietà.

Nel capitolo 7, sarà riportata l'analisi statistica di alcune proprietà meccaniche e composizionali dei fili in lega d'oro. L'obiettivo è di individuare un'approssimazione della possibile influenza e relazione esistente tra queste e l'energia assorbita durante il processo deformativo. Le proprietà che verranno analizzate sono l'allungamento, il modulo di Young, la resistenza a rottura e la concentrazione d'oro.

Nel capitolo 8, verrà descritto il processo produttivo delle lamine in lega d'oro. Lo scopo di questa parte di tesi è volto ad ottimizzare la microstruttura e le proprietà meccaniche dei prodotti, che, successivamente, verranno saldati ad una lamina di ferro per creare la base delle catene vuote finali. Verranno studiati i parametri dei cicli produttivi e le proprietà intrinseche delle diverse leghe d'oro,

con particolare attenzione agli stress e alle microstrutture generati attraverso il susseguirsi di step deformativi e di ricottura.

Infine nel capitolo 9 verrà analizzato il processo di placcatura, al fine di definire l'influenza dei parametri di processo sulle caratteristiche dei prodotti semi-finiti. Inoltre, verranno descritti diversi trattamenti di indurimento per varie composizioni di lega d'oro, i risultati ottenuti permetteranno di ottimizzare tempi e temperature dei trattamenti di indurimento per invecchiamento per le leghe d'oro utilizzate dall'azienda.

Tutti i test produttivi sono stati effettuati, con la collaborazione dell'Ing. Fabrizio Furlan, presso Filk S.p.A., l'azienda orafa partner di questa collaborazione e unico fornitore di materiale per la ricerca. Gran parte della caratterizzazione dei diversi campioni è stata effettuata presso i laboratori metallurgici del Dipartimento di Ingegneria Industriale, dell'università di Padova, sotto la supervisione del prof. Manuele Dabalà e con la collaborazione dell'Ing. Luca Pezzato.

Alcune analisi, specialmente l'attacco chimico sui campioni con differenti soluzioni di cianuri, sono state effettuate presso un'altra struttura: nei laboratori di Progold S.p.A. con la collaborazione dell'Ing. Daniele Maggian, il Dr. Patrizio Sbornicchia e il Dr. Valerio Doppio.

I risultati ottenuti hanno permesso di migliorare la lavorabilità delle leghe d'oro usate dall'azienda con una riduzione degli scarti di produzione. L'ottimizzazione dei parametri produttivi, nei diversi processi, ha permesso di aumentare la qualità microstrutturale dei prodotti semi-finiti con un miglioramento delle caratteristiche meccaniche e metallurgiche. Un opportuno controllo dei processi produttivi e, l'ottimizzazione delle composizioni delle leghe d'oro, hanno permesso di aumentare la costanza, la riproducibilità dei risultati e la qualità nella produzione di catene piene e vuote. I risultati ottenuti presentano inoltre una rilevanza scientifica tale da averne permesso la presentazione in numerosi convegni nazionali e internazionali e la pubblicazione in riviste scientifiche di settore come riportato nell'elenco delle pubblicazioni che conclude questo lavoro di tesi.

LIST OF CONTENTS

SOMMARIO	VII
<i>Chapter 1</i>	6
Supply and Demand of Gold	6
1.1 INTRODUCTION	6
1.2 GOLD PRICE	7
1.3 ABOVEGROUND STOCKS	8
<i>1.3.1 Scrap</i>	8
<i>1.3.2 Central Banks</i>	9
1.4 JEWELRY	9
1.5 OTHER FABRICATION	10
<i>Chapter 2</i>	12
Physical and Optical Properties of Gold	12
2.1 INTRODUCTION	12
2.2 ELECTRONIC STRUCTURE OF GOLD	12
2.3 CRYSTAL STRUCTURE AND ALLOYING BEHAVIOR	13
2.4 OPTICAL PROPERTIES	14
2.5 PHYSICAL PROPERTIES	17
<i>Chapter 3</i>	20
Metallurgy of Gold	20
3.1 INTRODUCTION	20
3.2 GRAIN REFINEMENT	23
<i>3.2.1 Solidification</i>	24
<i>3.2.2 Recrystallization during Annealing and after Cold-Working</i>	24
3.3 STRENGTH AND DUCTILITY	26
<i>3.3.1 Mechanisms</i>	26
<i>3.3.2 Precipitation Hardening</i>	28
<i>3.3.3 Solid Solution Hardening</i>	36
<i>3.3.4 Dispersion Hardening</i>	37
<i>3.3.5 Disorder-order Transformation Hardening</i>	38

3.4 COLOR OF GOLD ALLOYS	41
3.4.1. Yellow to Reddish, Greenish and Whitish	41
3.4.2 White Gold	42
3.4.3 Special Color of Gold	43
3.4.4 Thermal properties: Wetting, Fluidity and Other	44
Chapter 4	46
The Technology of Jewelry Manufacturing	46
4.1 INTRODUCTION	46
4.2 CURRENT MANUFACTURE	46
4.3 MAIN JEWELRY TECHNOLOGIES	47
4.3.1 Cold Forming Technologies	48
4.3.2 Electroforming	49
4.3.3 Investment Casting	50
4.3.4 Hollow-ware	53
4.3.5 Chain-making	54
4.3.6 Joining Techniques	55
4.3.7 Finishing	57
4.3.8 Manufacture of rings	57
4.4 OTHER TECHNOLOGIES	58
Chapter 5	62
Characterization System	62
Chapter 6	70
Study of gold-welding alloy wires: Effect of Production Parameters on Microstructure and Properties	70
6.1 INTRODUCTION	70
6.2 EXPERIMENTAL PROCEDURE	71
6.3 RESULTS AND DISCUSSION	72
6.3.1 9 Kt Gold Welding Alloy	73
6.3.2 10 Kt Gold Welding Alloy	75
6.3.3 14 Kt Gold Welding Alloy	78

6.3.4 18 Kt Gold Welding Alloy	83
6.3.5 Residual stresses and corrosion resistance tests	86
6.3.6 Concluding Remarks	91
Chapter 7	94
Statistical Analysis on a Mechanical Tests Dataset of Gold Alloy Wires	94
Chapter 8	102
Study of 10 Kt Gold Alloys Used in Cable Chain Industrial Production Processes	102
8.1 INTRODUCTION	102
8.2 EXPERIMENTAL PROCEDURE	102
8.3 RESULTS AND DISCUSSION	105
8.4 CONCLUDING REMARKS	115
Chapter 9	116
Study of Plating Process and Ageing Treatments for the Production of Hollow Gold Chains	116
9.1 PLATING PROCESS	116
9.1.1 Introduction	116
9.1.2 Results and Discussion	118
9.1.3 Concluding Remarks	121
9.2 AGE-HARDENING TREATMENTS	123
9.2.1 Introduction	123
9.2.2 Results and Discussion	123
9.2.3 Concluding Remarks	133
CONCLUSIONS	136
REFERENCES	140

Chapter 1

Supply and Demand of Gold

1.1 INTRODUCTION

All the gold diffused in the world comes essentially from two different sources, the new mine production and previously mined metal or aboveground stocked in various forms. In recent decades, the main of the two sources was the new mine production, which provides the bigger part of the total supply of gold to the market. The annual production has exploded from about 1,000 tonnes in 1980 to 2,645 tonnes in 2001, but recently this trend has fallen down. The greatest amount of supply from the aboveground stocks derives from the recycled part of metal contained in manufactured products, mainly comes from jewelry. Other fields of supply from aboveground stocks include hedging by mining companies, disinvestment from private holdings and sales by central banks. Hedging by the companies is, substantially, equal to selling the future production at current price. This was a big source of supply in the 1980s and 1990s, but in the last years, good sentiment about prices has resulted in a change of these actions.

Analyzing now the demand for gold, it's possible to individuate the greatest portion of this on jewelry manufacture. As for the supply, also for the demand is possible to define two distinct categories. The first regards the industrialized world, where jewels and adornments are the most important buying motive. The second category concerns the developing world, where investments motives dominate. Whereas the buying of jewelry productions are not that responsive to the price of gold, the second category is typically sensitive to price oscillations. Driven by market rising, population growth, and special gold price conditions, the demand for jewelry production reached the top in the 1980s-90s. However, some structural changes of the market, the coming of other applications and uses (e.g. electronics) and the rise in gold prices reduced the total impact of gold jewelry on the scene. The fabrication demand is covered, moreover, by dentistry and decorative uses, plating uses, coins production etc.

Investment in gold essentially consists on buying gold coins or bars by people or a large number of options, futures, dealings or share in exchange-traded funds. It is impossible to define the exact impact of these activities but they contribute to the total equilibrium of the supply and demand market.

The final aspect regards the price of gold. Usually, a deficit of supply means of a rising of the price while surpluses will drive to the opposite result. The precious metals market is different, a surplus

translates into an addition to stocks, which influences the investments and usually follow the rising prices. Selling from the investors (during the fall of the prices), is necessary to link the deficit to the main market.

1.2 GOLD PRICE [48]

Since antiquity, gold has been used in the exchange activities. The British monetary system adopted the use of gold against the pound sterling maintaining a fixed price (gold standard), therefore the sterling price became the international price of the metal. During 1930s, the U. S. dollar has been regarded as the first international currency, the price of gold was fixed at \$35 per ounce in 1934 and this has resisted till 1968, when it was entrusted to the global open market. Since this year, the gold price became highly variable, reaching a maximum of \$850 in 1980 before dropping again in the first 2000s. During the last years, the price of gold was characterized by a new increase, thus overcoming the \$1000 mark, but considering the inflation this remain still below the 1980 value. In Fig.1.1 is represented the trend of gold price in the last decades.

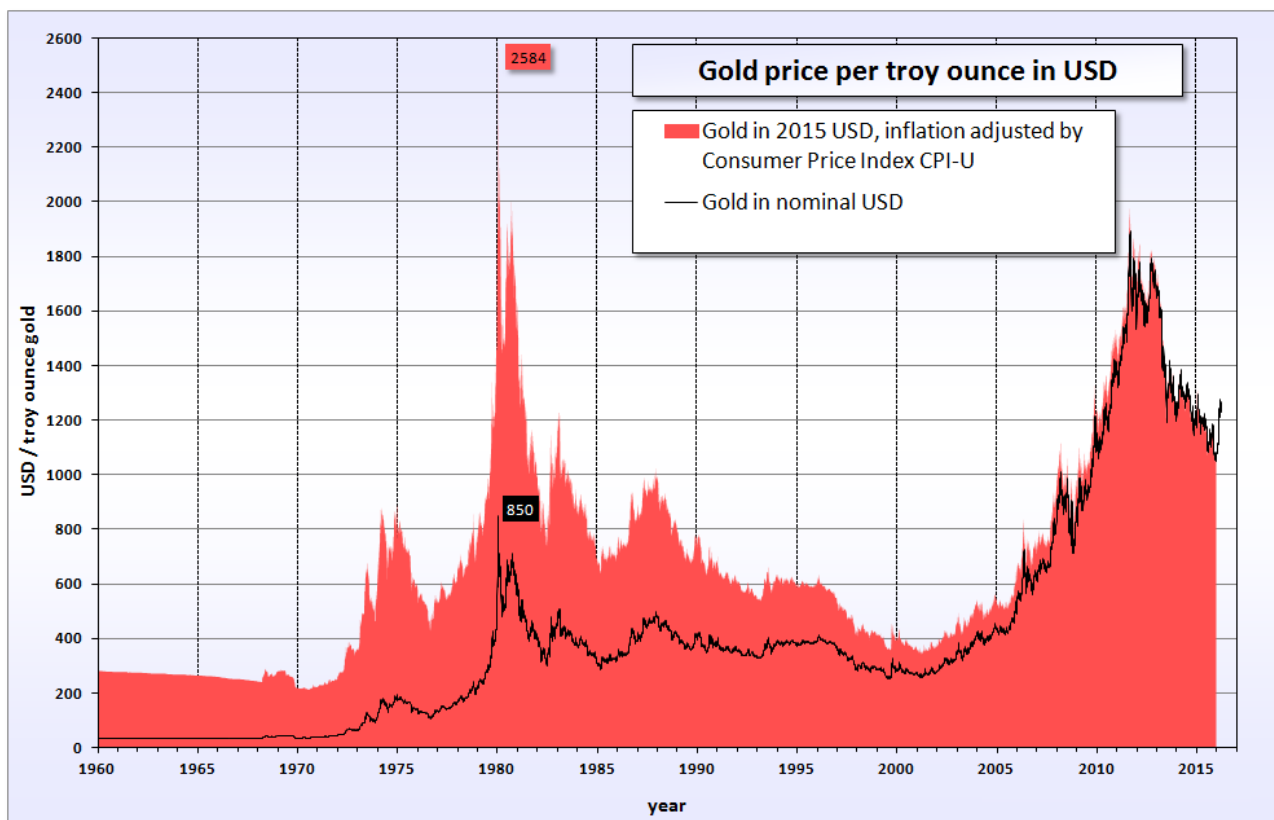


Fig. 1.1 – Gold price historic trend in 1960-2015

Since 1919, the London Fix is the primary reference price for gold, set by the members of the London Bullion Market Association. The currency fluctuations may have a considerable impact on the global market, producing different and divergent price trends within individual nations, although the international gold price is set in U.S. dollars. A close link between gold price and other industries exist, where the main is the correlation between the U.S. dollar and gold. Usually there is an increase in the value of gold in conjunction with a decline in the purchasing power of the U.S. dollar and vice versa. Also other precious metals, as platinum and silver, change their value with the gold market; or even oil is linked with its trend. In a time of politically and geographic tensions, when the price of oil increase, the appeal of gold investments is sold as a safe choice. The last bond of note is whit the stock market. Here, vice versa, during the period of boom, the investors move money from gold investments to equities.

1.3 ABOVEGROUND STOCKS

The recycling of all the industrial products and the displacement of ingots stocks are the main aboveground sources of gold, in addition to the extracted one. In the last year this type of supply has accounted for about 1/3 of total supply, certain estimates have suggested that these aboveground stocks amounted to about 150000 tons in the mid-2000s. Is this large quantity of aboveground stocks, which differs the gold market from the other precious metals. The whole gold extracted, until to date, also exist in various forms, due to its virtual characteristic of indestructibility. Ingot is the primary useful form for the return of gold into the market from the aboveground stocks; half of this bullion is held by banks, the other part by institutions and private individuals. About 75000 tons of aboveground stocks are held by jewelry products, the remaining part consists in other types of fabrication and includes, also, items containing gold lost or untraceable.

1.3.1 Scrap

Exist two types of gold wastes: the old scrap and the process scrap. The first, is the metal recovered from final products containing gold. The greater part coming from jewelry, although small amounts derive from other areas such as dental alloys or electronics. Old scrap is the largest source of supply, after mining, and it covers, for about a quarter, the total supply. In presence of a financial crisis, individuals sell their gold stocks inducing a phenomenon called dishoarding, although the first reason remains the volatility of the gold price. A change in the fashion trends or, for example, a recession, could prime an increase in scrap from producers until retailers, which are obliged to melt

unsold items. Usually, the old scrap is reused in the same market where it was inserted at the beginning but, sometimes, it is exported to other areas (such as Swiss refineries) when it exceeds the local industry needs.

The process scrap, instead, concerns that never result in a finished product. For example, the edges of a metal plate after the shearing process, the powder or filings recovered from the polishing or finishing processes, or even coins stamped incorrectly.

1.3.2 Central Banks

Once, gold was the dominant asset in the central banks stocks strongly linked to the dollar. But, with the dismantling of the gold standard in 1932 and, subsequently, other modifies, the gold price was allowed to vary freely with the different markets. The use of gold billion stocks allows to create a public confidence in the banks, and an idea of economic e financial security. The interest of the banks is also to generate income by lending of its gold ingots. The greatest holdings are in the Western world, while Japan, China and Taiwan, whose gold reserves are lower relative to other currencies, come after. The international gold market is provided, largely, by the official sector and the European banks have played an important role covering about 20% of the total annual supply.

1.4 JEWELRY

In jewelry, usually, gold is described in terms of karat that is a measure of purity of gold, defined as part per 24. This excludes, *e.g.*, all the articles which have a brass base and are plated with a gold coating. Pure gold exists in 24-karat form but the highest caratage commercialized is 22-karat, but this karat is mainly used in India. Other karat forms are: 21-karat, in the Middle East markets; 18-karat, in Southern Europe; 14-kt gold; and the lowest 8, 9, 10 karat forms are instead used in North America and in Northern Europe. Usually, the highest carat grades are bought only for economical investment [1].

The purchase of jewelry items is driven by fashion trends. 18-karat jewelry is the standard used in areas such as southern Europe to create high quality items, which can mount some precious stones as diamonds or other. This work is possible due to the particular concentration of gold in the alloy, in this way we are able to ensure a solid and sufficiently hard base to hold gems and to guarantee a permanent color over time. Is easy to find adornments in 18-karat gold alloy named “white gold”, the addition of elements like palladium or nickel can mask and move the color of the piece from the classic yellow to white.

Recently, fine jewelry has been blended with costume jewelry. A gold pendant or any other precious items could be found not only on a gold chain but, also, on a leather cord. Few grams of gold could be found also on steel or brass items, such products allow to raise higher markups over the real value of the gold content. In the industrialized markets, the segmentation of consumer spending cut the amount of money spent on gold and jewelry, moreover, the greater marketing helped other consumer goods. This would lead to assert that the amount of gold sold in form of jewelry will tend to a continuous decrease, which it's real considering the industrialized world but contrasts with the result obtained from the developing world. In these countries the economic growth has led to the opening markets, India became the largest consumer of gold followed by China and United States (in third position due to the recent crisis). In the global ranking of the jewelry production Italy claims fourth position, penalized by the structural change and market share loss. Although jewelry is the largest consumption of the yellow metal, accounting for about two-thirds of the total demand, often plays a minor role compared to investment. This last factor is the most important in the determination of the gold price due to its price sensitivity. The purchase of gold items varies depending on gold price and on balance between supply and demand.

1.5 OTHER FABRICATION

Jewelry is not the only field of application of gold. Other form of fabrication like electronics, dental alloys and decorative plating account for approximately 15% of total gold demand. Gold is used to isolate the plating of contacts with the aim to guarantee the corrosion resistance and for its ability to be drawn into thin wires. Regarding the use of gold in dental alloys, although the world population and standards of living are rising, gold dental demand decreased in the last years. Probably due to the substitution with other non-precious metals or with ceramic fitments. One of the main decorative uses of gold is the plating of costume jewelry and the clasps, buckles, and so forth of luxury accessories such as belts or handbags. Lastly, gold is used in coins, whether official or unofficial, and medals. Official coins are best categorized as a form of investment, unofficial coins and medals are often bought for various reasons such as for gifts or commemorative tokens, although an investment rationale will often still come into play to varying degrees.

Chapter 2

Physical and Optical Properties of Gold

2.1 INTRODUCTION

Gold was one of the first metals used by humans because of its particular characteristics: high malleability, considerable density (19.32 g/cm^3), excellent corrosion resistance and a shiny metallic yellow color. Gold occupies the position 79 in the periodic table and also other elements close to it present similar properties but, its special electronics configuration, explains the interest regarding the coexistent of these characteristics. The electronic configuration controls the optical properties, chemical reactivity and crystal structure of an element. Gold, being a heavy element, has other attributes like: a large number of isotopes or its opacity to x-rays which ensures that it interacts strongly with electrons in both scanning and transmission electron microscopy. Both of these characteristics allowed using gold in different technological applications [2-3].

2.2 ELECTRONIC STRUCTURE OF GOLD [48]

Elemental gold, normally, is free of an oxide coating. This considerable corrosion resistance is a result of its high first ionization potential, 9.2 eV, high compared to those of silver and copper (7.6 and 7.7). Gold has the electronic configuration $[\text{Xe}]4f^{14}5d^{10}6s^1$. The 4f electrons shield the other orbital electrons from the nuclear charge; this effect is called lanthanide contraction. This phenomenon causes the atomic radius of the lanthanides to decrease across the period as the quality of the shielding per electron decreases; in the 5d metal series this effect gives similar lattice constants to the 4d metals. The position of gold on the periodic table make it unique, because to this lanthanide contraction effect are added also some relativistic effects [4]. With the increase of the atomic number, the velocity of the 1s electrons approaches the speed of light. The increase in mass of these electrons causes the contraction of their orbital toward the nucleus. The higher s and p orbitals also contract trying to compensate this phenomenon resulting finally in the outermost 6s and 6p orbitals being smaller than they would otherwise have been without relativistic effects. The 5d and 5f electrons are more shielded from the nucleus due to the contraction of the s and p orbitals. Not having a high electron density approximately to it, are less susceptible to relativistic effects of their own, destabilizing and expanding outward with an associated increase in energy [5]. It was discussed how the stabilization of the 6s orbitals made up the first ionization potential of gold,

unlike the second and third ionization potential that follow the opposite trend. The oxidation states as +I, +II, +III are easily accessible, and +V state have been reported only for few compounds. The relativistic effect causes the shortening of the covalent bond lengths in several gold molecules, compared to the same Ag compounds. This characterizes the molecules Au-X⁺, while the contraction is smaller for the compounds Au-X⁻; the 6s orbital's contraction plenty reduces the dimension of the Au⁻ ion while the expansion of the 5d orbital increases the size of the Au⁺ ion [6]. Another non-negligible effect is the “aurophilicity” of gold, used to describe the interaction between the electrons of nonvalence orbitals, which generates unusual system bonding due to the small energy gap of the 5d and 6s electrons. The normal 5d¹⁰ configuration it is easily broken by the hybridization of the s-d orbitals [7].

2.3 CRYSTAL STRUCTURE AND ALLOYING BEHAVIOR

Gold, as other ductile metallic elements (Al, Ag, Cu,...), is characterized by a face-centered cubic crystal (f.c.c.) structure in its metallic form. One of the anomalies that distinguishes gold from other fcc metals is the possibility to easily reconstruct all the three high symmetry planes, included the (111), probably due to relativistic effects. The surface tension of liquid Au is approximately 1.1 to 1.2 J/m², increased by alloying with Cu and, vice versa, lowered with Ag or Zn [8]. The crystal structure of gold, with a multiplicity of close-packed planes on which slip can occur, makes it more ductile in comparison to iron or tungsten with their bcc structure, or Mg and Zn with their hexagonal structure. Referring to gold nanoparticles, instead, under 10 nm the fcc structure isn't the most stable but decahedral, icosahedral or defectives in structures are formed [9].

Some characteristics, like the electronegativity and the difference in atomic radius, limit the range of solid solutions that gold forms with other elements. Au-Ni, Au-Cu, Au-Pt and Au-Pd systems form solid solutions at high temperatures, but their mutual solubility decreases as the temperature drops [10]. Gold forms with other elements a wide range of intermetallic compounds, for example, AuAl₂, AuIn₂ or AuGa₂ have a well defined color due to their reflectance minimum in the visible part of the spectrum. This low energy behavior is caused by the presence of several bands of conduction electrons, in agreement with Fermi surface studies, and a developed secondary band edge in the visible [11]. Unfortunately, the fragility of these intermetallic compounds limits their commercial application in jewelry production.

2.4 OPTICAL PROPERTIES

The frequency-dependent permittivity or dielectric constant can describe the optical properties of all linear optical materials:

$$\varepsilon = \varepsilon_1 + i\varepsilon_2 \quad (2.1)$$

Related to the complex refractive index by

$$m = n + ik = \sqrt{\varepsilon} \quad (2.2)$$

Usually the permittivity of metals is modeled using a Drude-like function of the form:

$$\varepsilon_1(\omega) = \varepsilon_\infty - \frac{\omega_p^2}{\omega^2 + \gamma^2}, \quad \varepsilon_2(\omega) = \frac{\omega_p^2 \gamma}{\omega(\omega^2 + \gamma^2)} \quad (2.3)$$

$$\gamma = \frac{1}{\tau} \quad (2.4)$$

where ε_∞ is the real part of permittivity at high frequency, ω_p is the bulk plasma frequency, γ is the damping constant, inversely proportional to the relaxation time, τ , dependent on the individual electron scattering events [12].

So, physics and optical properties of gold are:

$$n = \sqrt{\frac{1}{2}(\sqrt{\varepsilon_1^2 + \varepsilon_2^2} + \varepsilon_1)}, \quad k = \sqrt{\frac{1}{2}(\sqrt{\varepsilon_1^2 + \varepsilon_2^2} - \varepsilon_1)}, \quad (2.5)$$

$$\varepsilon_1 = n^2 - k^2, \quad \varepsilon_2 = 2nk \quad (2.6)$$

The defined band edge at about 2.4 eV (in the field of green light – 500 nm) gives a strong yellow color to this precious metal. The energy of the hybrid transitions in gold is very low in comparison to the 4 eV of silver, the contractions of the s and p orbitals and the destabilization of the d and f shells are the causes of this characteristic [13]. An interesting properties of gold is the great increase of reflectivity in the middle of the visible spectrum that, as for many others metals, extends into the infrared. The interaction between the particular position of the band edge and the value of plasma frequency cause this phenomenon. A perfect metal is characterized by a value of ε_∞ equal to 1, and γ negligible. That cause the change of the real part of the permittivity from positive (transmission) to negative (reflection), at the plasma frequency. The reflection edge's energy is much lower than the plasma frequency, calculated from the electron density, due to the interbands transition in gold.

We perceive color when the different wavelengths composing white light selectively interfere with matter by absorption, diffraction, reflection, refraction or scattering, or when a non-white distribution of light has been emitted by a system [14]. The wavelength of visible light is of the order of 380-780 nm (Fig.2.1).

The formation of colour in metallic elements and their alloys can be explained by means of the band theory. When metal and light interact, electrons from the metal surface situated either below or on the Fermi level absorb photons and enter an excited state on or above the Fermi surface respectively [15]. The efficiency of the absorption and re-emission of light depends on the atomic orbitals from which the energy band originated. A white reflected light will result if the different colours in white light are

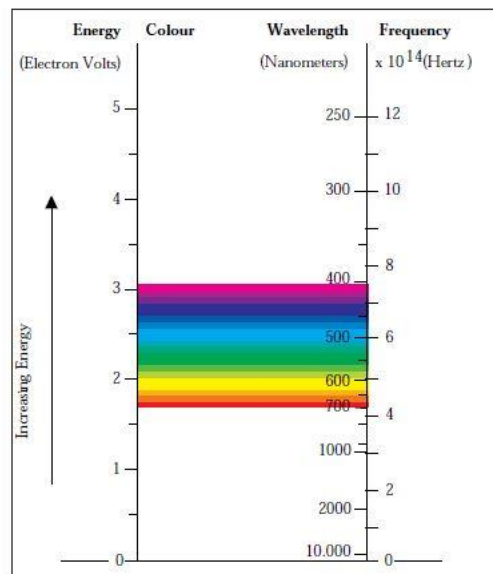


Fig 2.1 – Visible Spectrum [16]

reflected equally well. In the case of gold and copper, the efficiency decreases with increasing

energy, resulting in yellow and reddish colours due to the reduction in reflectivity at the blue end of the spectrum. Measurements performed on gold alloys with various amounts of silver (Figure 2.2) show a high reflectivity exhibited by fine gold for the low energy part (below 2.4 eV) of the visible spectrum. This means that the yellow colour of gold is formed by a selective reflection of the red-yellow wavelengths. As the silver content increases, a higher reflectivity is displayed for the high-energy part of

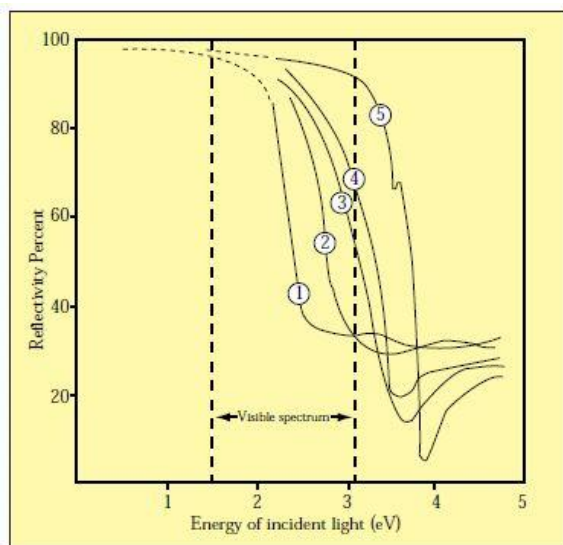


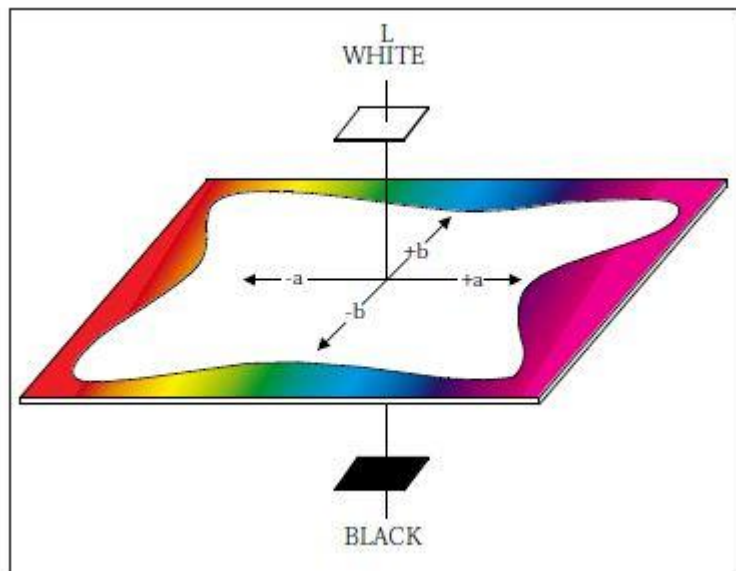
Fig. 2.2 - Reflectivity as a function of energy of the incident light. 1 - fine gold, 2 - Ag50at%Au, 3 - Ag10at%Au, 4 - Ag5at% Au, 5 - fine silver [16]

the visible spectrum. Silver has a very similar electronic structure to that of gold, but the transition of electrons above the Fermi level requires energy in excess of that of the violet end of the visible spectrum, and thus the entire visible spectrum is reflected, resulting in the characteristic white metallic colour [16]. The colour plays an important role in the field of jewelry and dentistry. Producer always estimated the colour of gold alloys visually but there are cases, where this characteristic is the unique condition for the selection. An example could be the need to select the suitable solder for repairing a well-defined item. The

variation in the colours of gold products are index of poor quality and professionalism and could be dangerous for the manufacturers. The need for accurate colour measurement led to the creation of different systems designed to assess the colour. The Munsell system describes the colour by using three co-ordinates: “hue”, “chroma” and “value” [17]. This system still relies on the human eye, and colours are described by visually comparing them with other standard and finding the closest match. Nevertheless, the jewelry industry needed a more objective system, whereby the point for the colour can be defined in order to have the same result and uniformity between the different producers. The DIN system is based on the comparison between, the colour investigated and, a standard gold panel. Also this system is affected by some problem: it depends on the human eye, and the gold panels with lower caratage are characterized by discoloration with time (tarnishing phenomenon).

The Manufacturing Jewellers & Silversmiths of America’s Committee for Color References has brought out a Gold Color Reference

Kit that is based on the CIELAB system [18]. The system, developed by CIE (International Commission on Illumination) and adopted since 1976, allows describing the color mathematically without relying on the human eye. The CIELAB method expresses the colour as three-dimensional co-ordinates: L^* , a^* , and b^* , where L^* is the luminance



(brightness) [19]. An L^* value of 0 means that no light is reflected by the

Fig. 2.3 - The three-dimensional coordinate system (CIELAB) [16]

sample, and an L^* value of 100 means that all incident light is reflected. The a^* co-ordinate measures the intensity of the green (negative) or red (positive) component of the spectrum, while the b^* co-ordinate measures the intensity of the blue (negative) or yellow (positive) component. The colour of a sample can be defined by plotting these co-ordinates as a point in the three-dimensional space represent in Figure 2.3. The values of L^* , a^* and b^* of a sample are obtained as direct readings from a spectrophotometer which is connected to a computer. The spectrophotometer has a resolving power between five and ten times greater than the human eye [16].

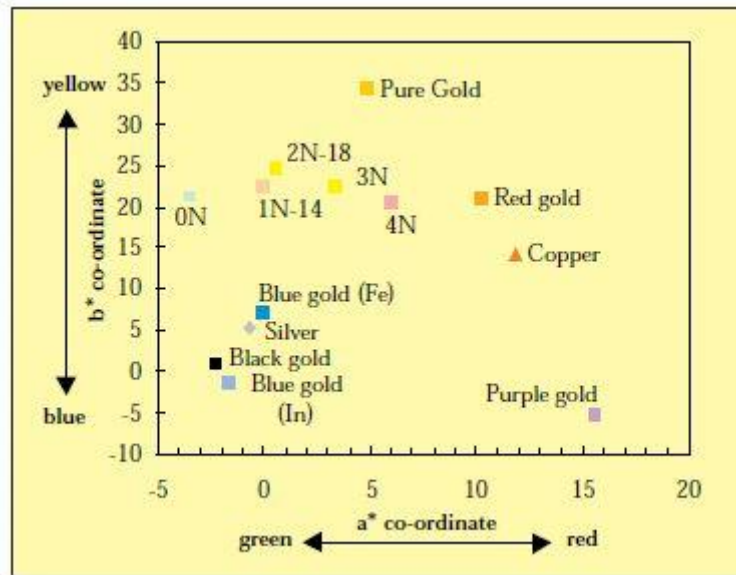


Fig. 2.4 – a^* and b^* for different coloured gold alloys [16]

As the colour of a sample depends on the illuminant, the sample itself and the observer, the spectrophotometer uses an artificial light source that simulates natural light, an array of photodiodes, and the computer as the observer.

The CIELAB co-ordinates of various gold alloys are shown in fig. 2.4, the distance, between two points in this system, is related to the difference in color and can be calculated and numerically described. The DE^* represents this distance and is described by the formula [20]:

$$DE^* = [(L_2^* - L_1^*)^2 + (a_2^* - a_1^*)^2 + (b_2^* - b_1^*)^2]^{1/2} \quad (2.7)$$

The subscripts 1 and 2 refer to the co-ordinates of the two different colors, usually used to describe the initial and the tarnished sample respectively. In fact, the DE value can also be a measure of the tarnishing of a gold alloy.

2.5 PHYSICAL PROPERTIES [48]

The possibility to create malleable gold ingots directly from the molten state, is due to the high resistance to oxidation of this metal, and to its high surface energy. The gold is characterized by a hardness of only 25 HV in the annealed state, which can be raised to about 60 ÷ 80 HV by application of various cold working processes [21]. The application of 60 to 70 % cold work can raise the flow stress of pure gold from about 30 to 220 MPa, but, a higher value of plastic deformation or repeated cold rolling steps, could increase it until 280 MPa.

An important industrial application of gold is the decorative creation of gold leaf, 30 g of gold can

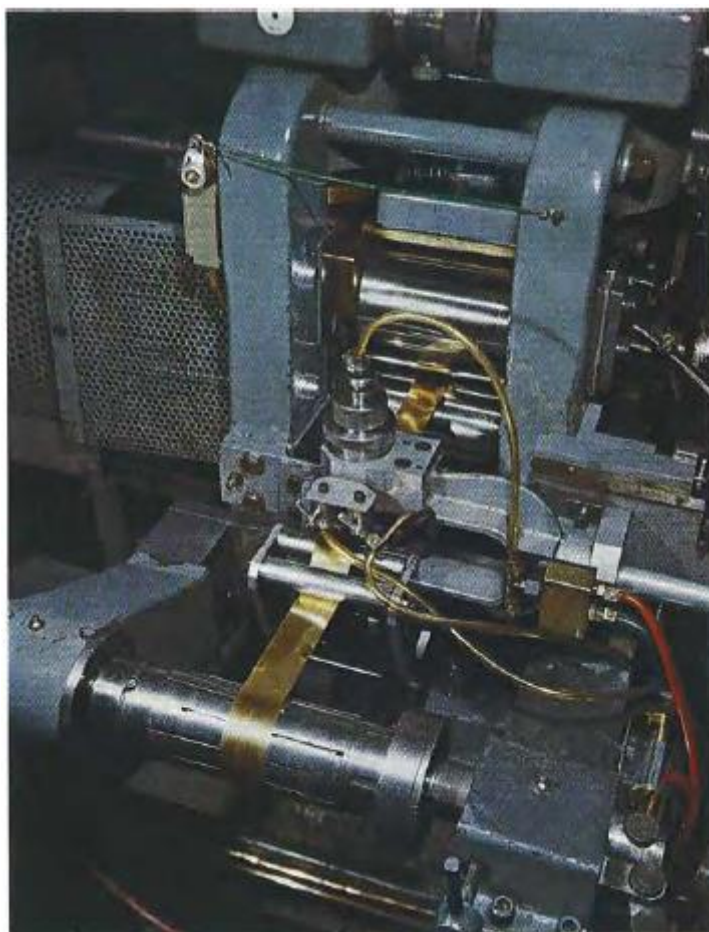


Fig. 2.5 – Example of rolling equipment in modern gold industry [22]

be plastic deformed to a sheet of about 25 m² in area.

The stacking fault energy of gold has an intermediate value between that of copper and silver. The metals with low stacking fault energies are never looked upon as being particularly ductile. The networks of stacking fault in the gold foil should, theoretically, result in a decrease of ductility, due to the greater difficulty in movement of dislocations. The reason of the high malleability of gold, in comparison with other metal characterized by the same fcc structure, is linked to its nobility. Gold, being a noble metal, does not have an oxide film on its surface [22]. Thus dislocations formed within the gold will be able to escape easily from the metal at the surface. With

metals having an oxide film on their surfaces the dislocations could well be held within the metal and this effect would become more noticeable as the total foil thickness decreased; thus the flow stress would be increased. In these conditions further strain may be accommodated by sub-grain boundary shearing, so giving rise to fragmentation at a foil thickness equal to the sub-grain diameter. Gold is, however, unusual in that it can accommodate plastic strain when the beaten foil thickness is less than the sub-grain size produced by plastic straining. In the follow table, Tab. 2.1, various physical parameters useful for the industrial applications are reported. In the late '90s the melting point of pure Au was moved from 1064.43 °C to 1064.18 °C, it is also one of the calibration point used for the International Temperature Scale ITS-90. The increase of the surface/volume ratio, in small gold particles, generates a decrease in the value of the melting point. This trend changes when the particles become even smaller, about tens of atoms, and the melting point increases again, probably because the elementary thermodynamic model does not considers the molecular regime [23]. Pure gold is characterized by a high thermal and electrical conductivity, albeit lower than silver and copper.

The extremely high resistance of this pure metal to corrosion has ensured its place in the connectors required for all types of performance-critical electronic devices.

Property	Notes	
Melting Point	1064.18 °C	
Lattice constant	4.07 Å	
Atomic Radius	1.44 Å	Metallic radius
Young's Modulus	79 GPa	Annealed material at 20 °C
Specific Heat	0.1288 J/(g·K) 25.4 J/(Mol·K)	
Electronegativity	2.44	
Electrical Resistivity	$2.05 \times 10^{-5} \Omega \cdot \text{cm}$	0 °C
Thermal Conductivity	314.4 W/(m·K)	0 °C

Tab. 2.1 – Various selected physical properties of gold [21]

Recent studies have demonstrated that, also if the bulk gold is diamagnetic and the magnetic fields repel it weakly, gold nanoparticles (about 2 nm of diameter) are characterized by a not negligible ferromagnetic behavior. The cause of that could be the particular electronic configuration of their surface [24].

Chapter 3

Metallurgy of Gold

3.1 INTRODUCTION

The properties of gold are unique; pure gold is soft, malleable, ductile and has a shiny yellow color. It is characterized by high thermal and electrical conductivities, it is the most noble of all metals and, due to this reason, it is not affected by corrosion, tarnishing and oxidation. This combination of properties and the persistent stability at high temperatures allows its use, not only in luxury and jewelry fields, but also in many other industrial applications: biomedical and electrical sector, nanotechnologies and others.

However, in the greater part of its applications, gold cannot be used pure but, usually, it is necessary to use other metallic alloying elements to ensure suitable properties.

In jewelry, usually, gold is described in terms of karat that is a measure of purity of gold, defined as part per 24. This excludes, *e.g.*, all the articles which have a brass base and are plated with a gold coating. Pure gold exists in 24-karat form. Caratage is defined as:

$$24 \text{ Kt} = 100 \text{ wt\% Au} \quad (3.1)$$

So, for other composition:

$$X \text{ Kt} = \frac{(X \cdot 100)}{24} \text{ wt\% Au} \quad (3.2)$$

For example, regarding 18 Kt gold alloy:

$$18 \text{ Kt} = \frac{(18 \cdot 100)}{24} = 75 \text{ wt\% Au} \quad (3.3)$$

Whereas, when we are talking about “microalloyed” gold, the additions of other elements are very small (about ≤ 1000 ppm).

The gold alloys composition varies over a wide range, primarily due to the need of particular range

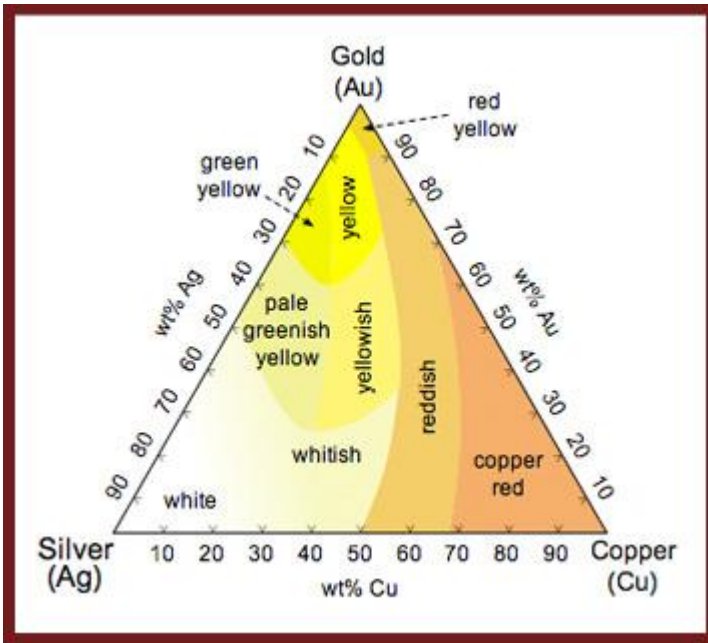


Fig. 3.1 – Au-Ag-Cu ternary phase diagram

of colors and mechanical properties and, secondly, to create products with different price for the consumers, depending on the gold content. The additions of particular elements into the gold alloy is very important, for example, in dental applications, where these are used to create a superficial bond with ceramic components. Another interesting aspect could be the use of lower melting elements to induce a decrease of melting temperatures, a higher wettability and fluidity of particular gold solders. The various phase diagrams are the basis for

any type of metallurgical approach, both binary and ternary gold alloy phase diagrams have been investigated and evaluated [25-26]. It is possible to correlate some specific aspects of the phase diagrams (formation of solid solutions, intermediate compounds, etc.) to a number of elemental atomic parameters, generally showing a gradual variation along the Periodic Table. These parameters could be the valence electron number (Periodic Table group number), electronegativity, atomic (and ionic) radius, Mendeleev number or elemental data such as melting and boiling point, sublimation heat, atomic volume, etc. [27].

Fig. 3.2 gives a sketch of the composition ranges of the solid solutions in gold of the transition elements for which reliable data are available. A complex trend can be noticed as a function of the position of the partner element in the Periodic Table. It is known that this trend can be related to the interplay of the different factors determining solid solubilities. An approach to this point may be given by the Hume-Rothery rules for primary solid solutions.

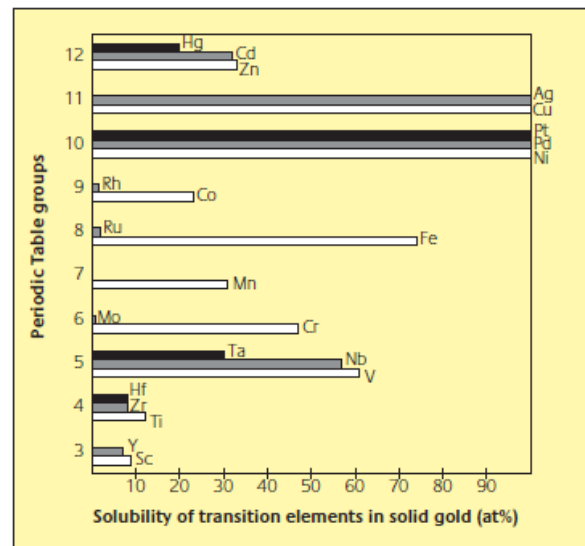


Fig. 3.2 - Solid solubilities of the transition elements in gold. The elements of 10th-11th groups present continuous solid solutions, usually at high temperatures [28]

In jewelry applications the analysis of Au-Cu, Au-Zn and Au-Ni binary systems is very important. All these systems are characterized by large fields of solid solutions, a single phase occurs in the Au-Ag, Au-Pd and Au-Pt systems at high temperatures. Whereas, decreasing temperatures, a solid-state decomposition phenomenon generates a miscibility gap with two final solid solution phases in Au-Ni and Au-Pt systems. Au-Pt and Au-Cu systems present a different behavior. A summary of the formation of these phases is represented in Fig. 3.3.

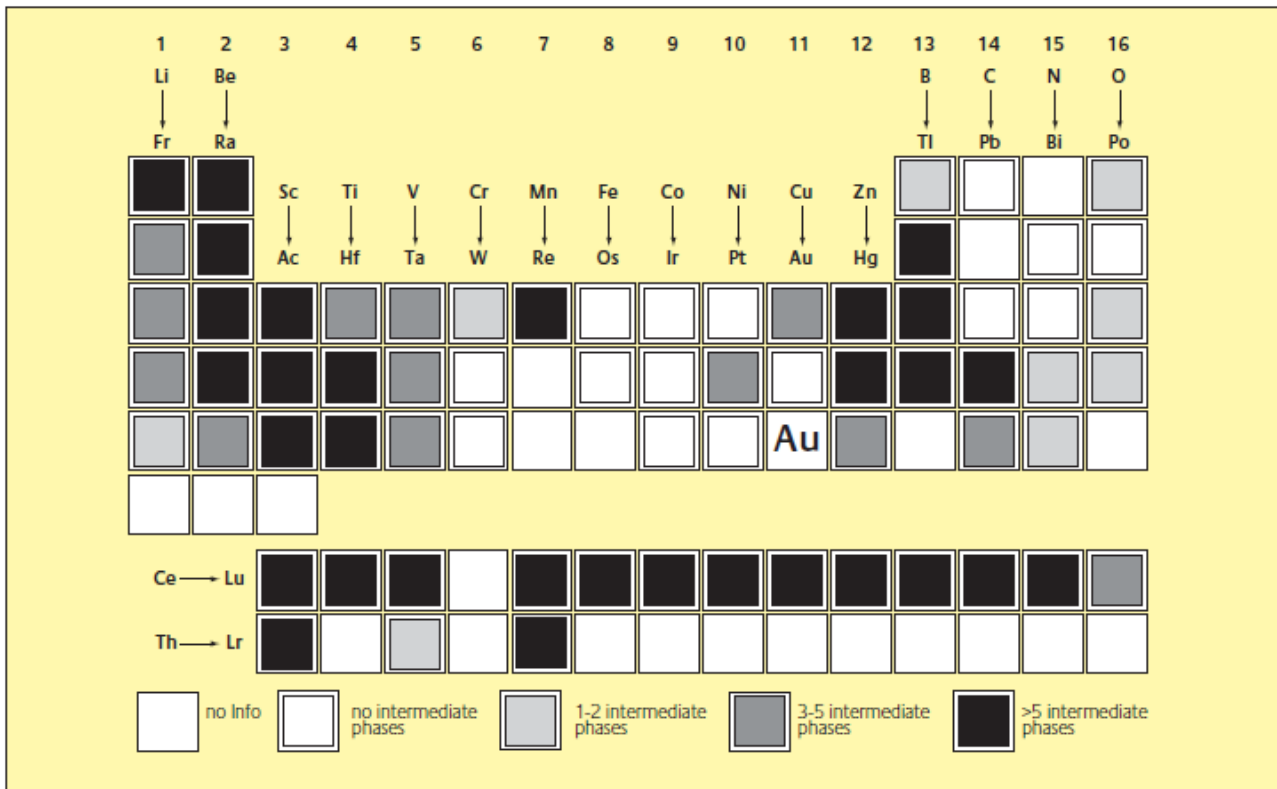


Fig. 3.3 - Indication of the number of intermediate phases formed in the binary Au-X systems, for different elements of the Periodic Table [28]

The mechanisms that overcome and lead to the formation of intermediate phases in the systems are various: crystallization phenomena from the melt or by ordering in the solid state. Mostly, two sets of elements giving intermediate phases can be observed. The first set is on the left of the Periodic Table and corresponds to the formation of stoichiometric compounds with high melting and strongly negative ΔH of formation [28]. The second set of alloys, moving towards the right side of the Periodic Table (e.g. Cd, Ga, In, etc.) generally showing low melting points, large solid solubility fields and lower ΔH of formation. A number of these phases are formed through solid-state reactions. Finally, at the far right of the Periodic Table compounds with semi-metals and non-metals are formed.

In this chapter, the metallurgical principles of alloying for grain refinement, strengthening, and further property adjustment of gold alloys will be introduced.

3.2 GRAIN REFINEMENT [48]

The grain refinement is a mechanism that provides several advantages to the material. Nowadays this form of control is used, by processing and microalloying additions, to optimize the gold alloys properties in different applications fields: dental, jewelry, electronics, etc. [29-30].

Trying to consider all the advantages and benefits related to the reduction of the grain size, it is possible to draw up a list:

- Increase of strength,
- Increase of malleability and ductility,
- Increase of work-hardening during cold-working
- Increase of microstructural homogeneity
- Reduction of alloying elements segregation during solidification
- Improvement of the quality of surface (orange peel effect avoided), and surface-finishing properties
- Increase of the corrosion resistance
- Reduction of the tendency to stress-corrosion cracking
- Reduction to risk of hot cracking during melting process
- Reduction of susceptibility to embrittlement

The grain refinement mechanism generates an increase of number of the grain boundaries and, at high temperatures, this could be a disadvantages due to the change in the deformation mechanisms that overcome. The diffusion processes along the grain boundaries generated cause a decrease in the material strength and of creep resistance.

In most of the application fields but, especially for the jewelry, two steps of the production process have a high influence on the grain size reduction or control: the solidification step of the material after melting process and the annealing step after the cold-working deformation process.

3.2.1 Solidification

When a metal or alloy solidifies from the molten state, as in casting for example, its structure is determined by the processes of nucleation and dendritic growth. The sizes of the grains and their shapes and orientations are determined by such factors as the rates of nucleation and dendritic growth, and by the tendency of crystals to form initially on the cold walls of the mould and to grow inwards towards the center of the casting. During the solidification from the melting process, the grain refinement can be achieved in different way: by promoting the formation of several new nuclei for grain growth, or else, by incorporating in the melt additives that decrease the rates of grain boundary migration and the rates of growth of grains once nuclei have been formed.

Different mechanisms are used to retard the grain growth, as cold pouring, mould vibration and agitation, gas-melting. It is known in the industrial world that the dimension of the grain obtained by gas-melting processes are smaller than in the induction-melted alloys. Depending on the absorption of impurities such, for example, carbon-containing gases [31].

To consider the homogeneous nucleation in the gold alloys, the formation of nuclei must depend on the segregation of particular additives during solidification phase. The suitable elements for this purpose are characterized by a high melting point and low solubility, such as iridium, ruthenium, molybdenum, tungsten and cobalt. The required concentration of additive depends on alloy composition and, usually, within the range between 50 and 1000 ppm. Higher presence of these elements in the composition could be detrimental, causing the formation of clusters or segregation, which reduce the refinement effect, and degrading the surface finishing of the items. Other problems, directly linked to the excessive concentration of grain refiners or the incorrect control of temperatures, which led to the formation of coarse particles, arise in the re-melting of scrap. Therefore, the homogeneous nucleation is a refining method useful for jewelry applications only if well-defined and controlled.

Other additives, which can be used to ensure a fine grain size, during solidification, are alkaline and rare hearth elements, as calcium, yttrium, barium or nonmetals like boron [31].

3.2.2 Recrystallization during Annealing and after Cold-Working

During deformation processes such as swaging, hammering, sheet rolling or wire drawing, the microstructure of metal alloys is heavily deformed with a reduction of the ductility to lower levels. The material becomes progressively harder and more difficult to work, as lattice defects increase in number. To restore the initial malleability of the gold alloys, an annealing process is required, in

order to soften the material and allow further deformation steps. The characteristics of the new structure, resulted from the recrystallization, depend on the parameters of the heating treatment and on the previous deformation performed. The value of deformation is very important to define the capability to recrystallize during annealing treatment, if the deformation produced is too small (about 20% e.g.), then the energy stored in the form of lattice defects may be insufficient to promote complete recrystallization of the metal. Usually, it is recommended to achieve between 40 ÷ 50% deformation in the as-cast product and about 70% in the annealed, before heating treatment.

The main mechanisms that cause the grain refinement during the annealing are: the increase of number of recrystallization nuclei and the decrease of grain growth velocity. The additives submitted before can promote also the formation of nuclei, by themselves or reacting with other grain refiner or impurities (generating inhomogeneities). These areas are energetically favorable for the nucleation phase but, if this mechanism is not adequately controlled, occurs an undesirable growth of a few number of preferentially formed nuclei. It is well known that, a fine-grained recrystallized microstructure is not stable and tends to achieve its minimum internal energy by different coarsen mechanisms during excessive annealing treatments.

The classic manifestation of coarse grain size in gold alloys is the 'orange peel' effect. This is characterized by the development during deformation of the material of a surface appearance similar to that of an orange skin. It results from a shifting of individual coarse grains relative to one another, in extreme cases to such an extent that the grain boundaries become apparent to the naked eye. Orange peel effects call for extra work in polishing or re-polishing of final products and this may result in excessive wear of tools and in loss of alloy [31].

For these reasons, the control of the annealing conditions (time, temperature, etc.) become increasingly important in industrial processes. In gold alloys, the addition of particular elements reduce the grain boundaries mobility, slowing down the kinetics both of the recrystallization and of grain growth, due to their diffusion processes. The foreign atoms' rate of migration controls the migration velocity of the grain boundaries, this interaction is negligible at low concentration and high temperatures. Accordingly, the grain boundaries move fast and the grain growth is not restricted. Increasing the concentration of grain refiner, however, the interaction becomes important causing a decrease of recrystallization rate and an increase of the alloy's recrystallization temperature. This effect increases comparably with the difference in atomic size between foreign and host atom [32].

Besides, other particles like oxides and intermetallic compounds can stabilize the grain boundaries, decreasing the velocity of grain growth, directly linked on these particles size and distribution.

In this process, the most important parameter is the recrystallization temperature, defined as the temperature at which we have the 50% of the material's recrystallization by 30 minutes annealing treatment after 90% deformation. Regarding jewelry applications, a scientific study showed that cobalt, zirconium and barium are very efficient grain refiners during recrystallization phase [33]. Cobalt, today, is probably the most used elements as grain refiner, in a range of 0.1 ÷ 0.5%, that become lower abreast with the gold caratage due to the reduction of solubility in the alloy.

3.3 STRENGTH AND DUCTILITY [48]

3.3.1 Mechanisms

The movement of dislocations, lattice defects, that causes the sliding of crystal planes of the structure, characterizes the deformation of the metals. The movement of these defects become more difficult with the increase of number of distortions, or various obstacles, presented in the crystal structure. This leads to a reduction in malleability of the gold alloys and an increase in hardness.

The as-cast state and, specially, the annealed state of pure gold are characterized by a very low hardness of 20 ÷ 30 HV and a deformability over 90% before ruptures. Fig. 3.4 showed the variation of hardness depending on the element added and its concentration in weight %, an overview of the influence of alloying addition and impurities on this property.

The main strengthening mechanisms valid for gold alloys, and other metals, are:

- ***Precipitation hardening***: mechanism of precipitation, with the decrease of the temperature, of dispersed particles by specific heat treatments. The solubility of the elements is very important and, lead to the formation of particular alloying elements or intermetallic compounds.

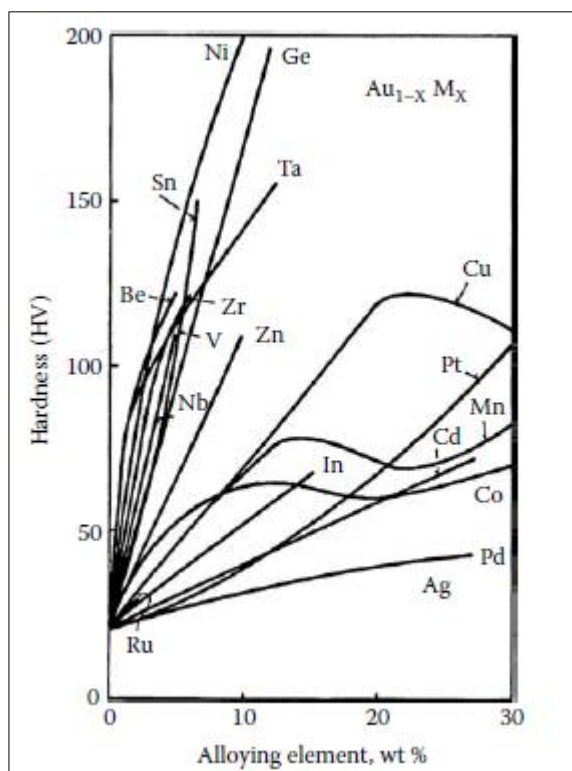


Fig. 3.4 – Overview of binary gold alloys hardness depending on type and amount of addition in weight [48]

- Solid solution hardening: the atoms of the alloying elements can modify the structure of the crystal lattice. If their size is much smaller than the gold atoms, they occupy the gaps between them; otherwise, they occupy the same sites of the gold atoms. The first case is called interstitial solid solution hardening, the second, instead, substitutional solid solution hardening.
- Disorder-order solid transformation hardening: with the lowering of temperatures, specific sites of the crystal lattice are occupied by different atoms, creating an ordered solid solution. This happens, usually, for well-defined alloys in the range of stoichiometric. The need to preserve the ordered state causes an increase in hardness and strength of the gold alloy, due to the elastic distortion and the difficulty of dislocations movement.

All these processes are reversible, using a homogenization heat treatment, unlike the following:

- Dispersion hardening: the reaction of the oxygen (or carbon, etc.) with the alloying elements generates the irreversible formation of dispersed particles.

In the industrial production world, great importance for the control of the semi-finished product properties, are the two mechanisms:

- Work hardening: this effect depends on the type and amount of alloying elements; the dislocations present within the crystal lattice react with these and each other. During the plastic deformation, the number of dislocations is increased by these reactions with not negligible strengthening of the gold alloy.
- Grain size control: as previously established, the grain boundaries are, effectively, obstacles to the movement of dislocations. The use of grain refiners, as stated by the Hall-Petch law, contributes to increase the strength of the material. This is, also, the unique mechanism that at the same time avoids the degradation of ductility and machinability of the material.

These two final mechanisms of hardening have particular importance for the optimization of sheets, rods and wires production cycle. The combination of alloying additions, plastic deformations and annealing treatments is decisive to define the grades of recrystallization of the microstructure, and the material's properties desired for every single step.

3.3.2 Precipitation Hardening

The base of this phenomenon is the reduction of the solubility in bulk gold of various elements added, such as Co, Fe, Mn, Ni, Pt, V and others. The characteristic of the phases generated depend on the composition of the alloy, for example considering binary gold alloys:

- In alloy systems like Au-Ti (figure 3.5) and others, with a low solubility in gold, solid solution phase exists at high temperature but, decreasing the temperature, a miscibility gap develops with the formation of various intermetallic phases
- In alloy systems like Au-Co (figure 3.6) or Au-Cr with a limited solubility, the miscibility gap extends up to the solidus lines (like above described)
- In alloy systems like Au-Ni (figure 3.7) or Au-Co, characterized by a complete series of solid solutions at high temperature, the miscibility decreases with the temperature.

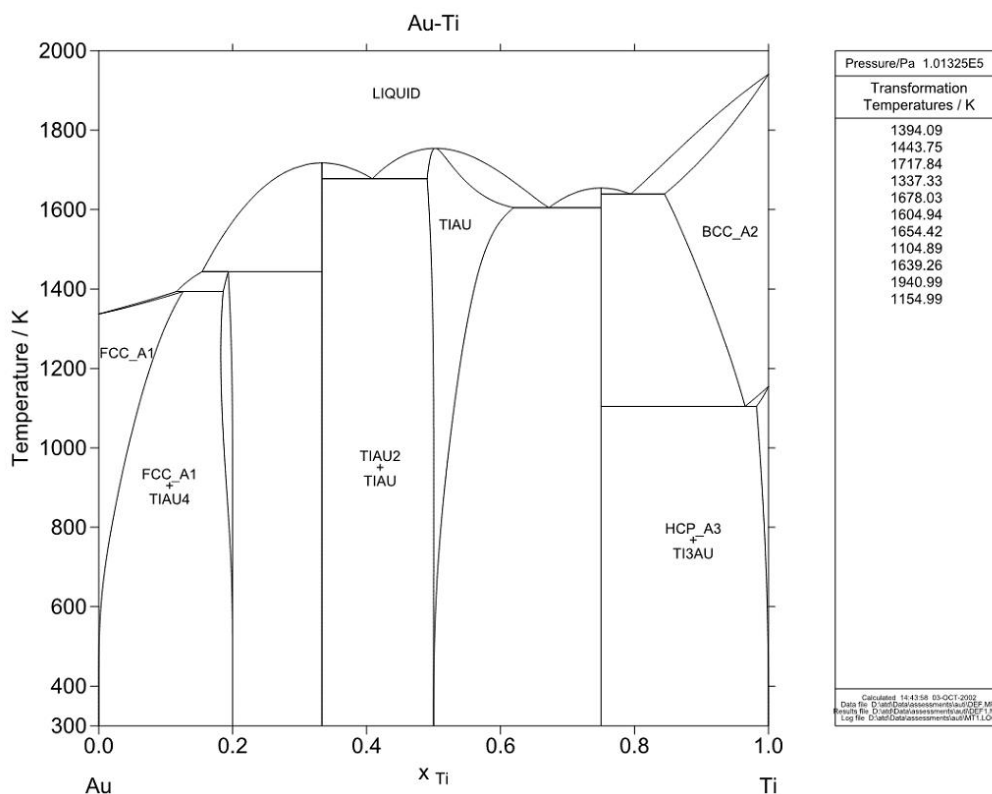


Fig. 3.5 – Binary phase diagram Au-Ti (MTDATA – Phase Diagram Software from the National Physical Laboratory)

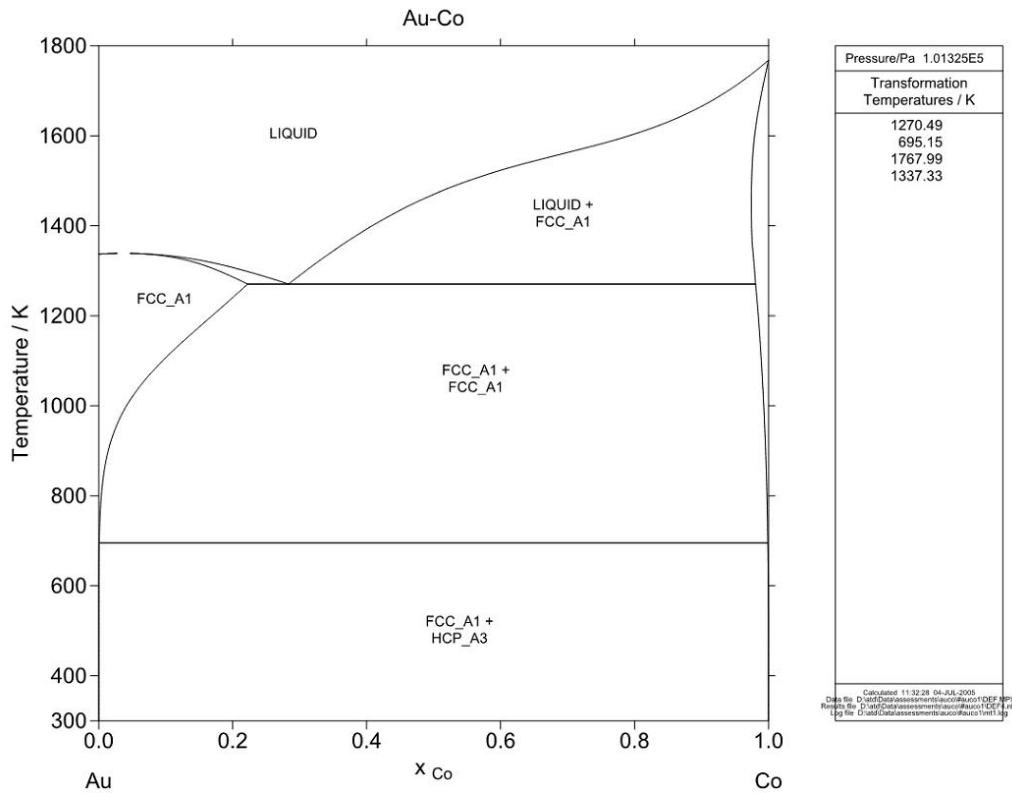


Fig. 3.6 – Binary phase diagram Au-Co (MTDATA – Phase Diagram Software from the National Physical Laboratory)

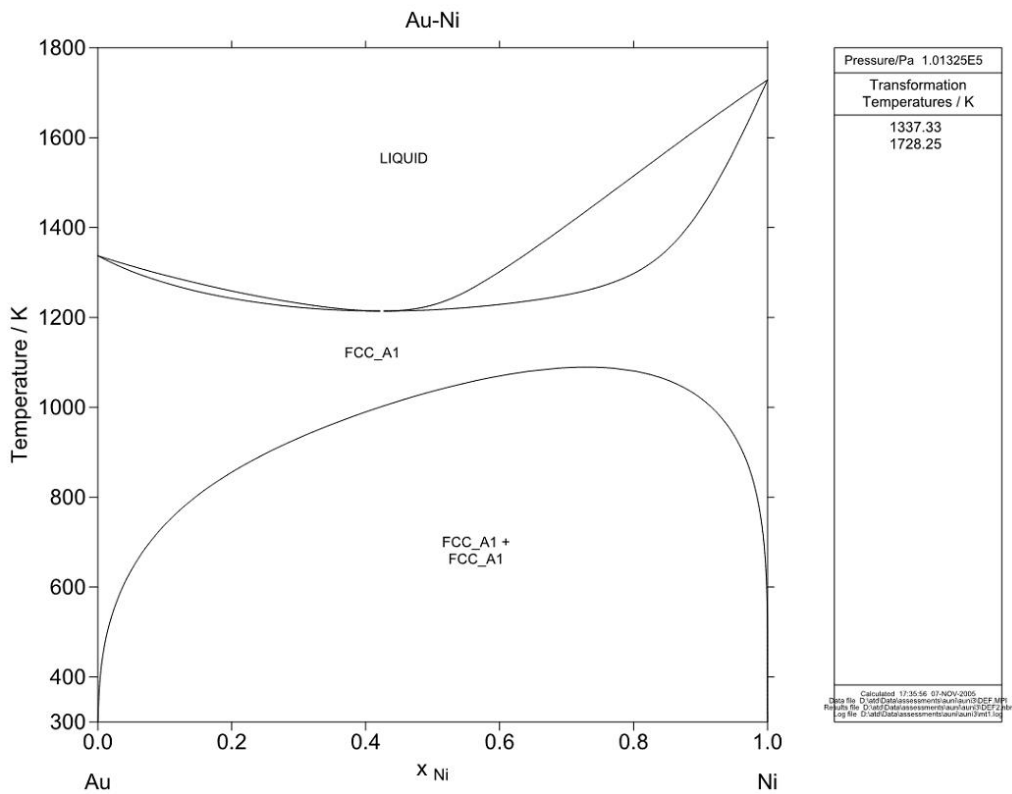


Fig. 3.7 – Binary phase diagram Au-Ni (MTDATA – Phase Diagram Software from the National Physical Laboratory)

This occurs, logically, also in ternary and higher order systems. However, to ensure a valid and pronounced age hardening of the material, a specific treatment should be used:

- Solution annealing (homogenization), typically between 700 °C and 900 °C, considering the example reported before, for a suitable time depending on the alloy composition and on the product dimensions. In this way, the alloying elements are again dissolved in the gold matrix,
- Exploiting a rapid quenching, into water, from the previous temperatures, in order to suppress the precipitation of the particles. A supersaturated solid solution is generated.
- Final age hardening treatment, usually between 200°C and 400°C, for a defined time, which depends by the alloy composition and other production factors.

The nature of particles that precipitates and cause the hardening of the material can be different, for example:

- ❖ An intermetallic phase, constituted by a compound of the alloying elements and the gold atoms
- ❖ An almost pure metal compound, usually linked to the low solubility of the element (especially grain refiner)
- ❖ Another phase enriched with the foreign element, e.g. Ni-rich phase (fig. 3.7)

Several studies on this phenomenon have demonstrated that during the age hardening treatments, some characteristics of the precipitates change comparably with the aging time. The variation of the volume fraction, the shape, the composition, the microstructure and sizes of gold alloys could lead to a hardening effect divided into different stages.

With the progress of the process, increase the risk of an excessive growth and coalescence of the particles precipitated, accompanied by a decrease in hardness. Usually, the precipitates form and grow at grain boundaries (energetically favorite), causing a not ideal and homogenous distributions between these and the grain interiors. The industrial production processes, and their difficult control, show the critical issue of suitable quenching and heat treatments for the gold alloys. The results obtained by the production trials are, too often, very different in comparison with the laboratory tests. The control of the quenching steps is critical for the strengthening effect, a too low cooling from the high temperature of homogenization causes the precipitation of coarse particles. This properties' degradation depends on the gradient generated in the potential for age hardening,

during the process, and could cause different results passing from the surface to the center of the products. In cases where, the risk of formation of precipitates during cooling from the melted state or after annealing treatment is high, is necessary a rapid quenching from higher temperature in order to guarantee the maintaining of the gold alloy workability and machinability.

The great miscibility gap, of the two main alloying element used in gold alloys, Ag and Cu, also extends in the ternary Au-Ag-Cu system. It allows defining specific age-hardening treatments for many alloys used in dental application and jewelry [34], figure 3.8.

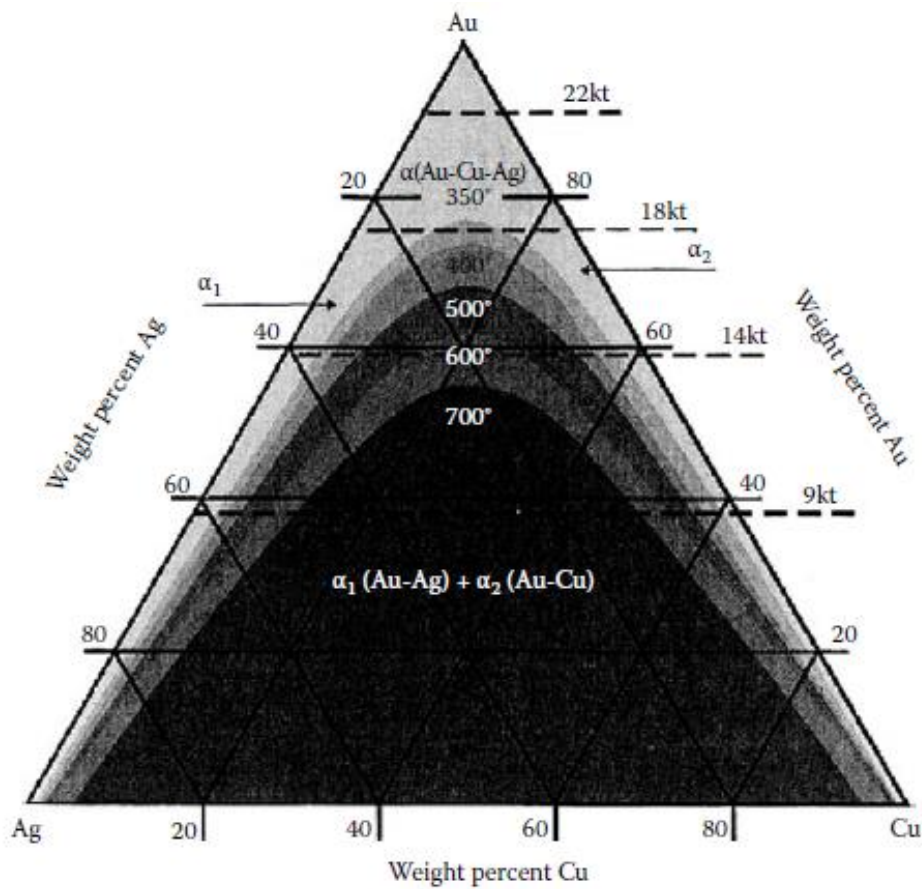


Fig. 3.8 – Projection of extent miscibility gap with temperature in the gold-silver-copper ternary system [47]

In figure 3.9, the influence of the Ag content on the hardness for the Au-Ag-Cu system is showed.

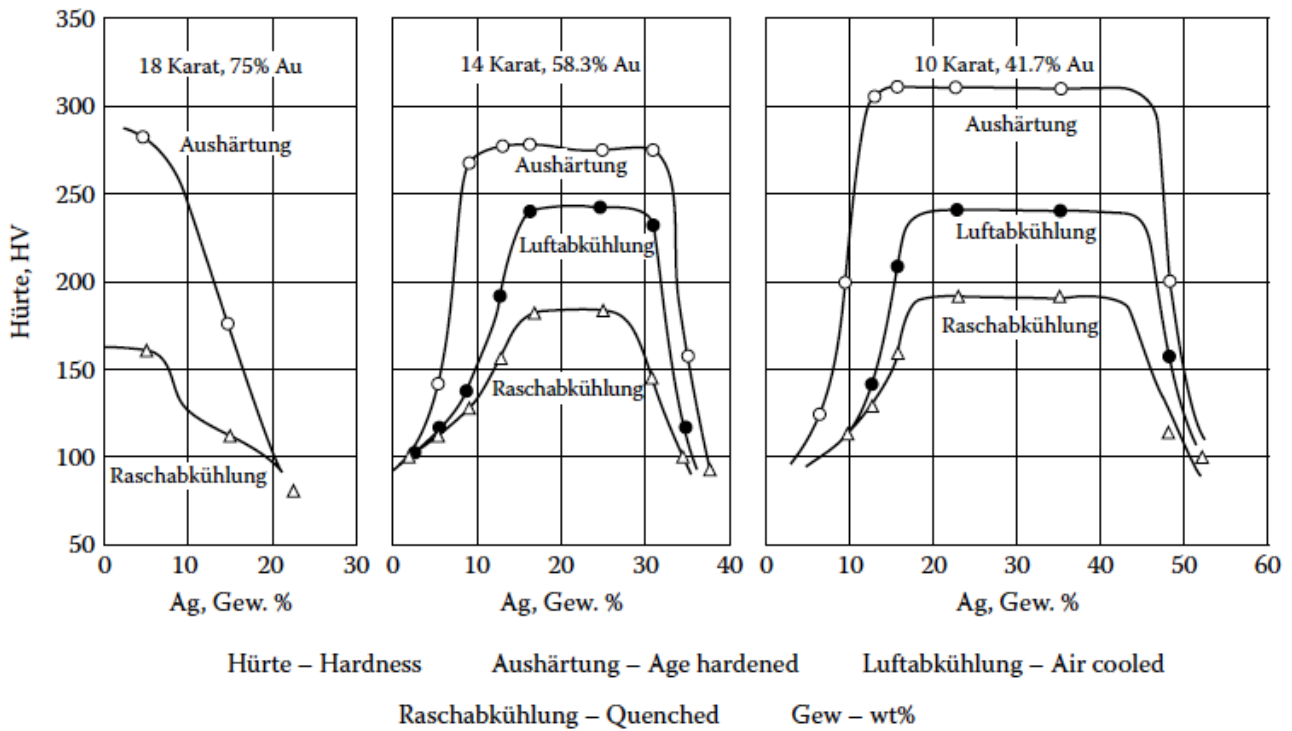


Fig. 3.9 – Influence of Ag (and Cu) content on hardness for age-hardened, aircooled and quenched gold alloys [48]

High values of hardness are achieved for an increasing content of Ag passing from the 14 Kt to 10 Kt gold alloy, respectively about 15 ÷ 30 wt% and 20 ÷ 40 wt%.

The silver, and copper, generate silver- and copper- rich phases' separation with the decrease of temperature from the solid solution state. It is possible to avoid this situation, only using very low concentration of the two elements (~ 5 wt%) or, instead, high (~ 40 wt% for 14 Kt and ~ 50 wt% for 10 Kt) obtaining single-phased alloy by quenching. These alloys can be hardened after, through a suitable heat treatment. For higher Ag content, a significant effect is not observable in this two different gold caratage. Regarding the 18 Kt gold alloy, decreasing the Ag content in the alloy, the hardness proportionally increases.

This is due to the hardening effect caused by the formation, related to the higher stability, of the ordered AuCu solid solution into the Au-Ag-Cu system. In the higher caratage gold alloys, the effects of precipitation and disorder-to-order transformation coexist, but one prevails the other depending by the composition [35].

The other important element added to the ternary system, previously presented, is the zinc. For the 14 Kt, 10 Kt and 9 Kt gold alloys, its amount is higher than 4% due to the necessity of guarantee, primarily, a certain defined color and, secondly, to restrict the volume of the immiscibility gap in these systems. In this way, it is possible to make more workable the gold alloys, though hardened or air-cooled. While the increase of Zn content in 14 Kt and 10 Kt alloys involves the formation of a not hardenable single-phase alloy, in 18 Kt alloys (characterized by medium to high Ag content) causes the increase of hardness, such as other elements: In, Ga, Sn, etc.

Other additions, like metals of the platinum group (Pt, Ru, Ir), increase the values of hardness achieved with the age hardening treatment (up to 330 HV), but at the same time, they are due to formation of dangerous inclusions. Referring to the white gold jewelry alloys, Ni is the most common element added to the composition

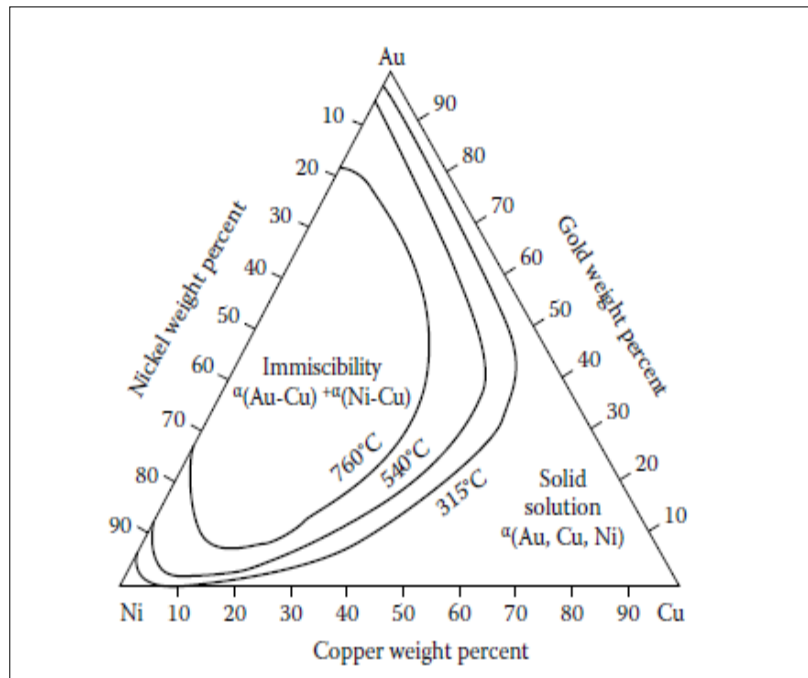


Fig. 3.10 – Miscibility gap depending by temperature in ternary Au-Cu-Ni system, isothermal section projection [47]

to shift color from the traditional yellow to whitish. Passing from the Au-Ni system (figure 3.7) to

Au-Ni-Cu system, the miscibility gap extends much more (fig. 3.10). With a concentration of nickel above ~ 15 wt% in 18 Kt and 14 Kt gold alloys, an increase of hardness occurs during slow cooling due to the formation of different X-rich phases in the material. Increasing, the content of this element and the time of the aging treatment, it is possible to achieve values of hardness closest to 350 HV.

In the industrial applications, anyway, this type of alloys are difficult to work, especially producing sheets or wires. Considering, instead, the Au-Ag-Pd system (18 Kt white gold alloys), the addition of Ni increase the possibility of age hardening, after heat treatment, to these relatively soft alloys.

In the binary Au-Pt system, with a content of Pt higher than 15 wt%, an age hardening treatment can shift the value of hardness from about 120 HV to 300 HV; and for a 50% Au – 50 % Pt balanced alloy, the hardness can increase up to 400 HV due to a precipitation of Pt-rich particles.

Usually, Au-Pt-Pd based alloys are used for dental application. In this alloys the miscibility gap extends significantly in comparison with the binary Au-Pt system and, as low as ~6 wt% Pt, they are age hardenable [36].

The highest caratage gold alloys, such as 22 Kt or 24 Kt, are difficult to use for the creation of plastic deformation jewelry, due to their very low hardness. For this reason, the research into precipitation hardenable alloys has been greatly developed, in recent years. Titanium was identified as the element with the best behavior for this purpose, a 990 gold alloy with a 1 wt% content of Ti can be age hardened till a value of hardness close to 170 HV. The process includes a solution annealing followed by aging at 500 °C for 1 h, figure 3.11 [37].

The enhanced hardening is due to the formation of fine Au_4Ti precipitates under the appropriate thermo-mechanical treatments. It has been shown that another hardening mechanism can be induced in wire having a diameter of less than 100 μm , which is stable to heating in air up to 200 °C. These observations are consistent with the formation of a network of titanium oxide inclusions up to 100 μm below the free surface [38]. The high reactivity of the Ti with oxygen, nitrogen and carbon, limits its use in jewelry production but, with a small increase in its content and the introduction of Ir as grain refiner, some gold alloy compositions were developed and used in dental sector.

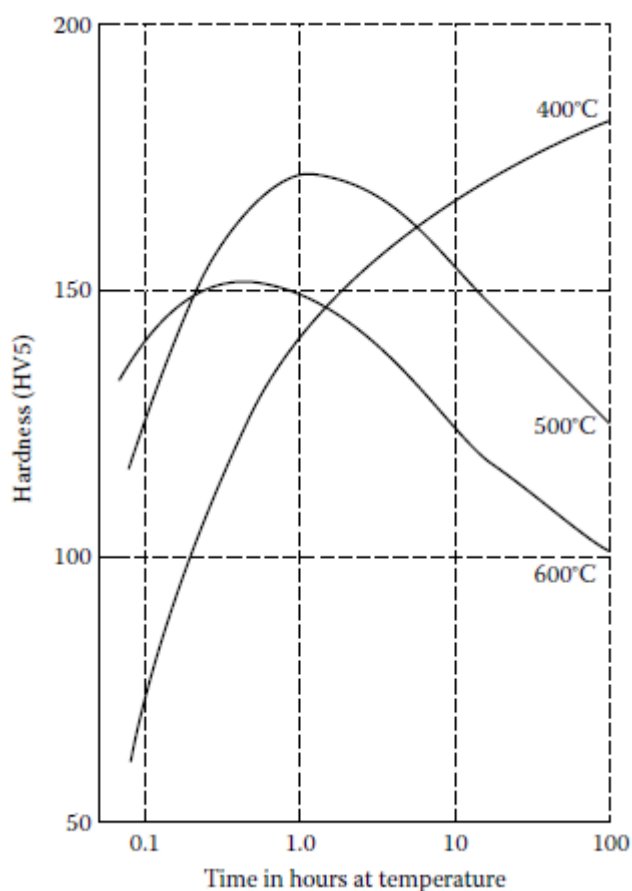


Fig. 3.11 - 990 Au-Ti alloy, age-hardening potential [37]

Exist several studies on the possibility to increase the hardness values not only for the 990 gold alloy, but also for the 995 gold alloys. The addition of particular elements like Co and Sb, allow improving the machinability properties of this alloys, introducing their use in the jewelry manufacturing. The alloy has a colour virtually identical to that of pure gold, and can be hardened to a peak hardness of ~ 140 HV using a combination of cold work and a low temperature (250 to 300°C) ageing heat treatment. This hardness is comparable to that of cold-worked 22 carat yellow gold, and almost double the maximum hardness that can be obtained in pure gold. The alloy

obtained is highly formable, and is amenable to casting, granulation, re-melting, wire drawing, forming and rolling [39]. The hardening mechanism that overcome, in these high carat gold alloys, is the precipitations of intermetallic compounds, and it is the same mechanism tapped to increase the hardness in the 24 Kt gold alloys using as additive rare-earth, alkaline and alkali metals or light metals.

The precipitation potential of these elements has been studied and the results showed that, only for Yttrium addition below 0.5 wt%, it is possible to achieve a notable hardening of the material.

For all the others elements the content must be higher. The age hardening treatment generates the precipitation of gold-rich compounds such as Au_4RE (for Er, Tm, Yb, Lu, Sc), Au_5RE (for Eu) and Au_6RE (for La, Ce, Pr, Pm, Sm, Nd, Tb, etc.). The solid solution strengthening effect of trace elements in gold is related to two factors. The first is the ratio of the atomic weight of gold to that of the alloying element. It is approximately directly proportional to the ratio of the numbers of gold and solute atoms at a particular weight percentage. The second factor is the relative difference in atom size between the alloying element and gold. It is proportional to the amount of lattice distortion caused by the presence of the solute atom. The alloying behaviour of the RE metals with gold is characterized by the formation of a series of eutectic reactions and limited terminal solid solubility [40]. The maximum solid solubilities of RE metals in gold increase as the lanthanide contraction becomes larger (ie the atomic radius becomes smaller). Thus, heavy RE metals have higher solid solubilities than light RE metals.

In 22 Kt gold alloys, the precipitation hardening was achieved through the addition of Co and Ni, the formation of new intermetallic compounds allows to increase the hardness up to 250 HV.

The addition, in the dental or jewelry complex gold alloys, of a few percent of elements, such as Sn, Ga, In or Zn, in order to reduce the melting point and increase the fluidity and wettability of the metal alloy, causes the strengthening of the products. Various thermodynamic modeling software are used to define age-hardening phenomena occurring in complex gold alloys, with five or more alloying elements, and to calculate the stability of the precipitated phases. The comparison of experimental results with thermodynamic stability calculations shows good correlation for the gold alloys evaluated. The interpretation of the experimental results with the help of the calculations leads to a reduction of the experimental work required to develop new alloy systems with specific properties [41].

3.3.3 Solid Solution Hardening

In the Au-Ag-Cu ternary system, the base of the common jewelry alloys, the value of hardness is strictly linked to the Ag-Cu ratio. Introducing alloying elements in the composition, the effect of solid solution hardening increases with the number of lattice distortions and with the atomic size difference between the precious metal and the added element. The dimension of Ag atoms are similar to the Au atoms, instead Cu atoms are ~ 12% smaller than Au atoms, and hence the effect of strengthening is higher for this element (substitutional solid solution). However, Cu is not completely soluble in Au, but only at temperatures higher than 410 °C, unlike Ag that is soluble at all temperatures. The formation, under 410 °C of intermetallic Au-Cu phases will be treated after. Pt and Pd are both completely soluble in Au at high temperatures, and are used in large amounts, over 15 ÷ 20%, for dental or white jewelry applications. These alloys need to be hardened by other mechanisms, because the solid solution hardening effect is too small. The addition of conventional base metals to gold alloys influences the mechanical properties of the material, through substitutional solid solution hardening, only for amounts above ~ 0.5 wt% [42]. For example, the influence of Co, Fe, Ni and Sb in 22 Kt gold yellow alloys (Ag:Cu = 1:1), is showed in figure 3.12.

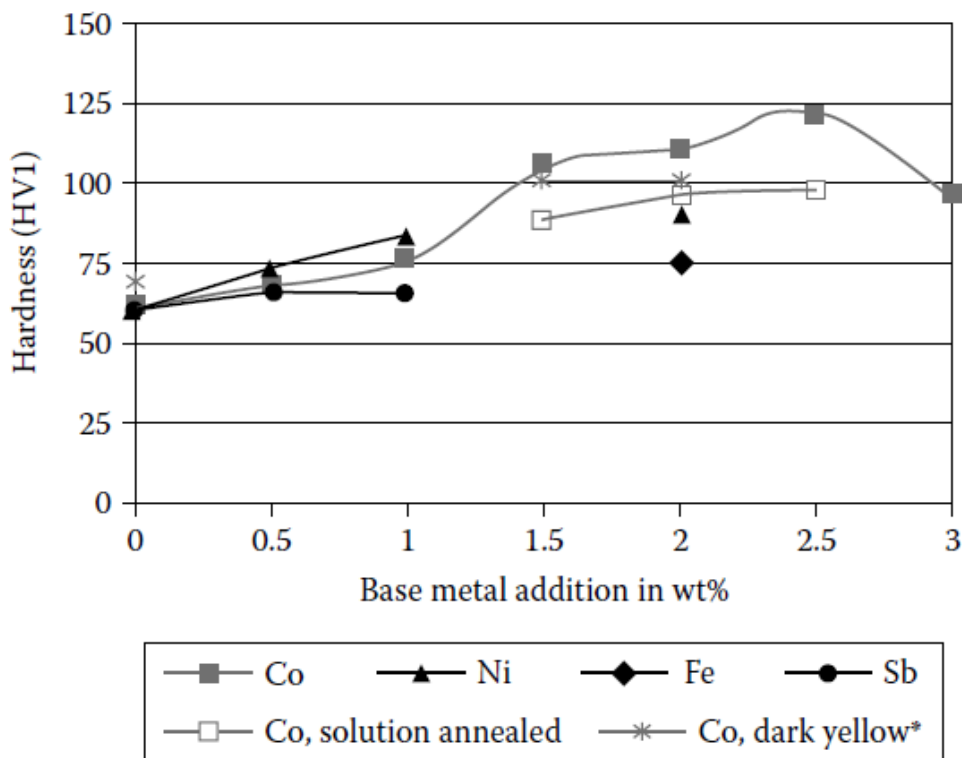


Fig. 3.12 – Influence of base metal additions on as-cast 22 Kt Au hardness values [42]

While, in white gold alloys, the use of Ni in content up to 15 wt% leads to strengthening mainly due to precipitation hardening mechanisms, instead small base metal additions (Zn, Sn, In, etc.) contribute to increase the hardness of the material by, in part, solid solution hardening.

The only valid approach, which allows to distinguish the contributions of the different effects, provides the homogenization of all the samples and the direct comparison between the quenched and the aged samples, after the solution annealing.

The larger difference in the atomic size between the rare-earth metals and gold atoms, gives to these elements a not negligible potential for substitutional solid solution hardening.

The low solubilities in gold of microalloying additions, generally, limits the solid solution strengthening effect due to the formation of eutectics that segregate and accumulate at grain boundaries during solidification. These segregated phases are undesired due to their embrittling effect [40].

In the jewelry industry, the additions of these elements are strongly controlled due to their tendency to oxidation. The processes are optimized in order to reduce the loss of microalloying additions, and the degradation of the material produced. In fact, the maintaining of the quality of the production scrap is important because, usually, is internally recycled for subsequent production lots.

3.3.4 Dispersion Hardening

At high temperatures, the precipitation hardening and disorder-to-order transformation, are not able to strengthening the material due to the reversibility of these mechanisms. Instead, using a mechanism based on the dispersion of fine particles (oxide, carbides and other stable compounds), it is possible to increase the strength of the gold alloy at high temperature. In particular, this type of hardening mechanism is irreversible. The method arrests dislocation migration under mechanical stress while building up thermally stable dislocation systems by the addition of extremely small extraneous particles, usually of an oxidic nature, of great thermodynamic stability. The diameter and distance apart of the dispersed particles combined with their distribution in the matrix are the decisive factors for the degree of hardness that can be obtained. Regarding the distribution and the dimension of the particles, the internal oxidation of the alloy can be achieved through the addition of elements with high enthalpy towards a stable oxide. For example an addition of ~ 0.4 wt% of TiO₂ particles, characterized by a diameter of 0.5 μm, causes a greater increase of strength [43]. The dispersion hardening mechanism can be achieved also, mixing gold with powder of cerium, aluminum or yttrium oxides. These particles are stable, in comparison to precipitates, but this method generally leads to inhomogeneous distribution of the dispersed elements.

3.3.5 Disorder-order Transformation Hardening

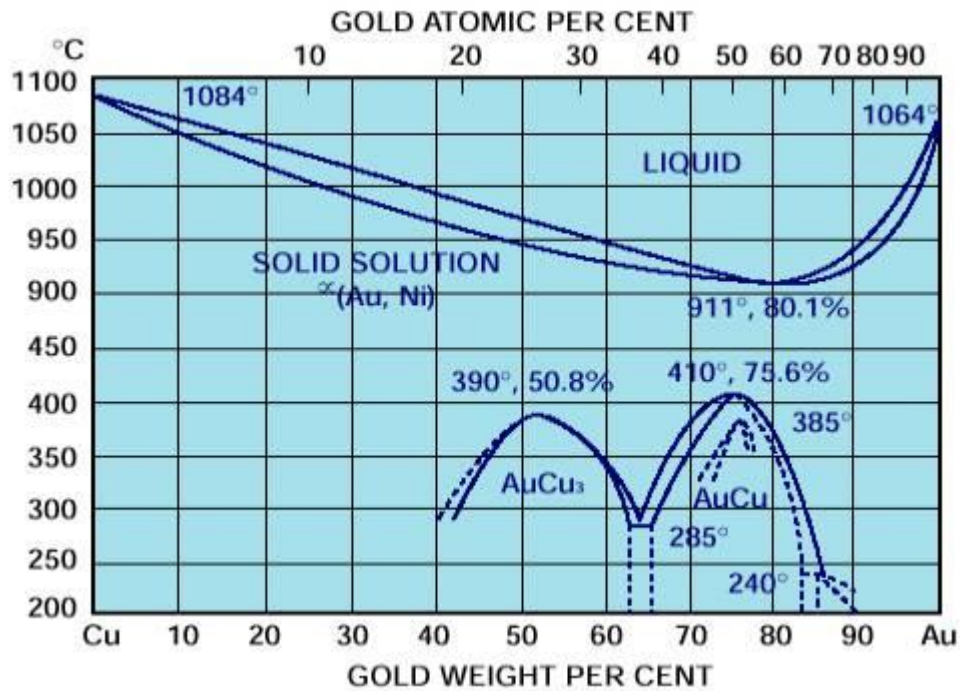


Fig. 3.13 - Binary phase diagram Au-Cu

The binary Au-Cu system (figure 3.13), is characterized by the formation of the ordered solid solutions AuCu and AuCu₃ (crystallographic structure) below defined temperature. This solid transformation from a disordered state to an ordered one is very important for the strengthening of Cu containing gold jewelry alloys.

Above 410 °C, independent on the content of Cu, the solid solution is disordered and the atoms occupy randomly the positions in a face centered cubic lattice, while at lower temperatures the equilibrium state is complicated.

Below 385 °C the stable arrangement for the alloy is a face centered tetragonal (f.c.t.) lattice, AuCuI, in which gold and copper atoms occupy (002) alternate planes, as is showed in figure 3.14.

This distribution of the atoms, considering the difference in the atomic radii, causes a distorsion of the lattice from f.c.c. to f.c.t. When the AuCuI ordering proceeds in the alloy, a considerable amount of strain associated with the change in crystal symmetry may develop in the surrounding matrix. A binary AuCu alloy shows an increase in hardness upon ageing at 200 °C but, after longer ageing periods, a softening began in the material [44]. At the beginning, the initial strain associated with the development of small tetragonally domains, leads to substantial hardening.

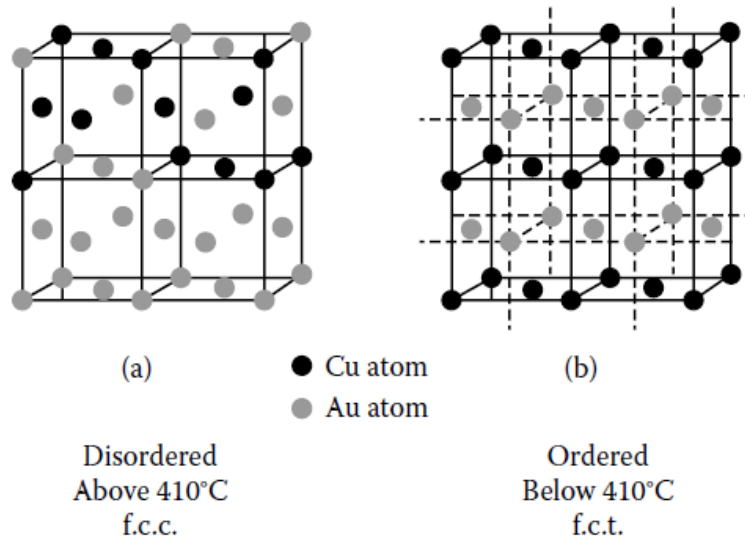


Fig. 3.14 – (a) Disordered crystallographic structure f.c.c. AuCu alloy, (b) ordered crystallographic structure f.c.t. AuCuI phase [48]

As the ordered domains grow larger, the strain field in the matrix becomes too great to be accommodated simply by a distortion of the lattice planes. When this happens, the strain field is released by the occurrence of twinning. Thus, the softening effect after prolonged ageing in the binary alloy is due to twinning [45].

Between 385 °C and 410 °C, an orthorhombic structure, defined AuCuII, being stable.

Figure 3.15 shows the crystallographic unit cell of AuCuII, which may be thought of as consisting of 10 AuCu I tetragonal unit cells placed side by side in the b-direction, with the content of (001) planes changed from all gold atoms to all copper atoms halfway along the new long cell. Thus, the structure is subdivided into domains with adjacent domains being in antiphase. The antiphase domain boundaries are parallel to the [100] direction and have a periodicity of five unit cells along the b-axis [46].

The addition of zinc, such as aluminum, tin, gallium, indium, manganese to the equiatomic AuCu causes a decrease in domain size of the AuCuII phase; whereas, the addition of silver, palladium, nickel or germanium causes an increase of the domain size. This effect becomes more and more significant as the concentration of the elements added.

All this occurs in the composition range where the atomic ratio of gold to copper atoms equals 1:1. Instead, when the atomic ratio is close to 1:3, two versions of AuCu₃ I+II of another ordered face centered phase form (L1₂-structure: Cu atoms on lattice faces, Au atoms on lattice edges).

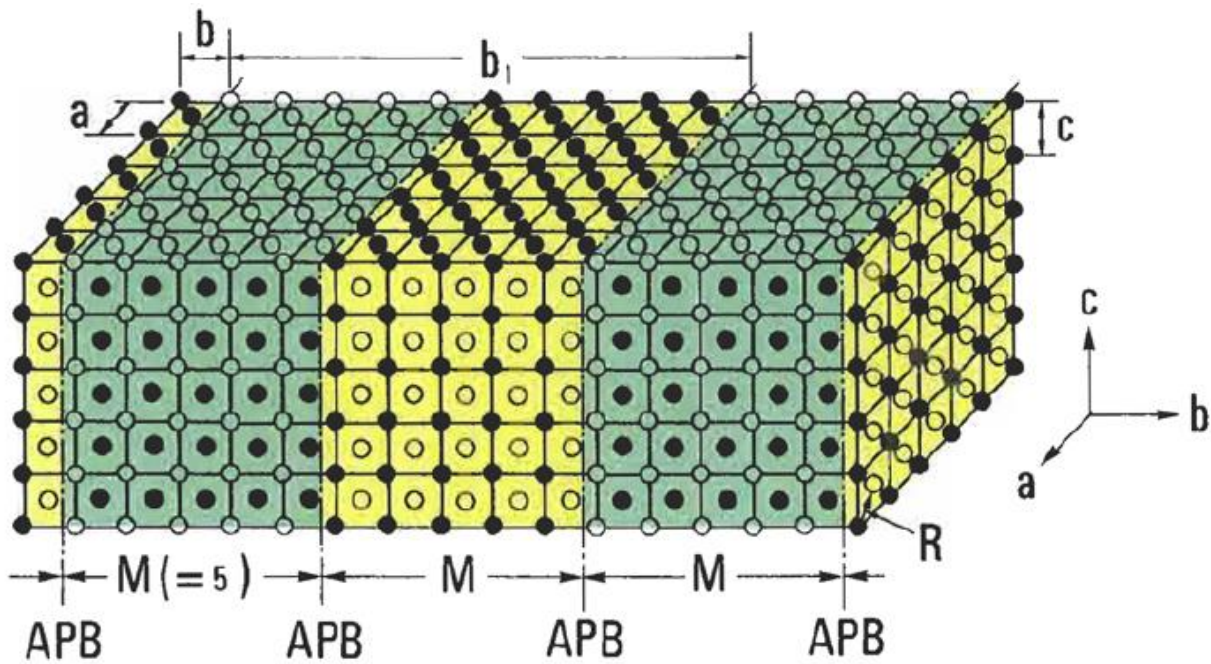


Fig. 3.15 – Example of the structure of antiphase domain boundaries in the AuCuII superlattice. The solid circles are copper atoms, while, the open circles are gold atoms [46]

This hardening mechanism, by solid transformation in the Au-Cu system, is an important characteristic for many gold alloys use in jewelry or dental applications [47]. The disorder-to-order transformation is obtained in different way, by aging between 150 °C and 400 °C or by slow cooling from high temperatures. If the aging treatment is too prolonged, a decrease in hardness of the material is observed due to a greater hardening effect generated by a partially ordered state in comparison to a fully ordered state (“overaging effect”). A binary Au-Cu alloy containing 25 wt% Cu, can be strengthened to ~ 350 HV starting from as-cast hardness of 165 HV, with an increase of ~ 300 N/mm² in tensile strength (figure 3.16). On the other hand, however, the ductility and the tensile elongation drop to the minimum values. In the industrial jewelry processes, usually, it is preferable to avoid this transformation, during the plastic deformation steps, by rapid cooling from elevated temperatures.

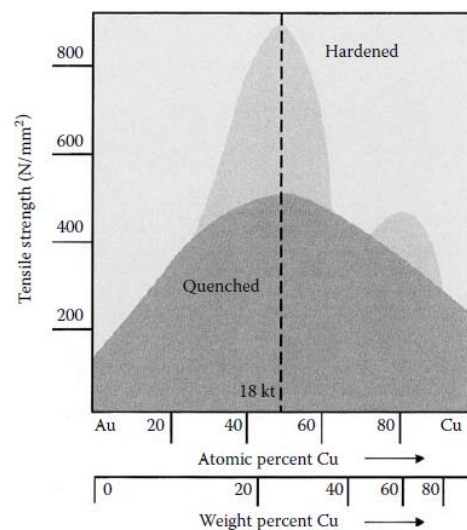


Fig. 3.16 – Tensile strength trend of Au-Cu alloys depending on heat treatments [47]

The disorder-to-order hardening mechanism prevails in Cu-rich 18 Kt gold jewelry alloys, due to the extension of the ordered phases into the ternary system. The precipitation hardening overcomes, in Au-Cu-Ag based dental alloys, only for high Ag content. In the Au-Cd and Au-Zn systems, the martensitic transformations, related to the ordering phenomenon, increase the strength of the alloy and are important for shape memory applications.

3.4 COLOR OF GOLD ALLOYS [48]

3.4.1. Yellow to Reddish, Greenish and Whitish

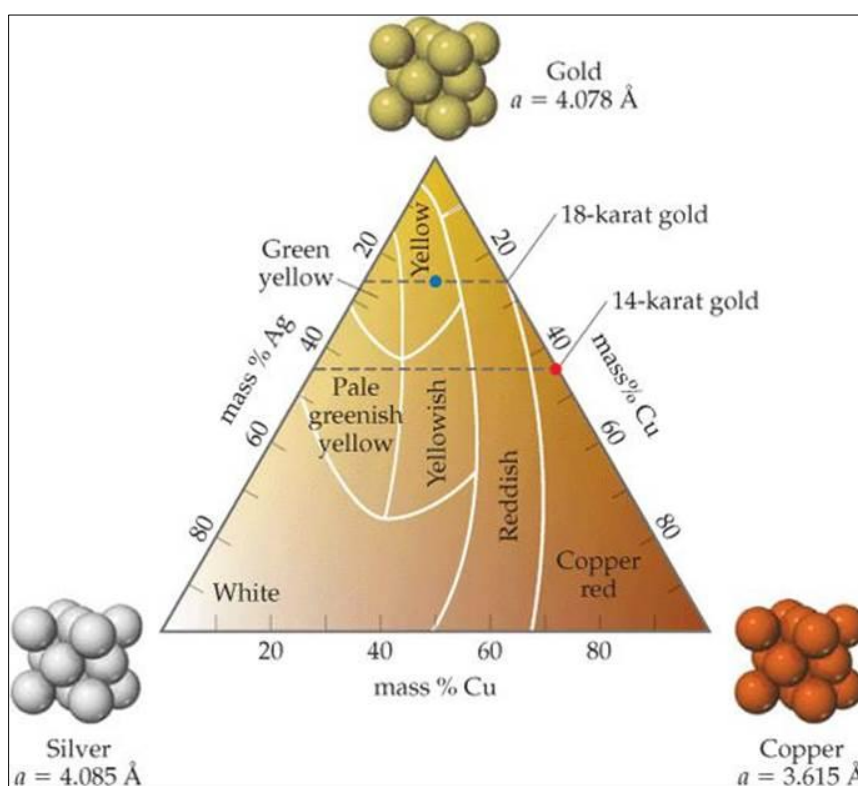


Fig. 3.17 - Color variations in the ternary Au-Ag-Cu system

All the pure metals appear white or grayish, except gold and copper that are characterized by respectively, a yellow and a red color. Regarding the particular reflectivity of gold, see chapter 2.4. With the addition of copper to pure gold, the drop in the reflectivity curve shifts toward the low-energy part of the visible spectrum. The color moves from the traditional yellow, to a deeper yellow to reddish hue.

Adding Ag, instead, the drop in the reflectivity curve moves to the high-energy end of the visible spectrum or, also, the addition of nickel, palladium and platinum, results in a flattening of the

reflectivity curve. Controlling the addition of the various elements, the color of gold alloys can be modified generating a huge range of different coloration dependent on the caratage of the alloys, figure 3.17. For example, the addition of zinc to the main alloying elements, Ag and Cu, shifts Cu-rich phase color from reddish to dark yellow.

In order to make easier the qualitative color characterization and comparison, defined range of composition and color was developed and distributed, besides, other methods for quantitative color measurement was improved and applied [49].

3.4.2 White Gold

For the lower carat gold alloys (8 Kt and 9 Kt), the whitish color is achieved using very high Ag contents while, for the higher caratage, Ni and Pd are the most common elements added to the gold alloys. They are introduced as lower-cost alternative to platinum jewelry, despite Ni has problems related to skin allergy and Pd remains a quite expensive elements to use in large amounts [50].

The most common systems used for the base of these alloys are the Au-Ni-Ag-Zn or Au-Pd-Ag-Zn systems, Cu is introduced only for guarantee a little improve in workability.

The Pd - based white gold alloys are characterized by a more grayish – white color, in comparison to the Ni – based alloys recognized for the cold white color. The behavior of these two white gold alloys, during the industrial processing, is substantially different. The Pd – based alloys are difficult to melt, due to the high melting point of this element and the high reactivity with crucible and mould's graphite, but are quite soft and workable. Whereas the Ni – based white gold alloys, are easy to cast but are characterized by higher values of hardness with a decrease in workability.

As mentioned before, the European legislation and the attention for skin allergies, for Ni, and the much expensive use of Pd, restricting the addition of these elements in jewelry alloys. Owing to these limits, a large variety of white gold alloys made with other elements, such as Co, Mn, Fe, Ga and Cr, are developed [51]. However, probably due to the poor white color or the degradation of the working properties of these new alloys, the use of the common alloys with a reduction in addition of Ni and Pd remains widespread. Only for particular fields of application, or high quality sectors, alloys with high content of Pd (with the addition, further, of Ni and Pt) are used in order to guarantee a suitable whiteness [52].

The presence of white gold alloys with high differences in the base color leads to the definition of the reference color, based on yellowness index. Nowadays, a galvanic process with rhodium is used to plate all the white gold jewelry produced, in order to achieve a brilliant white color of surface. This coating, however, covers the real, too often poor, color of the base material. This standard

index allows to divide the white gold alloys in different categories: premium, standard, off-white and non-white).

The dental sector represents an exception, because the use of high content of Pd and Pt is used not to bring out the color, but to increase the melting point making viable the ceramic firing process without degrading the properties of the metal part.

The additions to these dental alloys, of base metal such Zn, Sn, In and Ga (from 0.1 to 3 wt%), are used in order to improve the investment casting properties.

3.4.3 Special Color of Gold

The whole color spectrum can be obtained as result from optical interference between the light and the nature or the thickness of coating applied to gold alloys. Special colors can be realized by the formation of particular oxides (or other material layers) on the surface of the products, using chemical or thermal treatments [53]. The possibility of varying color or reproducing a large number of shades is important for jewelry application. However, this approach leads to a coating characterized by a low wear resistance, a discoloration in short time and some difficult in process realization, due to the use of particular alloys (as base for the oxide formation) rich in Co, Cr, Fe or Mn content.

Some special color, like purple and blue, are obtained alloying gold with other metals, respecting a well-defined stoichiometric composition. The particular color derived from the precipitation of intermetallic compounds with particular electron band structures. An absorption for particular range of the light occurs, while all the rest is reflected. These intermetallic compounds are respectively, AuAl₂ for the purple color, AuIn₂ and AuGa₂ for the blue color.

The best known among these compounds is AuAl₂, which is formed at 79 wt% Au and 21 wt% Al. The melting point of this compound is higher than its constituents, indicating its higher thermodynamic stability. The purple colour do not change for content of Al higher than 15wt% [54]. However, this phase is the final equilibrium phase. In fact, Au₂Al and Au₅Al₂ form first in the binary system [16]. This intermetallic form, however, is characterized by an intrinsic brittleness that limits its use. In order to avoid the problem of fragility, several alternative manufacturing process and alloy additions were investigated [53]. The introduction of ~ 3 wt% of Pd, Ni or Cu, for example, increase the workability of the gold alloy probably due to the formation of ductile second phases. It was demonstrated that, a rapid quenching and the addition of a little content of Si+Co into the gold alloy, reduces the grain size of two order of magnitude (reaching ~ 5 μm), with a change from brittle to ductile of the fracture [55].

The ternary system Au-Al-Cu for 18 Kt gold alloy, its mechanical properties and color trends are were studied in detail [56].

Other two metallic compounds that gives a different color to the gold alloys are AuIn₂ and AuGa₂, which show a bluish hue. Both are characterized by a crystal structure similar to the AuAl₂ compound, based on the CaF₂ prototype. The gold-indium intermetallic compound AuIn₂ forms at 46 wt% Au, and AuGa₂ at 58.5 wt% Au. In figure 3.18, the reflectivity as a function of the light energy for the three intermetallic compounds is showed. It falls in the middle of the spectrum and rises again towards

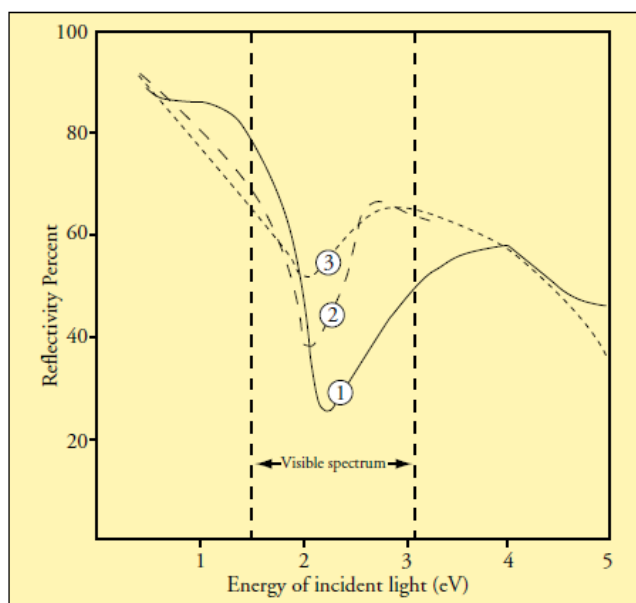


Fig. 3.18 - Reflectivity as a function of energy of the incident light. 1 - AuAl₂, 2 - AuIn₂, 3 - AuGa₂ [16]

defined ranges, resulting in various colors in each case. Microalloying additions improve the mechanical properties of the intermetallic compounds, reducing the fragility of these cubic fluorite structures. The use of alkali metals or light metals in addition to gold alloys generates a list of brittle and unstable compounds. Analyzing the Au-K system, two intermetallic compounds occur: Au₂K (deep green) and Au₅K (violet), while in the Au-Rb system a single colored compound, Au₅Rb (olive green) crystallizes [57]. Other colored intermetallic compounds are reported below:

- Au₇K₄Ge₂, black and lustrous;
- Zintl phases: Li₂AuPb, purple / Li₂AuSn, orange-reddish / Li₂AuTl, greenish / Li₂AuGe, orange, etc. [58];
- MgAuSn, red-purple.

3.4.4 Thermal properties: Wetting, Fluidity and Other

The addition of elements such Zn, Sn, In, Ga, is usually used to guarantee an appropriate behavior during casting, to improve the wettability and the fluidity properties of dental and jewelry gold alloys.

Interfacial tension decreased rapidly with additions of less than 0.5 wt% zinc, but the rate of decrease fell significantly with zinc additions of more than 1.5 wt%.

The addition of zinc, with the reduction of interfacial tension, improves the surface quality of the product [59]. Zn decreases the probability of dendritic surface structure formation, often observed on articles cast in a reducing or inert atmosphere, reducing the roughness of the final surface.

The use of elements with high affinity for oxygen causes the loss of them from the gold alloy to a slag formed, especially, during re-melting or re-casting processes. Establish the proper content of addition is complicated. The use of low-melting elements allows to decrease the liquidus temperatures but, also, the solidus temperatures of alloys, with an increase of the width of the melting range. This increases the risk of segregation during solidification phase, and the formation of low-melting compounds leads to embrittlement during plastic deformation.

P, S, Pb and B generates the same undesired effect.

These elements can give to the alloys many benefits but require a well-defined preparation step, ensuring the suitable distribution of the additions and the right dosage for each application. Usually, nowadays, prepared master alloys are used, containing particular percentage of grain refiners.

The additions of Zn and Si to gold alloys have not a relevant influence on the heat of solidification and on thermal conductivities, while the modifications that these additions generate to the characteristics of the melting range are not negligible.

The differences in melting range and heat of solidification, combined with the various values of thermal conductivities for 18 Kt yellow, red and white gold alloys, can explain the high susceptibility to shrinkage porosity of these alloys.

As seen before, the additions of Zn, In and Sn result necessary for the formation of thin surface layers in metal-ceramic applications, which are the base for a suitable bond between the metal surface and the ceramic [60].

Nowadays, the above constituents are added in large amount in gold soldering and brazing alloys, used in dental and jewelry applications, due to their capability to reduce the surface tension, lowering the melting range and increase the wettability. Only Cd is no longer used because of its high toxicity.

Other elements used, in the industrial applications, are Si, Ge and Sn.

Soldering alloys thus created are based on eutectic compositions, in the binary and ternary systems of these low-melting elements, and are the basis for bulk metallic glass alloys [61].

Several thermodynamic models of multiple component alloys are developed with the aim to study and predict important thermal alloy properties, improving alloys for casting, brazing or soldering and optimizing heat treatments and deformation processes in the industrial production cycles.

Chapter 4

The Technology of Jewelry Manufacturing

4.1 INTRODUCTION

Gold was one of the first metals discovered, its beauty, color, sheen and rareness makes it suitable for artifacts and adornment realization. The rich colour, its malleability and the high resistance to oxidation made it useful material for jewelry applications. A greater part of the technologies adopted nowadays, derive from the early ages of gold, for example, over 6000 years ago the investment casting was developed in the Middle East.

The first gold alloys, with copper as additive, was created around 4000 years ago; the refining processes of impure gold, instead, date back to 2500 years ago. The use of soldering, brazing and welding processes was attributed to the Egyptian populations in ca. 1350 BC.

However, the use of gold as a valuable material for economic exchanges was developed in the 7th century BC in Asia Minor and this is, also, the first time that appears the assaying method to certificate the purity of the coinage. With the aim to avoid the danger of fraud, by debasing precious metal, the need for hallmarking of jewelry became necessary about 700 years ago; so, in London, the oldest consumer protection legislation was created. The term “hallmark” was born in the London Assay Office, where the jewelry items were assayed and hallmarked. The first testimonials regarding the use of gold in medicine refer to dental applications, index of the affirmed ability to manipulate and shape pure gold or gold alloy, since ancient times.

4.2 CURRENT MANUFACTURE

Nowadays, a large part of the jewelry artifacts is still produced in traditional workshop, where the goldsmith, using its craft knowledge and approaches, limits the use of modern equipment and scientific investigation. This leads to a low design innovation, a large manual labor and a low production efficiency and repeatability, resulting in a time-consuming production technique.

However, with the increase of the world demand for jewelry items, the industrial mass production adopted a new trend, based on modern machines, improving quality, velocity and productivity.

The adoption of massive production leads to a decrease of the labor costs and, besides, this modern technique allows guaranteeing compliance on the fineness, health, safety and environment standards.

For outsiders to the jeweler sector, it may seem that, over years, the jewelry manufacturing has not changed much. Nevertheless, only analyzing the manufacture sites, it possible to notice that these shift from the West to the East, probably due to the lower costs. The customer's demand and the expectations on the quality and design changed. This, combined with the introduction of other luxury goods into the world stage, increased the pressure on the jewelry manufacturing industry. All of this caused profound modifies on the approach and the methods of industrial jewelry production. The major driver for change in jewelry is the cost competitiveness, depending on the increasing internalization. The consumer is increasingly demanding innovative jewelry design, improving the develop of new superficial effects and decorative material. Other decisive factors for the goldsmith company are:

- the production's velocity and the efficiency, in order to get to market rapidly and take the bigger awards;
- The respect of the pollution standards;
- The scrupulous control imposed by hallmarking and similar regulations on export.

These factors have led to large improve in quality control, safety technology and suitable production approaches, with a particular attention to the product differentiation in the market and to the customer requirements. In order to guarantee these new objectives of the jeweler sector, more sophisticated quality assurance and production systems were developed and optimized [48].

4.3 MAIN JEWELRY TECHNOLOGIES [48]

The improvement of jewelry alloys and the introduction of modern techniques of fabrication, in jewelry manufacturing, were developed at the same time. Here, for example, some of the major modern production technologies are listed and, afterwards, illustrated:

- Cold forming technologies (stamping and other),
- Electroforming,
- Investment casting,
- Hollow-ware,
- Chain-making,
- Joining techniques,
- Finishing,

- Manufacture of rings

Other example could be the following set of technologies derived from engineering applications and adapted to jewelry manufacturing needs:

- a) Robotics,
- b) Use of laser and laser sintering,
- c) Powder metallurgy,
- d) CAD: computer aided-design, CAM: computer aided-manufacturing

Regarding the material used for the realization of jewelry artifacts, suitable alloys for any type of production processes are developed and optimized, in order to meet special request or to guarantee well defined characteristics and properties during casting, microalloying, deformation and annealing processes.

4.3.1 Cold Forming Technologies

The most widespread cold forming process is stamping, it is used to create hollow lightweight jewelry such brooches, pendant, claps and components for particular design of chain.

In the first part of twentieth century, this process was the primary machine technology adopted to



Fig. 4.1 – Gold alloy flowers obtained by stamping process

produce precious metal items, replaced later by investment casting.

Usually, the stamping process is used to create thin sheet (or other three-dimensional shapes, figure 4.1) of gold after a series of plastic deformations carried out by hardness steel dies, particular attention is given to the amount of material employed in order to reduce the fabrication costs and the industrial scraps resulting from the shearing process. The hardness of the material is an important characteristics, a harder material allows to increase the quality of the blank, to reduce distortions and burring [62].

The suitable force to guarantee the required deformation is defined by the thickness of the gold alloy, the composition and the mechanical properties of the material. Furthermore, the tooling design is important and, the final clearance in between plate and punch, in blanking, depends on all these material and machine characteristics. The stamping process becomes viable only with a mass production, due to the high costs of steel dies manufacture (wire electrical discharge machining and CAD technique).

The production of medals and coins derived from the blanking and stamping process, with the reproduction, in several steps, of the design on both sides. The surface quality and the embossed pattern precision in the final product depends on the gold alloy sheet and dies surface finish.

In ancient times, the single parts was moved through a sequence of individual dies, obtaining the final shape at the end of different deformation steps hand-operated or steam powered.

Nowadays, it is not necessary any more to move the single parts through the process but is the strip, which passes, in several steps, through a single die, resulting as piece in the final shape. The dies are moved by hydraulic pressure.

When the pieces are stamped in matching pairs, these are soldered together, using welding wire or solder paste or solder flush trip, in order to create the hollow jewelry item, ready for final polishing [63].

The higher prices of gold (and other precious metals), and the reduction of the purchasing power of consumers, have led to the diffusion of lighter hollow products that guarantee a lower price, due to the lower weight, maintaining unchanged the jewelry items volume. Using stamping technologies the thickness of the final pieces produced can be reduced until 0.10 mm, with an ever faster and cheaper production.

4.3.2 Electroforming

This particular technique allows to obtain very complex three-dimensional items, and offers the possibility to create unique designs in various jewelry applications [64]. Pure gold or gold alloy are electroplated onto a shaped former but, recently, it was developed a new process where the bulk is a wax model (coated with a conductive layer) [65].

The control of the plating bath becomes the fundamental parameter, in order to guarantee uniformity, homogeneity and caratage/fineness of the coating, especially when the process is used on several pieces at the same time [66].



Fig. 4.2 – *Rigid yellow gold bracelet produced by electroforming*

The thickness of the coating depends on the final dimension of the jewelry artifacts; usually it is between 100 μm and 250 μm , as a function of mechanical strength and costs. The wax or metal core is removed in the final step of production by chemical dissolution or melting through holes in the semi-finished product. At the end, a soldering process of the end fittings may be necessary. Electroplating is used to obtain alloy deposits from 8 to 18 Kt.

With the 22 Kt gold alloys it is possible to achieve red and white colors, while the pure 24-carat gold is used as coating in the Far East.

The microstructure of the coating depends on the deposition rate, for example, high velocity of deposition produces a dendritic surface, avoiding further finishing. The base of the galvanic baths used in electroforming is the gold potassium cyanide (GPC), which constitutes, also, the main component of the coating.

One of the guaranteed benefits of this process is the production of low-stress decorative deposits.

4.3.3 Investment Casting

This is one of the oldest methods to produce jewelry items, developed for copper and gold in ca. 4000 BC. Nowadays, it is the most widespread mass production process in jewelry field.

During the years, the equipment and the materials have become more advanced and sophisticated, in order to satisfy the increasingly stringent requirements of many applications [67].

Using lost wax casting, near-net shape products are obtained through different production steps:

- A hard copper-nickel zinc alloy, or often silver, is used to create a master model,

- A rubber mold is obtained surrounding this master model with a sheet rubber, placed later in a heated press and vulcanized, at the end of the process it is cut into two halves,
- This new mold is used to create a large number of copies of the master model, through a molten wax injecting process into the mold cavity. Eliminating the air from the cavity using a vacuum system, it is possible to reproduce an exact copy of the original model,
- The waxes are arranged around a central feeder, like a “tree”. This particular shape is placed in a metal cylinder (the “flask”). Silica powder with, usually gypsum as binder, is mixed with water and poured into the cylinder to cover the tree. All the system is placed under vacuum in order to remove air and guarantee to form the refractory mould,
- After this, the flask is inverted, allowing to remove the wax by a melting process in a furnace (the burnout oven), the investment mould is heated to the maximum temperature of 750 °C, maintained at this temperature for several hours and then cooled down to the casting temperature (usually between 450 °c and 650 °C),
- The pure gold or gold alloy is melted in a crucible and then cast into the hot investment mould, after a small cooling it is quenched into water. The thermal shock allows breaking off the investment mould and releasing the cast tree (figure 4.3), the final shapes are cut off from the tree, assembled and prepared for the polishing process.



Fig. 4.3 – *Example of casting tree*

Over the years, more and more tests and researches were performed in order to control all these steps properly, because the high quality of the final results depends on every single pass.

The investment casting is affected by defects in casting that are dangerous for the major quality demanded for particular jewelry applications.

The porosity in the as-cast products is due to the presence of gas dissolved in the molten alloy or to shrinkage during solidification. The reaction between the refractory mould (gypsum or calcium sulfate) and the molten metal or, worse, the use of unclean scraps in the charge causes the formation of gas porosity in the products. A reducing atmosphere accelerates the generation of sulfur dioxide gas derived from this reaction, which is expelled during solidification phase, figure 4.4.

Usually, it is possible to observe this defect, round in shape, near the surface of the products.

A bad design of the casting tree, instead, could generate other problems of porosity. The premature solidification in particular sections of the tree, in the thinner section or in the feed sprue, causes shrinkage porosity due to the failure of molten metal feed to the heavy sections of the casting (figure 4.5).

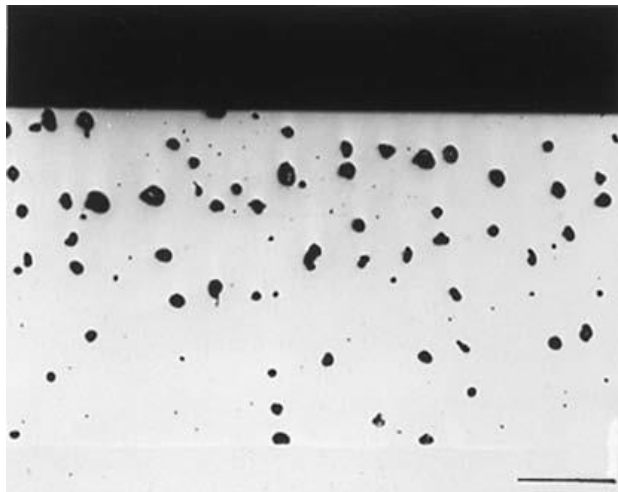


Fig. 4.4 - Gas porosity defect in gold casting product



Fig. 4.5 - Shrinkage porosity defect in gold casting product

The poor control of temperatures and mold practice can cause these porosity defects, fins and unfinished surface problems [68].

Today, two different type of casting machine are used: the older centrifugal casting machine and the modern static vacuum-assist machine. In the first system, using a horizontal rotating arm, the molten metal is accelerated from the crucible to the mould. In the other static system is the gravity that promotes the filling of the mould from the crucible, often a gas overpressure is used also to assist the melting process. The flask is placed below the crucible, in a second chamber under vacuum or inert gas.

The static method is preferable due to the higher control of casting parameters, the higher quality of the products, the greater productivity.

The use of induction heating increases the velocity of production and, the risk of operator error is decreased by the introduction of artificial intelligence computer technologies for a better control of the total process. Recently, a casting machines containing a vibration system to the flask is developed with the aim to improve mould filling and refine the grain size.

Improvements in waxes composition, wax injectors, natural and synthetic rubbers for moulds leads to a lower degrade of investment powders and, to a better production quality [69].

Important trend in investment casting is, also, the increasing use of placing gemstones directly in the waxes prior to investing and casting. This is an economic process because avoids the time-

consuming hand set operation to collocate the individual stones [70]. Special powders are developed to protect the gemstones during burnout process.

Currently, a computer modeling of the investment casting has been optimized, in order to predict the temperature distributions, to control the metal flow and mould filling, the wax feed sprue size and orientation, and to define the probability of casting defects generation [71].

4.3.4 Hollow-ware

Several jewelry products, such as earrings or hollow bracelets, are produced with a large number of different techniques, figure 4.6. The gold strip is formed into tubes by drawing steps, using steel dies, or by lamination process using a rolling mill. The final tubes can be welded or simply seamed (with the seam hidden in particular positions) and, after, the surfaces can be worked or textured.

Usually, the tubes are formed around a metal core, which is eliminated by chemical dissolution at the end of the process. A specific shape able to contain a welding wire, necessary to create the final hollow products, characterizes this metal core.

To complete the jewel produced end fittings and findings are added, or final polishing and diamond-cut processes are used to produce decorative pattern and increase the surface gloss [72].



Fig. 4.6 - *14K Yellow Gold Hollowware Hoop Earrings*

4.3.5 Chain-making

Starting with a round, square or oval wire, the chain production technology is the unique jewelry continuous production system.

Nowadays, the continuous casting system is the most used method to produce gold wire. The gold alloy is melted in a crucible by induction and then, the molten metal passes through a hole in the mould. The shape of the hole defines the final section of the rod: round, rectangular or tubular. The temperature of the graphite mould is lower than the solidus temperature of the gold alloy, and a traction system of rollers allows to pull out the solidified rod.

Using this method the microstructure of the material is characterized by a higher homogeneity and a lower presence of porosity in comparison with that obtained through solidification of ingots in bracket.

Furthermore, the gold product presents a lower content of inclusions and oxides due to the lower interaction with the mould and to the particular method of extraction.

The rod obtained from the melting process pass through different alternating steps of lamination and annealing treatments that allow to properly reduce its section. The final diameter of the wire is achieved by a drawing process [73].

The wire is inserted in the machine, wrapped around a steel former to create the link shape and cut, this process cycle repeated to form the chain. In a second step the link are welded using a powder welding technique.

The process involves the passage of the chain in a mixture containing an organic solvent, oil and a dispersed powder, made by silver, copper, zinc and addition of other elements. Then they are rubbed with talc to remove excess mixture and to insulate them from the high temperature used in the belt furnace, necessary to melt the welding and join the link.

Since the welding powder does not contain gold, the gold alloy, used to create the wire, has to be overkarated in order to ensure the required karatage after soldering process.

Other solution consists in the use of a welding core wire (of the same caratage of the chain), post soldered in the welding furnace. With the

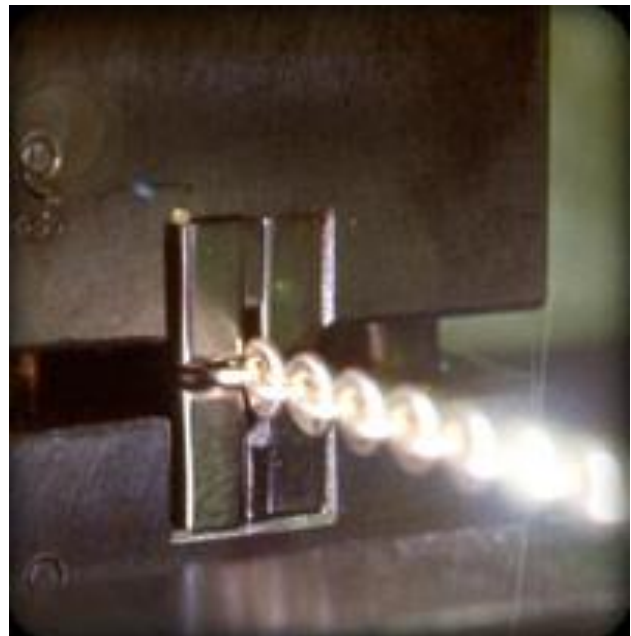


Fig. 4.7 - Chain production machine

introduction of the modern machine, laser in situ on the machine directly welds the link of the chain [74].

The dimensional tolerance of the wire and its metallurgical and mechanical conditions are important factors, they have to allow a suitable strength to cope with the stresses and the deformations generated from the rolling and drawing processes; maintaining, however, a good ductility in order to avoid the possibility of fractures [75].

Final decorations on chain surface can be added by diamond machining, the quality of the processing is guaranteed by the use of ice to fix the chain on large drums, in order to maintain the same position during the all process.

Laser welding is used to create more complex chains, it is also possible to create hollow products by the use of a metal core, often containing a welding wire. The thin gold sheet is wrapped around the core, which is eliminated, at the end of the chain formation, through an industrial emptying process using acids. With these methods, solid and hollow chains can be produced in all the color range and caratage (from 8 Kt to 24 Kt) to satisfy the world markets demand.

4.3.6 Joining Techniques

These technologies continue to represent a fundamental process for joining the different component into the final jewelry artifacts. Soldering and brazing, at temperatures below 450 °C, allow joining the various parts of the final piece, using a welding alloy melted along the joint gap. Usually, a gas torch is used to achieve the suitable temperature. Considering mass production system, such chain-making production, the soldering process can be done in a belt furnace under controlled atmosphere.

Welding alloys must guarantee, first, a suitable joint and then, they have to respect several requirements:

- The welding gold alloy has to present melting range lower than the liquidus temperature of the gold alloys used to create the parts to be welded,
- The diffusion at liquid-solid interface produces a strong bond and it occurs without the melting of the parent metal parts,
- The welding alloy has to be metallurgically and chemically compatible with the parent gold alloy, and has to be characterized by a high fluidity and wettability, in order to avoid the formation of brittle intermetallic compounds,

- The solder alloy must have the same karatage of the gold alloy parts joined and, if possible, a similar color, in order to hide the welding lines in the final jewelry piece.

The welding can be applied to the joint or in the form of wire or strip, that melts and wets the gap, or as cut thin pieces of sheet placed in the gap before the heating process. The use of solder pastes is much diffused, due to its several benefits such as the velocity of production, less rework post soldering, costs reduced, etc. [76].

In the mass production jewelry process, the welding step is performed in a belt furnace, using the solder alloy in the form of paste or present as solder flush sheet and solder filled parts. The part surfaces are cleaned and degreased and the solder are placed in position before the introduction in the furnace. The welding process performed in the furnace allows a better control of the temperatures through the process and the uniform heating of the products.

Until today, the most common elements added to the alloy in order to achieve a low liquidus temperature have been cadmium and zinc. The use of the first one was eliminated due to its toxicity, it melts at 321 °C and boils at 767 °C reacting with air to form poisonous fume. The use of this element in welding alloys was banned in many countries, regardless of the presence of absence of good ventilation and exhaust system in the industrial workshops.

Other elements that are used to depress the melting range of the welding alloys are tin, gallium, indium, germanium and silicon.

Generally, the welding alloys are divided in different categories due to their liquidus temperature, from the lower melting range to the higher we find the “easy”, the “medium” and the “hard” grade solder. However, this designation is not the same for all manufacturers and, its use is not progressed by the industry.

Other alternative approaches to the soldering technique are:

- Laser welding: used in chain production and repair processes, avoids karatage and color compliance problems,
- TIG welding,
- Electrical resistance welding,
- Diffusion bonding: this result is obtained, for machined components, using pressure and heating under inert atmosphere for a suitable time. Multicolor rings are obtained with this technique [77].

4.3.7 Finishing

At the end of the production cycle, all jewelry items need to present a glossy and brilliant surface, accessible only with a polishing process. Motorized wheels filled with polishing compounds are used. Unfortunately, this process generates a high gold loss and inconsistent quality results. Therefore, in mass production workshops, mechanized polishing methods are introduced, such as tumbling with abrasive shapes of sintered ceramic (balls, cones, etc.), or with natural compounds as wood chips. The final polishing process can be carried out by hammering the surface with hard materials in a sequence of different steps (both wet and dry) with a reduction of surface roughness. Centrifugal disc machine, vibratory polishers and magnetic burnisher are the typical industrial machines used for this purpose [78]. Also electropolishing is another polishing technique used in jewelry production field.

Wire brushing, acid etching and sandblasting are processes used to create satin or matt surfaces, while diamond machining is used to give brightness to the artifacts.

Finally, some chemical methods like acid treatment or “bombing” (treatment using a mixture of cyanide-hydrogen peroxide), are increasingly less common due to their degree of danger. These treatments give high finishing and the color of pure gold to the material, by dissolving silver and the base metal from the surface.

4.3.8 Manufacture of rings

The most common plain rings are produced by sheet, strip or solid tube after a typing process, while the complex shapes are often obtained by investment casting. If the ring has a thin section, it is simply obtained from a curved strip soldered along the edge. Considering greater section rings, the production process involves blanking washers from gold sheet, forming these in several steps over a conical die into a ring shape, rolling process to the final size [79]. The disadvantages of this method are the high part of unused material (about 70% of gold sheet) and the low velocity of production.

Other diffused methods involve the production of rings from solid tube, made by extrusion or by forming strip, generally soldered to give a seamless final artifact.

Trying to satisfy specific requests of customers or to produce more complex designs, multi-axis machining centers, controlled by CAD systems, are increasingly used in mass production jewelry industry.

A powder metallurgy technique was developed to produce wedding bands. The pieces are sintered at high temperature, cold forged to increase the density for the final mechanical deformation by

rolling to the suitable size. The reduction of the scrap, high velocity of production, finer grain size and increase in ductility make this method very interesting for jewelry applications [79].

4.4 OTHER TECHNOLOGIES

As previously discussed, modern technologies derived from engineering uses have found application in the jewelry industry.

a) In jewelry production, the use of robots is limited to grind e polish operations, with the aim of improve quality and velocity of production.

Other potential application could be the use of robots in the production of waxes for investment casting from rubber moulds on wax injectors. A higher control of the injection parameters can be planned for the robots, resulting in a greater flexibility of the system.

Furthermore, robots are used for the handling of molten metals to the casting system, in the mixing of investment powders, and in the quenching steps.

b) Regarding the operations of welding, marking, cutting and others, the use in jewelry manufacturing of lasers (based on the Nd:YAG type) is spreading. Their applications in the production processes are various [80]:

- Production of the final jewelry piece through the laser welding process of single components,
- Soldering and welding in the repair of broken jewelry,
- Repair defects as casting porosity,
- Decoration laser engraving, aided by CAD,
- Laser sintering (DMLS)



Fig. 4.8 - Jewelry laser welding

Some examples are showed in figure 4.8.

c) Powder metallurgy processes give a superior quality product, an increase in velocity, a decrease in production scrap and a reduction of the costs (only for high production quantities), figure 4.9.

The more complex products are obtained by MIM (Metal Injection Molding), where the powders combined in a binder are injected into the final mould shape, which is then sintered [81].

Recently, the use of a technological system that allows sintering single layers of powder together, in order to build a three-dimensional piece of jewelry, was evaluated and developed in jewelry production. These production methods find applications in particular areas, such as custom-designed jewelry which can be obtained in one single step.

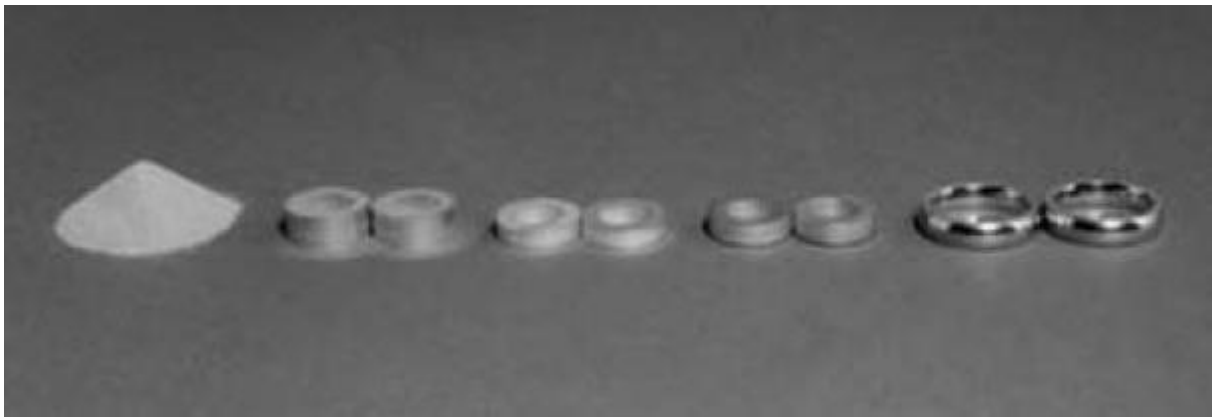


Fig. 4.9 – *Production of gold wedding bands from powder*

d) CAD (computer-aided design) systems for jewelry are developed, in order to use the high possibility on creating complex shapes rather than working to particular engineering parameters [82], figure 4.10 and 4.11. The software allow to cut drastically the time of design and prototyping, the three-dimensional virtual CAD-project can be coupled electronically with CAM or RP (Rapid Prototyping) technology [83].

This production approach has various advantages:

- CAD allows an easier and direct design capability,
- Increase the velocity of product development,
- Jewelry can be designed in a single place and then sent to a production site anywhere,
- CAD allows to easily change the product characteristic without the need of creating several physical models,
- The software allows to increase the freedom of the designers,
- After electronically coupled, the physical models can be produced without any difficulty.

The introduction of RP and other technology leads to the development of direct metal laser sintering of powders (DMLS), figure 4.12.



Fig. 4.10 – CAD design of jewelry artifact



Fig. 4.11 – Cad design of jewelry ring



Fig. 4.12 - Jewels produced by Direct Metal Laser Sintering (DMLS)

Chapter 5

Characterization System

In this chapter will be illustrated the instruments use to characterize all the samples taken from the whole gold chains production process of Filk S.p.A, figures 5.1 and 5.2.

All the characterization has been performed at University of Padua, in the metallurgical laboratory of the industrial engineering department. The chemical etching are performed at Progold S.p.A.



Fig. 5.1 - *Example of sampling in Goldsmith Company*



Fig. 5.2 – *Samples of semi-finished products after metallographic preparation*

CUTTING PROCESS



Fig. 5.3 - *Cutting Machine*

The tool is constituted by a very thin flexible grinding disc (≈ 2 mm), with a diameter included between 100 and 200 mm. The cutting discs are constituted by a binder in which is inserted an abrasive substance; the binders normally used are the rubber and bakelite. Considering, instead, abrasive agents, the most common for such uses are the aluminum oxide (Al_2O_3), silicon carbide (SiC), and diamond powders. Generally, the soft cutting discs are used for processing the samples characterized by high hardness and hard disks for processing samples with low hardness. Particular attention should be given to the temperature in the cutting area, in order to minimize the alteration of the structure of the specimen. To avoid the excessive heating up during the process, the cutting machine, (figure 5.3), is already designed to operate with a considerable flow of fluid refrigerant.

MOUNTING PROCESS



Fig. 5.4 – *Mounting machine*

The samples, suitably obtained from semi-finished gold products, are dissected and embedded in a thermosetting resin, having to meet the following requirements:

- impossibility of manipulating the specimen in the case of small size,

- need to perform microscopic examination on the sample edges (electrochemical coatings, thermochemical diffusion treatments, ...),
- Use of automatic systems of preparation of specimens,
- need to easily locate the specimen under test (n° specimen, n° protocol, annotations, ...),
- ease of storage

The sample, after being inserted in the machine, is compressed together with the resin powder, through a piston, which eliminates the porosity of the compound and maintains the pressure also during heating, which allows the melting of resin (figure 5.4). At the end of cooling step, the result obtained is no more than a solid disc, on its basis appears the face of the sample that will be subsequently subjected to polishing.

POLISHING SYSTEM

This step is very important for the success of the test, because a surface with a high degree of roughness, or not perfectly finished, does not allow an optimal vision, due to the distortion of the light beams. Furthermore, there are essential parameters to be taken into account as the choice of abrasive discs, which must possess a higher hardness than the sample, the speed of polishing, because the discs (with increasingly finer abrasive grains) must be replaced with the progress of polishing process. This preparation step of the samples allows to eliminate all the structural modifies undergone by the metal during cutting process, generally a grinding or a pre-polishing are performed before the real polishing. However, both the processes are similar and serve to remove increasingly thinner thicknesses of material making use of abrasives via finer way.

The last steps of the specimen preparation process provide the step of polishing, where the abrasive is sprayed in form of suspension on the polishing cloths. Aluminum oxide, silica dioxide and amorphous diamond are the mostly used abrasives for this final part of the process, and, with the exception of the latter, they are all suspended in distilled water. In the case, the use of water is not compatible with the sample, alcohol, ethylene glycol, etc. are used. The choice of the type of polishing cloth and the grain size of the abrasive depend on the characteristics of the material that is polished. Usually, for the final polishing steps, multiple soft polishing cloths and more viscous lubricants are used (in comparison with the initial part of the process).

In this study, all the different gold alloys investigated are polished with the following sequence of abrasive paper and polishing cloths:

- abrasive paper: P320 - P500 - P800 - P1200 - P2500/4000

- polishing cloths: 3 μm – 1 μm

In the following figures, (fig. 5.5 and fig. 5.6), the two type of polishing machines are presented.



Fig. 5.5 - Polishing automatic machine



Fig. 5.6 - Polishing manual machine

OPTICAL MICROSCOPY



Fig. 5.7 - LEICA DMRE optical microscope

Optical microscopy is the basic method of investigation for the structural analysis of materials. The technique is particularly efficient for the study of abnormalities resulting from heat treatments, for evaluation of inclusions, for the interpretation of breakage and for the evaluation of welds and coatings. With the ability to magnify the images, through the objective of the optical microscope, we can distinguish two points close to each other, up to a distance equal to 0.3 μm , which coincides with the resolution power of the instrument. However, one of the limits of this technique is the low depth of field, or the inability to focus optimally the parts of the sample that lie, even only slightly, outside the optimal focal plane. This forces the metallographic polishing to a face, or a section of the sample, to expose a flat portion

to the observation of the prepared test specimen. The characterization of all samples taken from the goldsmith company was performed with a LEICA DMRE microscope, figure 5.7.

SCANNING ELECTRON MICROSCOPY (SEM)

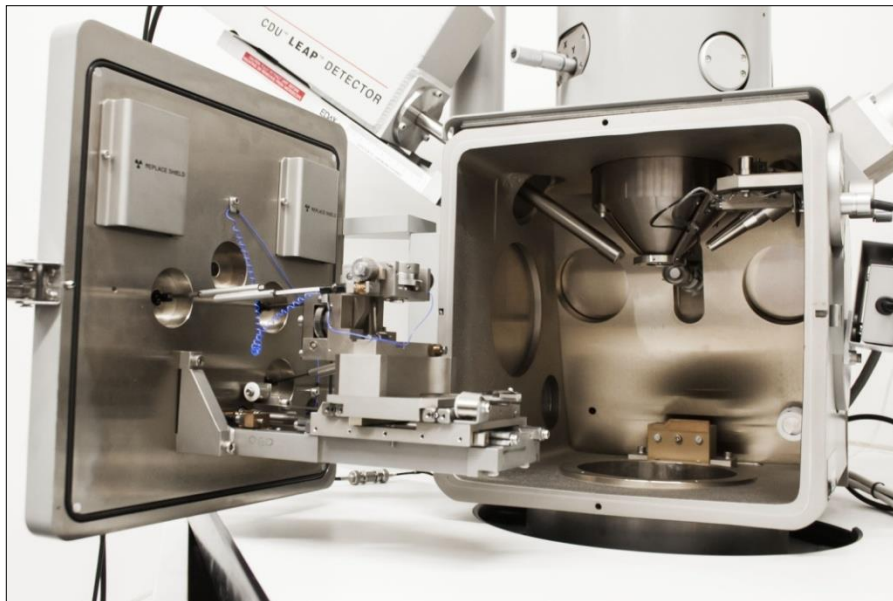


Fig. 5.8 - *Scanning electron microscope (SEM) used in the characterization of the samples*

It allows to easily observing the bulk samples, obtaining images with high quality and great depth of field, transmitting information with great immediacy. The use paired with a microanalysis system widens the possibility of working: it is possible to obtain qualitative and quantitative informations about the elements present on a given area of the sample.

Secondary electron images are usually used to study the morphology of the samples. The contrast in the images, thus obtained, depends on the relative variation in the number of detected secondary electrons, to which two effects contribute: change in number of electrons emitted from the sample and variation in the population of electrons collected by the detector. Regarding the first effect, the number of emitted secondary electrons is always proportional to the number of primary electrons incident, while, the fraction of electrons collected by the detector depends only on the angle of incidence. The combination of the two discussed effects implies that, the number of detected secondary electrons depends essentially on the angle of incidence of the local probe, therefore on the sample topography.

The contrast in the images obtained through backscattered electrons is due, equally, to the material's nature of sample and to the topography of the surface; in fact, the backscattering coefficient is a function of the atomic number of the sample. The final image quality depends on the resolving power of the instrument.

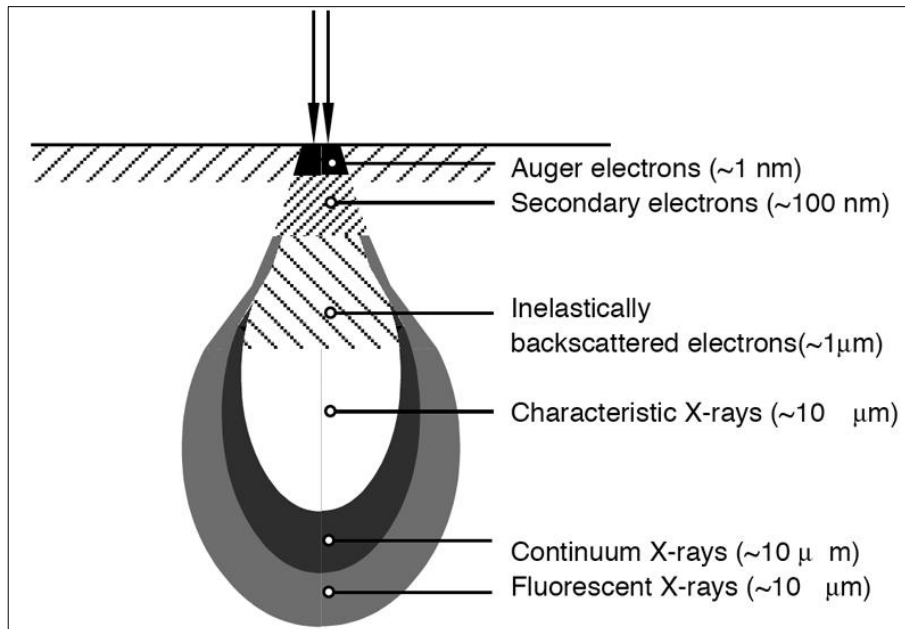


Fig. 5.9 - Emission volumes of the various signals generated from a sample excited with an electronic probe

Using the SEM, the achievable resolution depends on the section of the electronic probe, on the penetration and diffusion effects within the sample, on the signal/noise ratio, on the accidental presence of external interference fields, on the presence of vibration. Generally, with commercial instruments, the resolution is comparable to 10-30 nm in the secondary electron images, while it is worst (50-200 nm) in those to backscattered electrons, figure 5.9. In this work, the characterization of the gold samples (obtained after metallographic preparation) was mainly performed with a Cambridge Stereoscan 440 scanning electron microscope (SEM), equipped with a Philips PV9800 EDS (Fig. 5.9).

MICROHARDNESS TESTS



To evaluate the mechanical properties of the samples, hardness tests were performed using a LEITZ microdurometer (figure 5.10) with a Vickers penetrator set with a 25 g load and with 30 s of loading time.

Fig. 5.10 - Microdurometer LEITZ

CORROSION TESTS

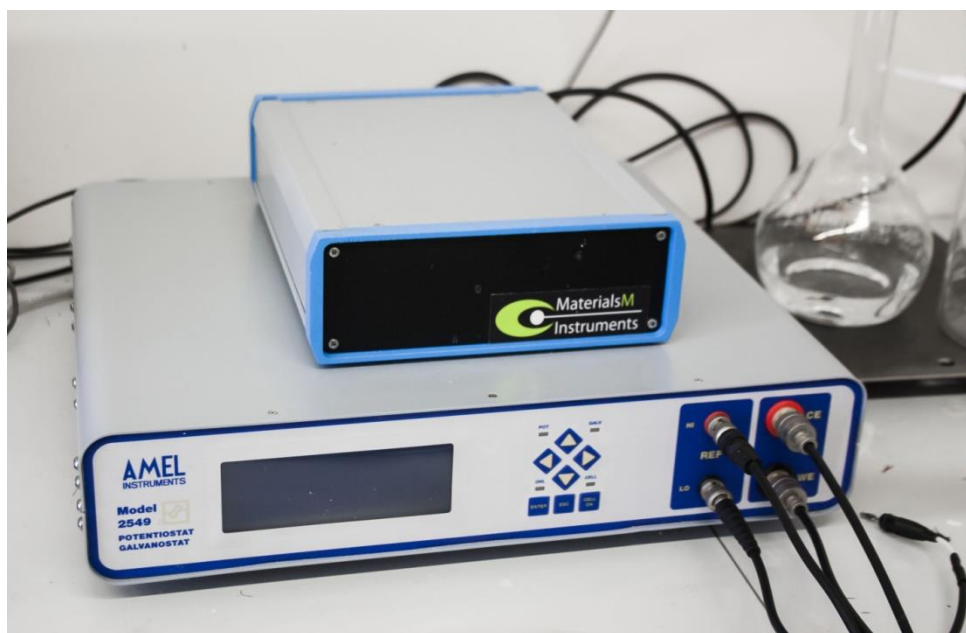


Fig. 5.11 - Experimental setup used for corrosion tests on gold alloy samples

The corrosion resistance of the gold alloys employed for the production of gold sheets and wires was evaluated with potentiodynamic polarization tests. Anodic polarization tests were performed with an AMEL 2549 Potentiostat (figure 5.11), using a saturated calomel electrode as the reference electrode (SCE) and a platinum electrode as the counter electrode, with a scan rate of $8 \times 10^{-4} \text{ Vs}^{-1}$.

X-RAY DIFFRACTION TECHNIQUE (XRD)

The residual stresses were evaluated using a Siemens D500 X-ray diffractometer using CuK α -radiation, showed in figure 5.12. The strain in the crystal lattice was measured and the combined residual stresses were defined from the elastic constants. Several grains contributed to the measurements. The number of grains in each sample depended the size of each grain and on the geometry of the X-ray beam [84].

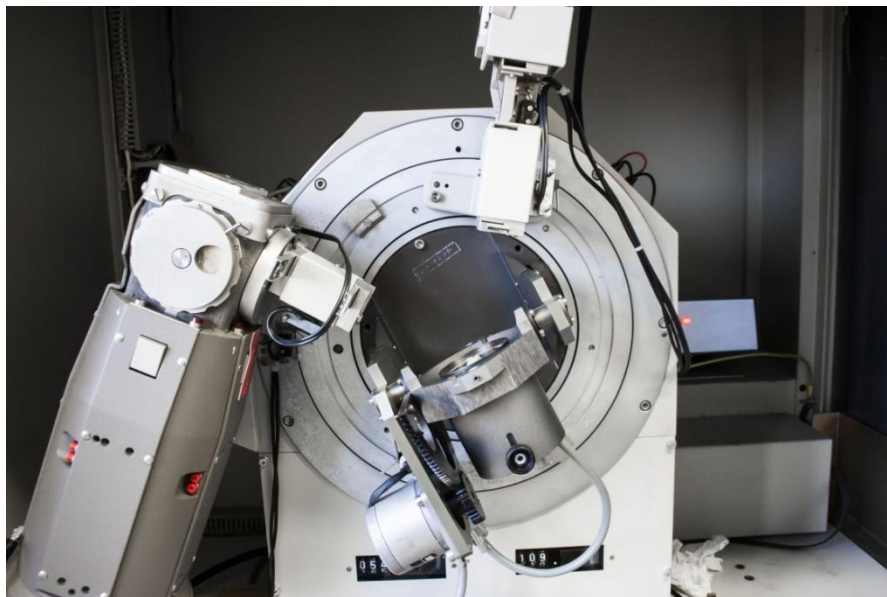


Fig. 5.12 - *X-Ray diffractometer used in the characterization of the gold alloy samples*

Chapter 6

Study of gold-welding alloy wires: Effect of Production Parameters on Microstructure and Properties

6.1 INTRODUCTION

Gold-welding alloys, which are used in the production of both hollow and solid gold chains, affect the optical and mechanical properties of various gold products because the corrosion resistance of the individual links depends on these properties. It is important that welding alloys with high corrosion resistance do not degrade during or after the production process.

The mechanical properties of gold-welding alloy wires is strongly influenced by the alloy microstructure, which has a key role in both the machinability and the quality of the wires. In this thesis, various physical and mechanical properties of gold originating from different industrial deformation processes are evaluated. Specifically, various plastic deformation grades caused by different annealing and rolling steps are analyzed. The change of the temperature, time and velocity parameters in the annealing and lamination processes leads to the formation of different levels of residual stresses in the material, which can generate a variation in the corrosion properties of the gold wires. Moreover, the influence of these residual stresses on the corrosion resistance of the welding is studied, since it represents a fundamental characteristic that guarantees suitable properties in a gold chain's final environment of use. The most important phenomenon characterizing the corrosion of gold alloys is the selective dissolution of the less noble elements [85].

6.2 EXPERIMENTAL PROCEDURE

Measurements of the melting and annealing parameters for three different welding alloys have been performed. Their respective compositions are shown in Table 6.1.

Tab. 6.1 - Chemical compositions of the yellow welding alloys studied

Kt	Au [%]	Cu [%]	Ag [%]	Zn [%]
14	58.5	18.6	17.1	5.8
10	41.7	23.6	17.6	17.1
9	37.5	29.1	15.1	18.3



Several tests were implemented in order to optimize the continuous melting and the annealing processes. In particular, microstructural analyses and hardness tests were performed, in which the temperatures, time of melting and quenching, and velocity of melting and rolling are the relevant parameters.

Fig. 6.1 - Example of master alloy First results obtained by optical microscope (OM) analysis were used to modify some production parameters. The melting temperature in the crucible was increased in order to optimize manual and induction mixing. The same conditions were created in the mould with the aim of maintaining a good solubility of the low melting elements. The number of water jets, in the continuous casting operation, was increased in order to homogenize the system of cooling out of the furnace. As the cooling time in air before the water quenching was suppressed, the jets of water were moved to a zone closer to the mould's exit.

After solidification, the cross-section of the rods was reduced from about 6.00 mm to a diameter of 1.00 mm, by applying the sequential steps of rolling, annealing and final drawing. A similar investigation was performed for the annealing process in the static furnace. Time, temperature and cooling parameters were modified in order to improve the resistance of the wires during rolling steps, and with the aim of obtaining a satisfactory recrystallization after deformation.

A statistical analysis on different annealing tests at various temperatures (from 560 to 610 °C), times (30 and 45 mins) and air cooling (from 0 to 60 s) showed that it is possible to reduce the hardness with suitable heat treatments. To evaluate the mechanical properties of the final annealed products, tensile and hardness tests were performed. OM observation was performed with a LEICA DMRE microscope. The samples were prepared with the standard metallographic technique of polishing and the etch was performed with different solutions of cyanide.

The corrosion resistance was evaluated with potentiodynamic polarization tests, using as electrolyte a solution that simulates human sweat in order to replicate the environment of final use. By mass, the solution consisted of 0.5% NaCl, 0.1% lactic acid and 0.1% urea. A solution of NaOH was used to guarantee an acidity of pH 6.5. Anodic polarization tests were performed and, the electronic scanning microscope (illustrated before) was used, in order to study the microstructures obtained from the variation in processing parameters. The residual stresses were evaluated through XRD measurements, the operating parameters are shown in tab. 6.2.

Tab. 6.2 - *Parameters of the XRD analysis*

Material	Lattice structure	Simmetry	Diffraction Plane	Radiation type	Collimator diameter
Gold alloy	FCC	Fm3m	(2 2 0)	CuKalpha	4 mm

6.3 RESULTS AND DISCUSSION

During the microstructural and mechanical analysis, several different process parameters of the production cycle were tested for different welding alloys. The aim was to identify the relationship between the parameters of the processes, the microstructures and the mechanical qualities of the semi-finished products. Furthermore, the influence of these characteristics on the residual stresses

and the corrosion resistance was evaluated. In this part of the thesis work, four different carat gold alloys were considered; 9, 10, 14 and 18 Kt.

6.3.1 9 Kt Gold Welding Alloy

An analysis of the lowest commercial carat gold alloy allows the possibility to attempt to reproduce the results observed for the other carat gold-welding alloys, by optimizing the entire production cycle. The two different processes for the 9 Kt gold alloys are shown in Table 6.3.

Tab. 6.3 - Melting and annealing process parameters for two different production paths for the 9 Kt gold alloy

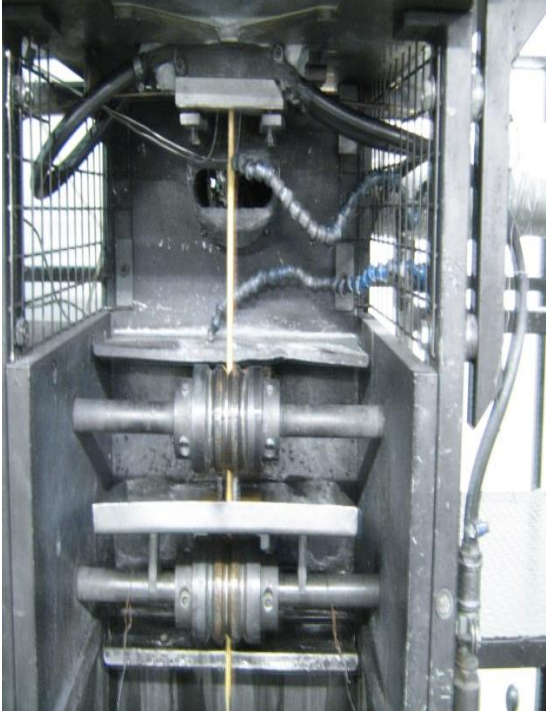
	OLD PROCESS	NEW PROCESS
Crucible Temperature	930 [°C]	930 [°C]
Mould Temperature	640 [°C]	640 [°C]
Melting velocity	6 [mm/s]	6 [mm/s]
Working time	1.8 s	1.8 s
Pause time	1.4 s	1.4 s
Time before quenching	60 s	0 s
Annealing Temperature	610 [°C]	600 [°C]
Annealing time	30 [min]	45 [min]
Time before quenching	60 [s]	0 [s]

The deformation cycles are the same as in the 10 and 14 Kt gold-weldings. An immediate cooling of the wires between the melting and the annealing furnaces allowed for the hardness of the gold alloy to be reduced, as shown in Table 6.4.

Tab. 6.4 - Micro-vickers hardness for the final annealed wires obtained with the two different production paths for the 9 Kt gold alloy

		Micro-hardness [HV _{0.025}]
1.00 mm diameter final annealed wire	OLD PROCESS	202 ± 5
	NEW PROCESS	175 ± 5

Immediate cooling also allows for an increase in the malleability and the workability during rolling, drawing, and in the chain production machines, figure 6.2.



The microstructures of the final annealed, and previously deformed, samples obtained with the new production processes are shown in fig. 6.3. In fig. 6.3(a) the slip bands due to plastic deformation are shown, whilst in fig. 6.3(b) it is shown how the annealing process allows for the restoration of the fine grain microstructure. The tensile tests indicated a considerable increase in the elongation for the final annealed wires obtained after the change in the parameters of the whole production process, as shown

Fig. 6.2 - Continuous casting system for the production of gold alloy rods in Fig. 6.4.

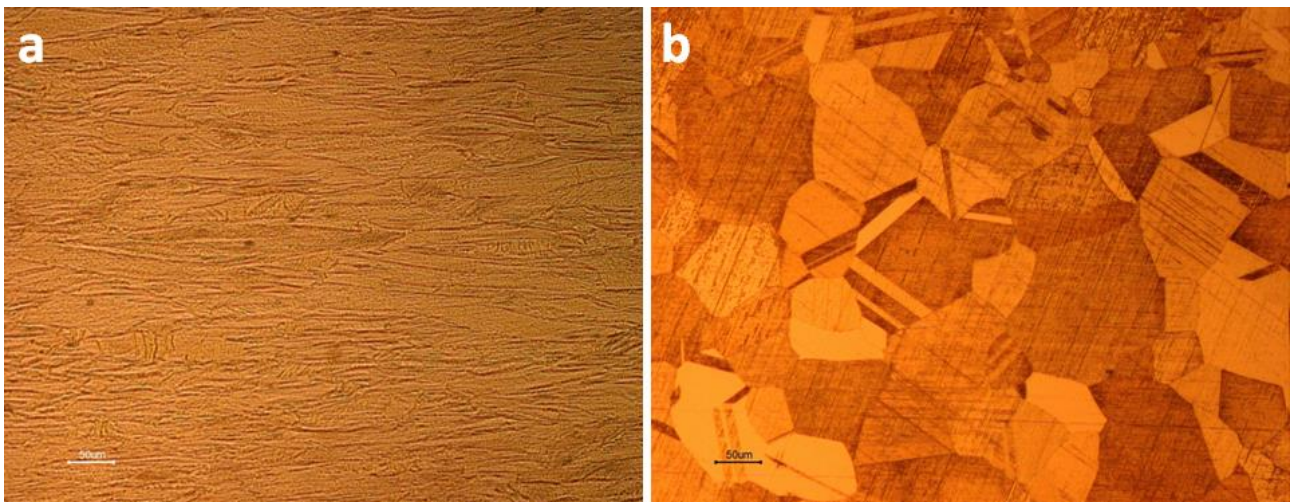


Fig. 6.3 - Microstructure of the gold alloy wire obtained with the new optimized process for the final drawn step (a) and after the last annealing process in the static furnace (b)

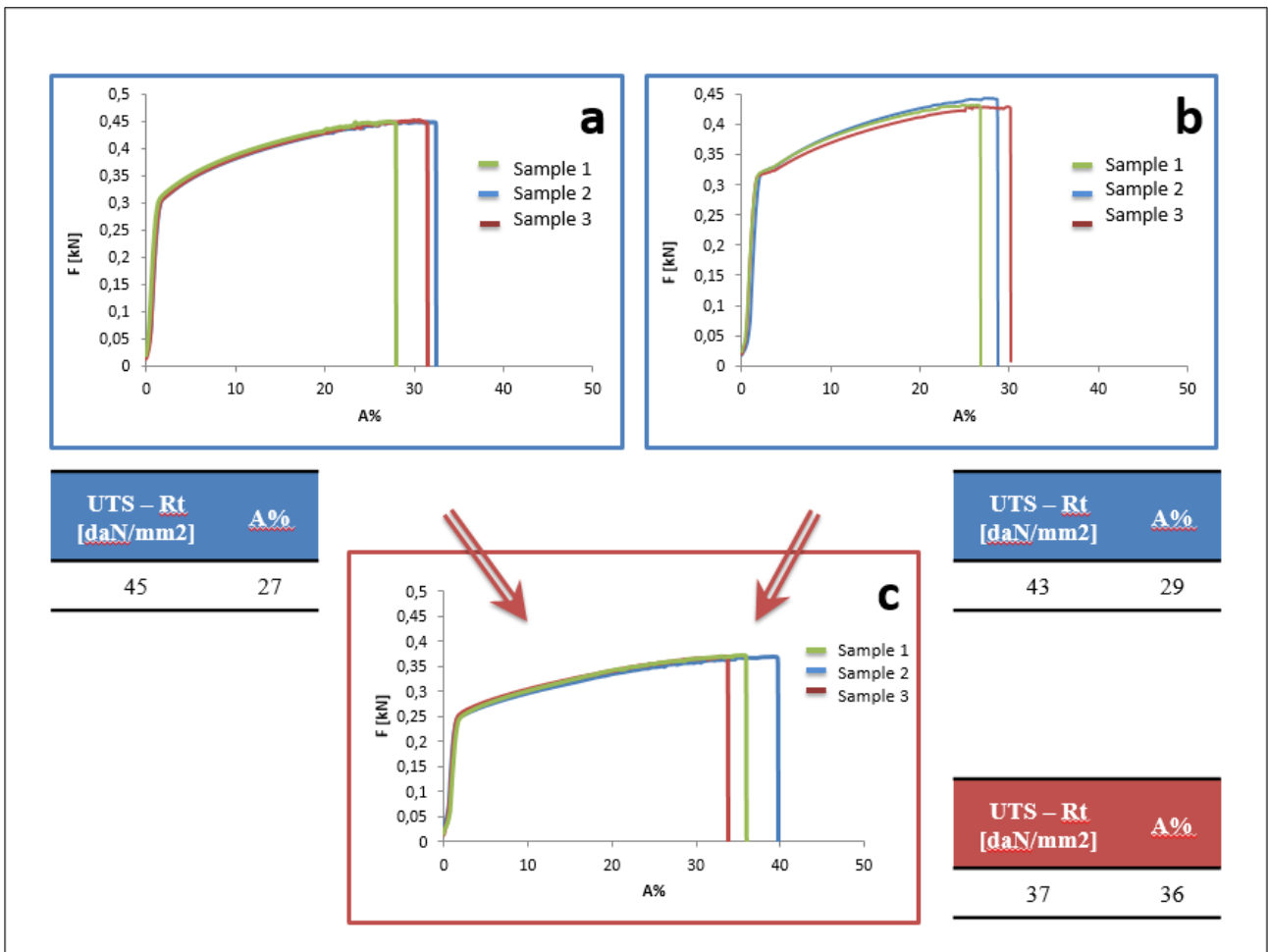


Fig. 6.4 - Tensile curves and the average values of strength and elongation for the final annealed wires obtained with the old process (a), (b) and the new one (c)

6.3.2 10 Kt Gold Welding Alloy

For low carat gold and gold-welding alloys such as the 9 and 10 Kt samples, the addition of zinc has an important effect on the properties of the material. Zinc causes a reduction in the volume of the immiscibility field, and this affects processes such as annealing, solution annealing, susceptibility to softening or overageing and temperature of precipitation hardening. The presence of a higher fraction of less noble elements, in comparison with the 14 Kt sample, increases the fragility and the sensitivity to ruptures in the solidification phase during the melting process.

In order to reduce stresses generated from the solidification phase and the superficial interaction between the rod and the graphite mould, the velocity of melting, the total time of work and pause of

the rollers downline of the crucible, and the time before quenching were reduced, as indicated in Tab. 6.5.

Tab. 6.5 - Melting and annealing process parameters for two different production paths for the 10 Kt gold alloy

	OLD PROCESS	NEW PROCESS
Crucible Temperature	930 [°C]	930 [°C]
Mould Temperature	640 [°C]	640 [°C]
Melting velocity	6 [mm/s]	3.5 [mm/s]
Working time	1.8 s	1.2 s
Pause time	1.4 s	1.0 s
Time before quenching	60 s	0 s
Annealing Temperature	610 [°C]	600 [°C]
Annealing time	30 [min]	45 [min]
Time before quenching	60 [s]	0 [s]

The microstructures resulting from the optimization demonstrated greater homogeneity and a non-negligible decrease in the hardness of the melting specimens. The immediate cooling of the rod after the melting furnace allows one to maintain a smaller grain size than obtained in previous production processes, figure 6.5.

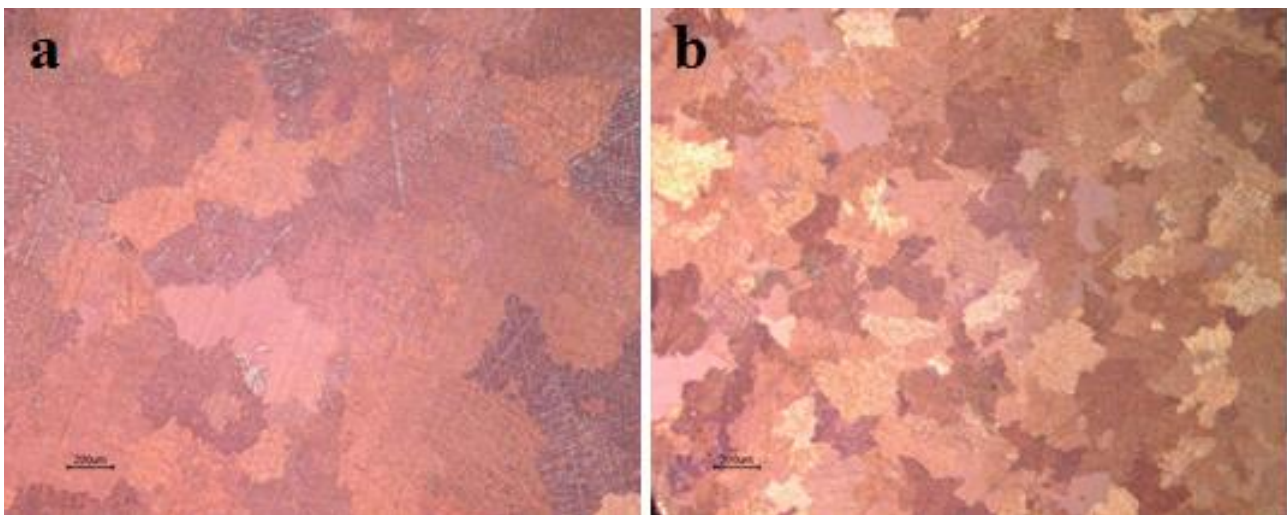


Fig. 6.5 - Microstructures of the as-cast wires obtained with the two different processes, the old (a) and the optimized one (b)

A similar procedure was followed for the microstructures of the samples at the end of the production process, as shown in Fig. 6.6.

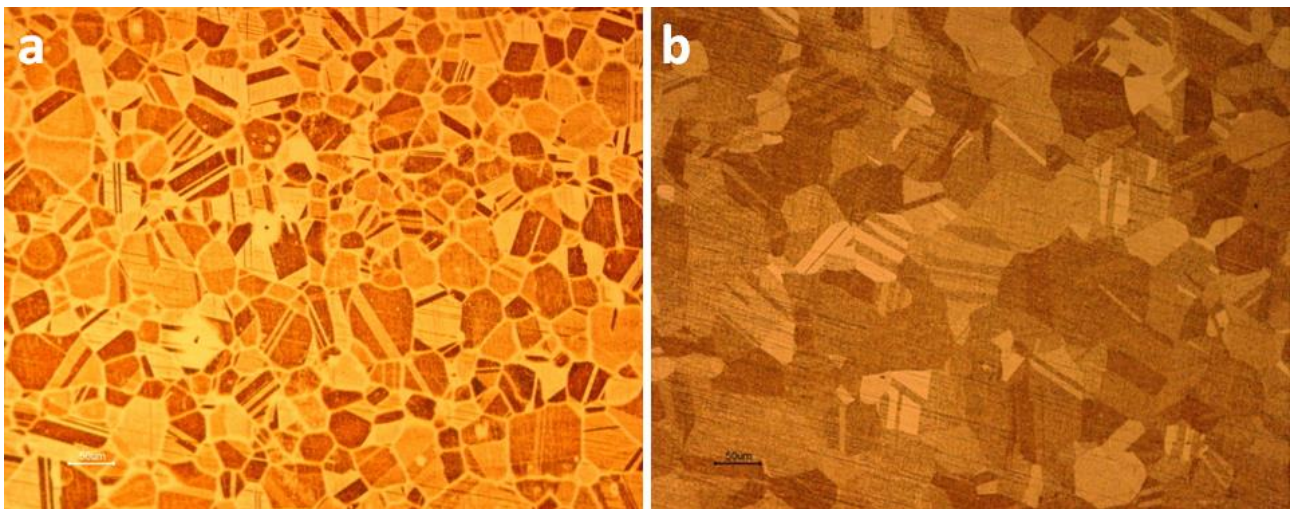


Fig. 6.6 - Microstructures of the annealed wires obtained with the two different processes, the old (a) and the optimized one (b), at the end of the production cycle

Although the hardness remained approximately constant in the final annealed wire specimens during the annealing process, as shown in Tab. 6.6, the decrease in temperature and the increase in time of the treatment allows one to avoid precipitation phenomena, ensuring that a single-phase material is produced with a uniform distribution of grain dimensions. This improvement in the uniformity of the microstructure leads to an improvement of the mechanical properties, as shown in Fig. 6.7.

Tab. 6.6 - Micro-vickers hardness for the final annealed wires obtained with the two different production paths for the 10 Kt gold alloy

		Micro-hardness [HV_{0.025}]
1.00 mm diameter final annealed wire	OLD PROCESS	190 ± 10
	NEW PROCESS	175 ± 10

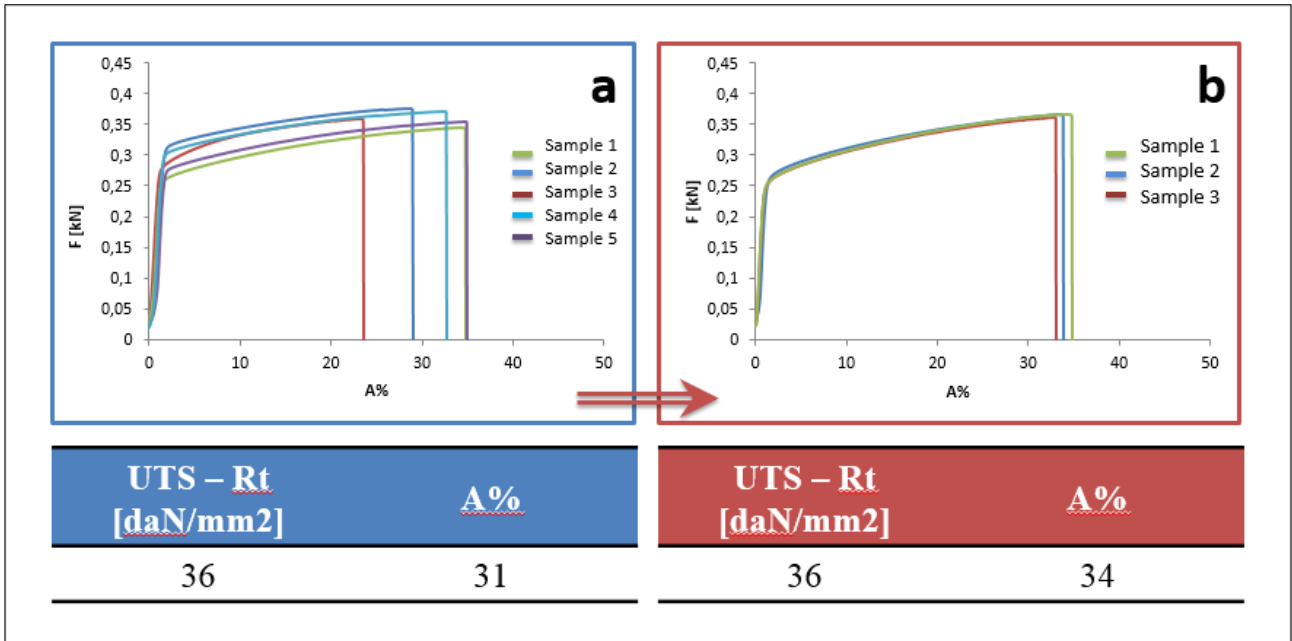


Fig. 6.7 - Tensile curves and the average values of strength and elongation for the final annealed wires obtained with the old process (a), and the new one (b)

6.3.3 14 Kt Gold Welding Alloy

In the case of the 14 Kt samples, three different production processes were implemented using the parameters indicated in Tab. 6.7.

Tab. 6.7 - Melting and annealing process parameters for three different production paths for the 14 Kt gold alloy

	PROCESS 1	PROCESS 2	PROCESS 3
Crucible Temperature	930 [°C]	930 [°C]	930 [°C]
Mould Temperature	640 [°C]	640 [°C]	640 [°C]
Melting velocity	6 [mm/s]	6 [mm/s]	3.5 [mm/s]
Working time	1.8 s	1.8 s	1.2 s
Pause time	1.4 s	1.4 s	1.0 s
Time before quenching	60 s	0 s	0 s
Rolling velocity	35 m/min	35 m/min	20 m/min
Annealing Temperature	610 [°C]	560 [°C]	600 [°C]
Annealing time	30 [min]	45 [min]	30 [min]
Time before quenching	60 [s]	0 [s]	0 [s]

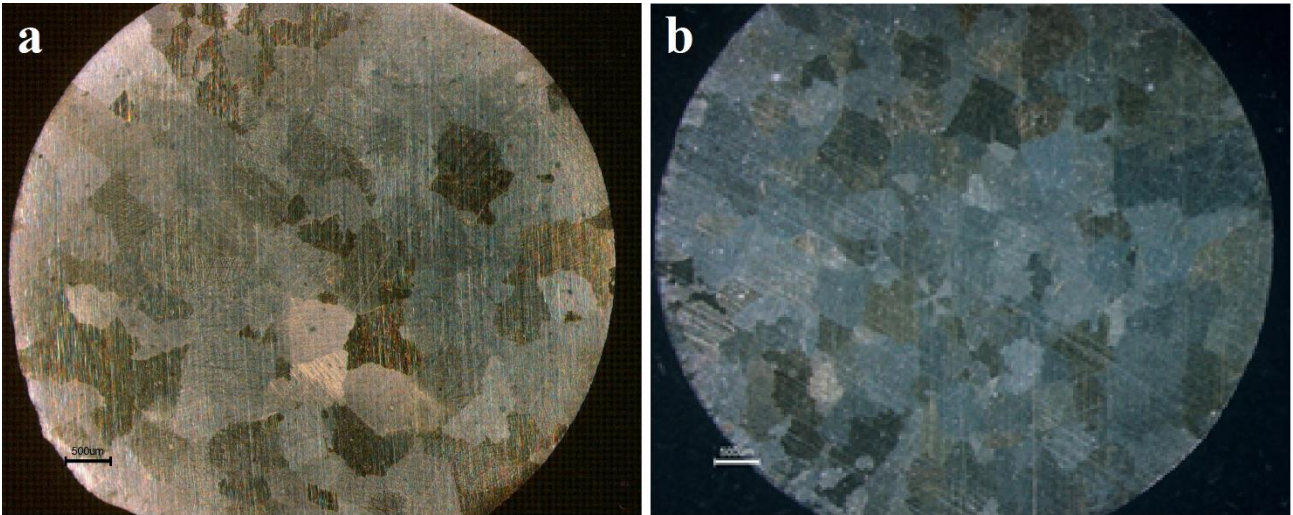


Fig. 6.8 - *Microstructures of the as-cast rod obtained with the process 1 (a) and the process 3 (b).*

Figure 6.8 shows the microstructures of the as-cast gold rod obtained with the process 1 (figure 6.8a) and the optimized process 3 (figure 6.8b), the grain size remains substantially the same but, it is possible to notice a greater homogeneity and uniformity of distribution passing from the old production process to the new one. The microstructures of the final annealed wires obtained with the first two processes and the deformed and annealed microstructures for the samples treated with the third optimized process (“process 3”) are shown in Fig. 6.9.

The comparison of the microstructures shows a refining of grain size, and a greater homogeneity for the specimen obtained with process 3. In particular, by employing process 3, the grain size is shown to be very fine.

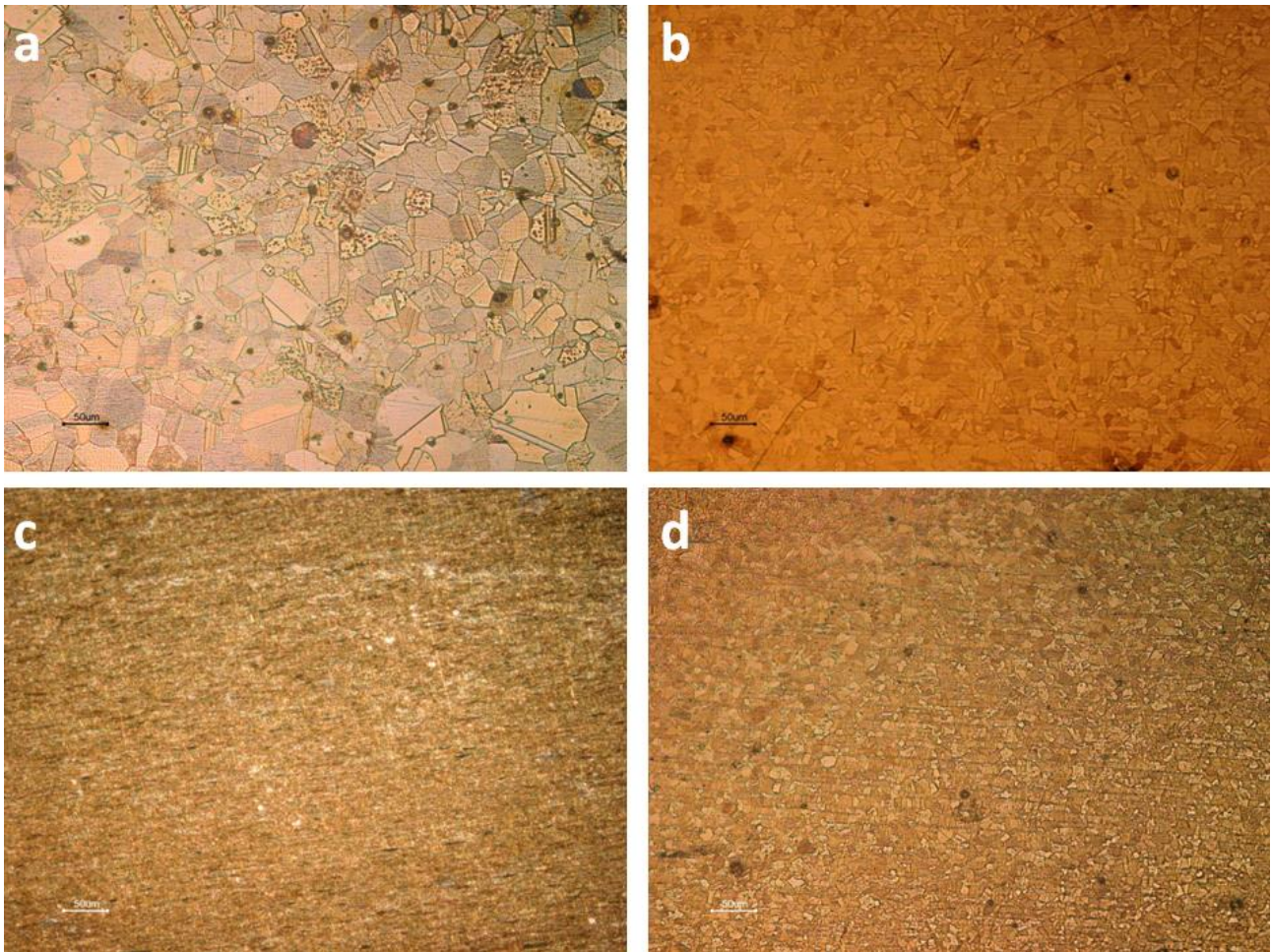


Fig. 6.9 - Microstructures of the 1,00 mm final annealed wires obtained with the process 1 (a) and the process 2 (b). Rolled and final annealed microstructures of the sample made through the optimization of the production parameters with the process 3, respectively (c) and (d)

To better understand the structure in these samples, SEM analyses were performed.

Figure 6.10, shows the SEM microstructures analyzed with backscattered electrons. This change in the structure of the material causes a significant decrease in hardness of the specimens derived from process 3.

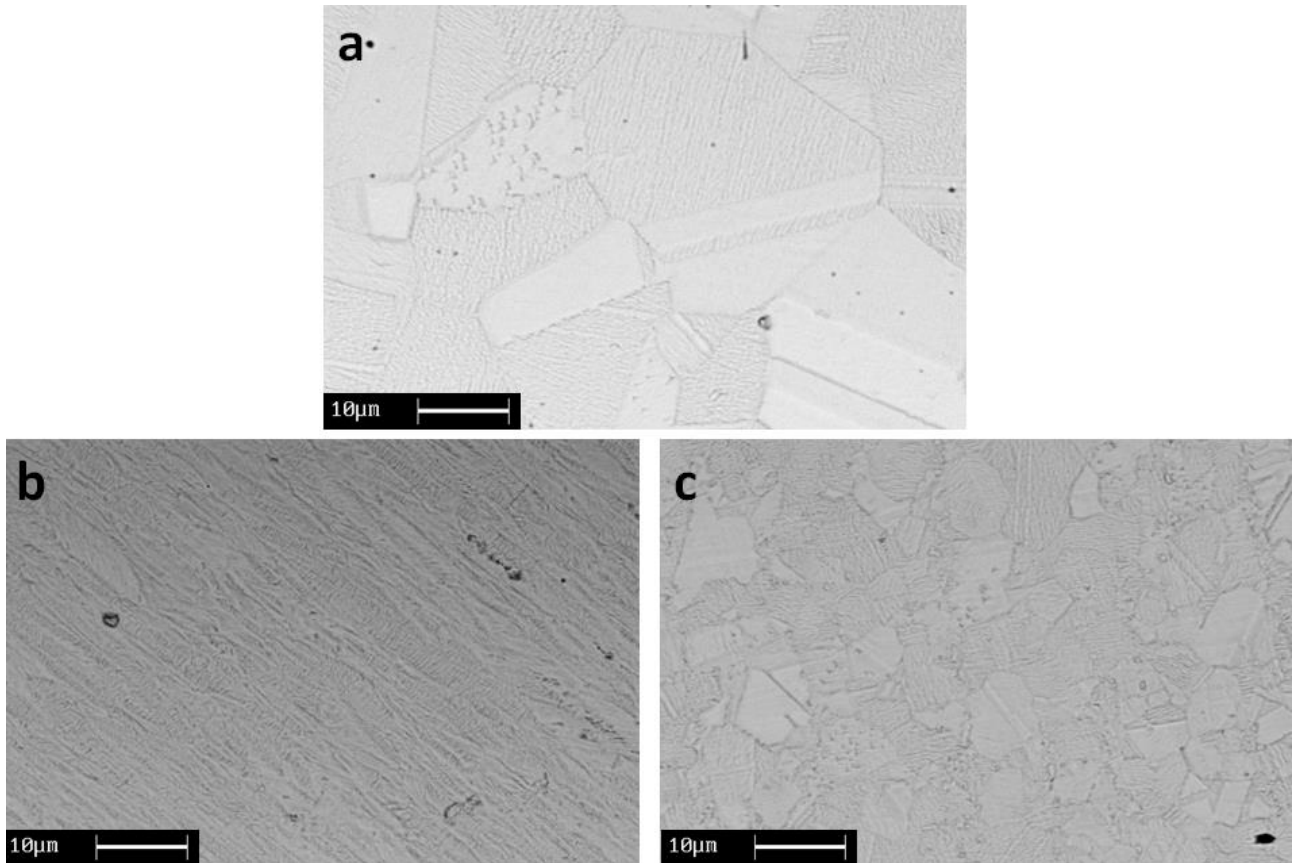


Fig. 6.10 - SEM micrographs obtained with backscattered electrons diffraction of the final annealed wires for the old process (a) and those deformed (b), and annealed (c) for the last optimized process

The corresponding data are reported in Tab. 6.8.

Tab. 6.8 - Micro-vickers hardness for the final annealed wires obtained with the three different production paths for the 14 Kt gold alloy

		Micro-hardness [HV _{0.025}]
1.00 mm diameter final annealed wire	PROCESS 1	210 ± 10
	PROCESS 2	175 ± 10
	PROCESS 3	155 ± 5

The optimization of the annealing steps in process 3 led to a more regular growth of the grains and a large reduction of the grain size in the final annealed wire. As for the other welding alloys, this was achieved by a decrease in the temperature by about 10 °C and by the immediate cooling after removal from the furnace, which avoids undesirable grain growth.

The air cooling time is a critical variable in the process, as the hardness of the gold wire decreases due to cooling in water immediately after the furnace. Hardness can there be used to quantify the role of air cooling, as the rearrangement of the atoms in the crystal lattice gives the material a greater hardness due to the transition from a disordered distribution to an ordered one.

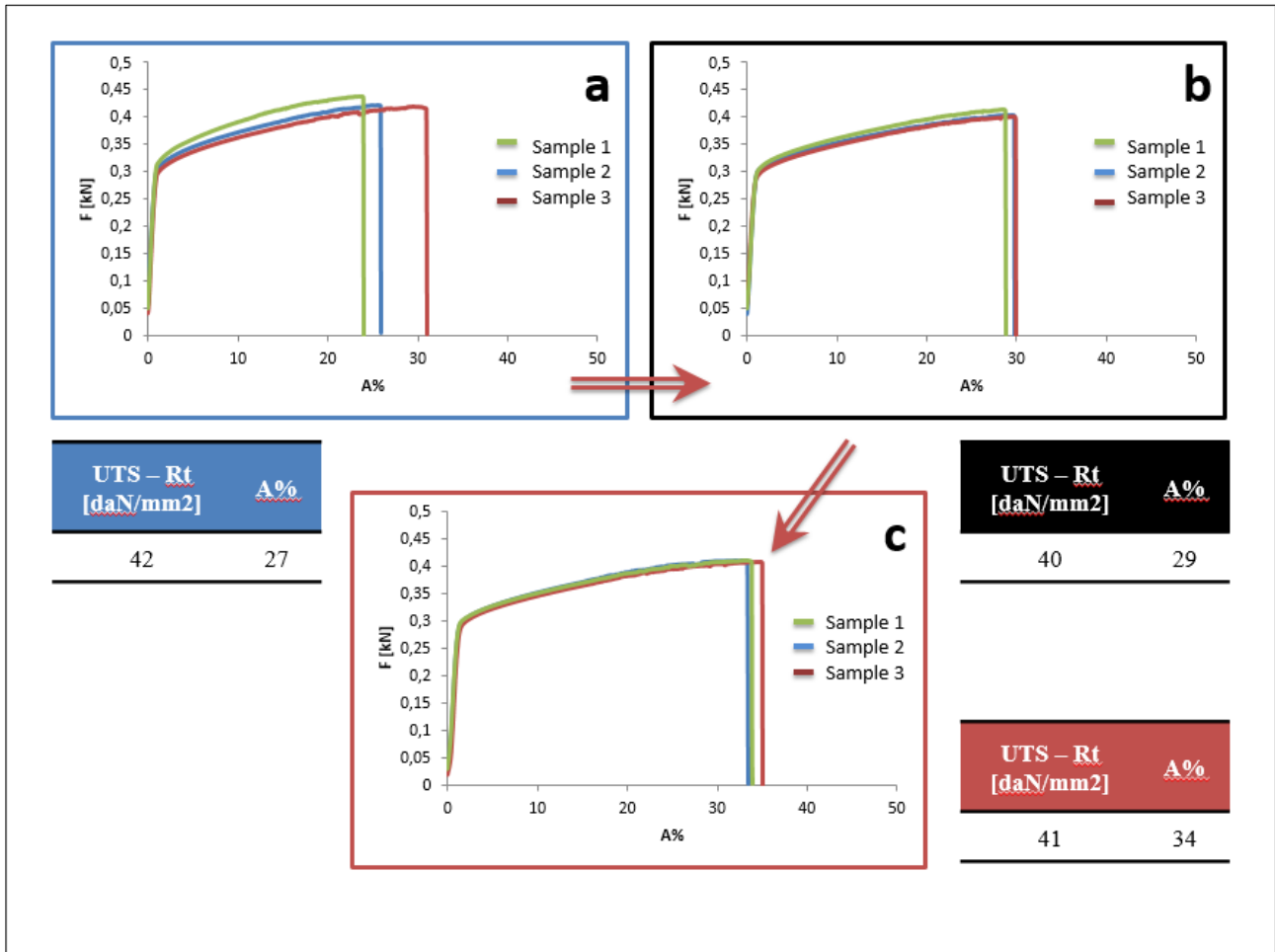


Fig. 6.11 - Tensile curves and the average values of strength and elongation for the final annealed wires obtained with the process 1 (a), process 2 (b) and process 3 (c)

In figure 6.11, the tensile tests show a degree of uniformity in the relationship between elongation and the tensile stress of the specimens taken from the skeins of wire produced by process 3. As observed in the previous process, the values of strength and elongation in the same skein showed significant variation, which demonstrates the presence of crystallized and non-crystallized zones.

6.3.4 18 Kt Gold Welding Alloy

Also the 18 Kt welding wires alloy for the production of cable pipe were studied; part of these were discarded during the deformation and annealing process due to breakages immediately out of the annealing furnace or under the rolling, figure 6.12.

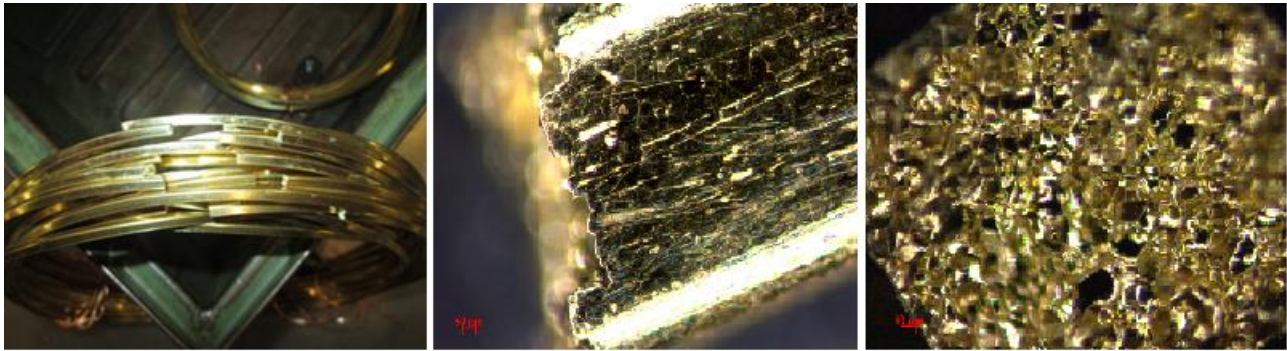


Fig. 6.12 - Broken gold welding wires during production process

Several analysis of the temperatures, during the operation, were made to confirm the constancy of the work parameters and none abnormalities were found.

With the aim to reduce these drawbacks, the parameters of melting process and the treatments in the annealing furnace were modified, after a microstructural analysis and hardness tests the condition of continuous casting were optimized. In Table 6.9, the old and the new optimized process are showed.

Tab. 6.9 - Melting and annealing process parameters for two different production paths for the 18 Kt gold alloy

	OLD PROCESS	NEW PROCESS
Crucible Temperature	950 [°C]	980 [°C]
Mould Temperature	650 [°C]	670 [°C]
Melting velocity	6 [mm/s]	6 [mm/s]
Working time	1.8 s	1.8 s
Pause time	1.4 s	1.4 s
Time before quenching	60 s	0 s
Annealing Temperature	610 [°C]	560 [°C]
Annealing time	30 [min]	45 [min]
Time before quenching	60 [s]	0 [s]

After the first results from the microscopical analysis, some production's parameters were modified. The melting temperature in crucible was increased to allow a better manual and induction mixing, the same condition were created in the mould with the aim to maintain a good solubility of the low

melting elements. The number of water jets, in the continuous casting operation, was increased to guarantee a more homogeneous system of cooling out of the furnace.

The cooling time in air before the water quenching was suppressed, the jets of water were moved to a zone close up at the mould's exit.

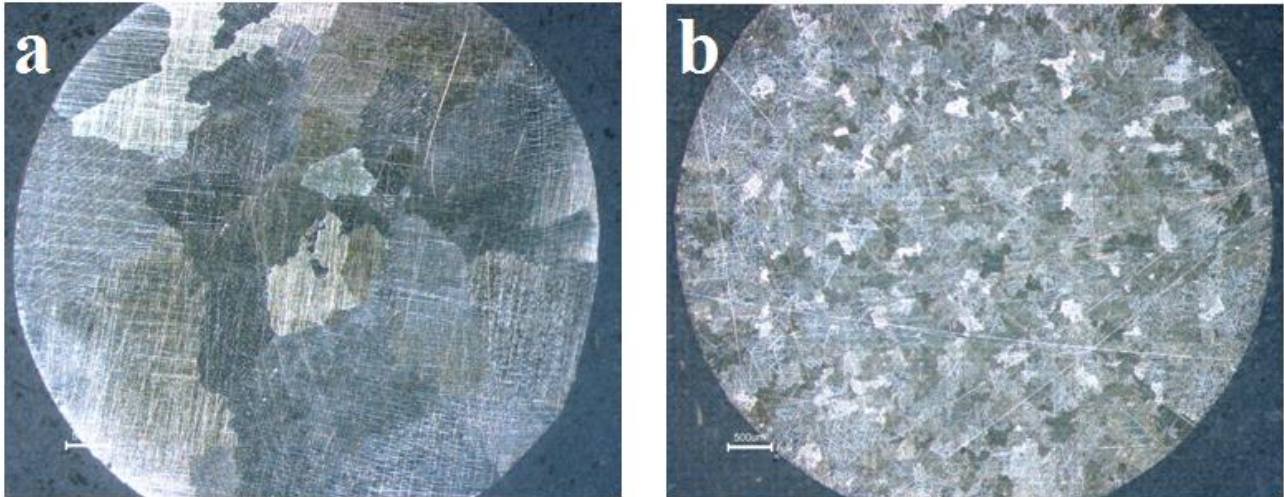


Fig. 6.13 - Microstructures of the as-cast rod obtained with the old process (a) and the new optimized process (b)

Figure 6.13 shows the smaller grain size obtained in the melted rod with new optimized process (b) and the more uniform distribution, in comparison with the old process (a).

An analog investigation was done for the annealing process; times, temperatures and cooling were modified in order to improve the resistance of the wires during rolling steps and to obtain a good recrystallization after deformation. The change in microstructure passing from the old production process to the new optimized one is showed in fig. 6.14, a reduction of about 50% of the grain size was achieved.

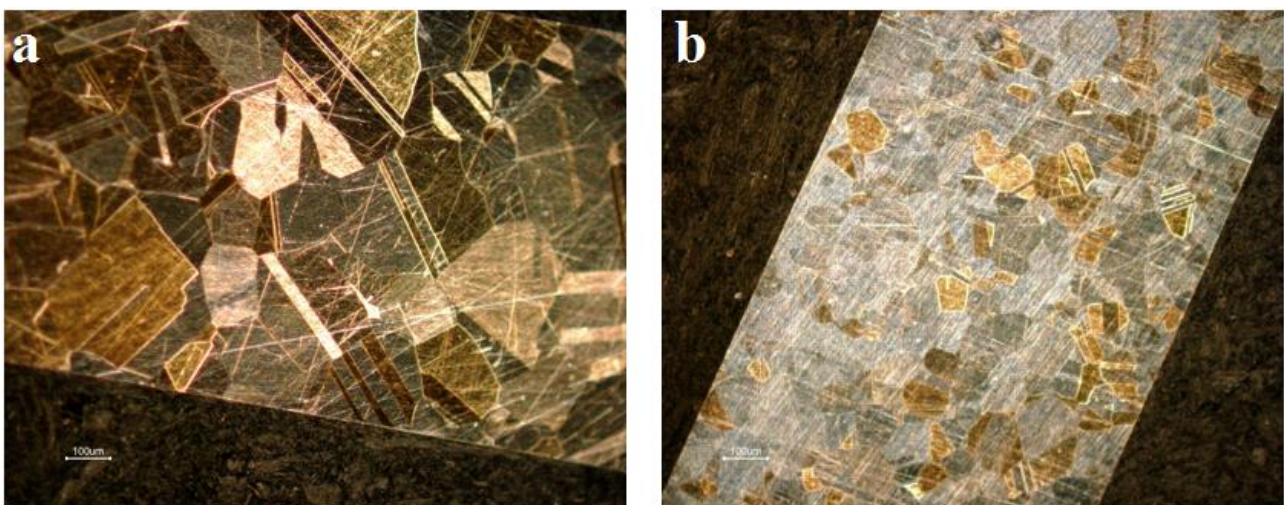


Fig. 6.14 - Microstructures of the final annealed wires, obtained with the old process (a) and the new optimized process (b)

All these devices were taken to improve the surface characteristics and to get a lower hardness of both the as-cast rod and the final annealing wire, as it is demonstrated by the hardness results, in table 6.10.

Tab. 6.10 - Micro-vickers hardness for the melted rods and the final annealed wires obtained with the two different production processes for the 18 Kt gold alloy

		Micro-hardness [HV _{0.025}]
As-cast rods	OLD PROCESS	200 ± 10
	NEW PROCESS	185 ± 5
1.00 mm diameter final annealed wire	OLD PROCESS	180 ± 10
	NEW PROCESS	165 ± 10

Also for this carat gold alloy several tensile tests were performed. Passing from the old to the new optimized process the gap of elongation and strength values, between the specimens taken from the same skein of yarn, become smaller. In figure 6.15, it is possible to notice a greater uniformity of the curves obtained with the tensile tests, index of a suitable recrystallization process.

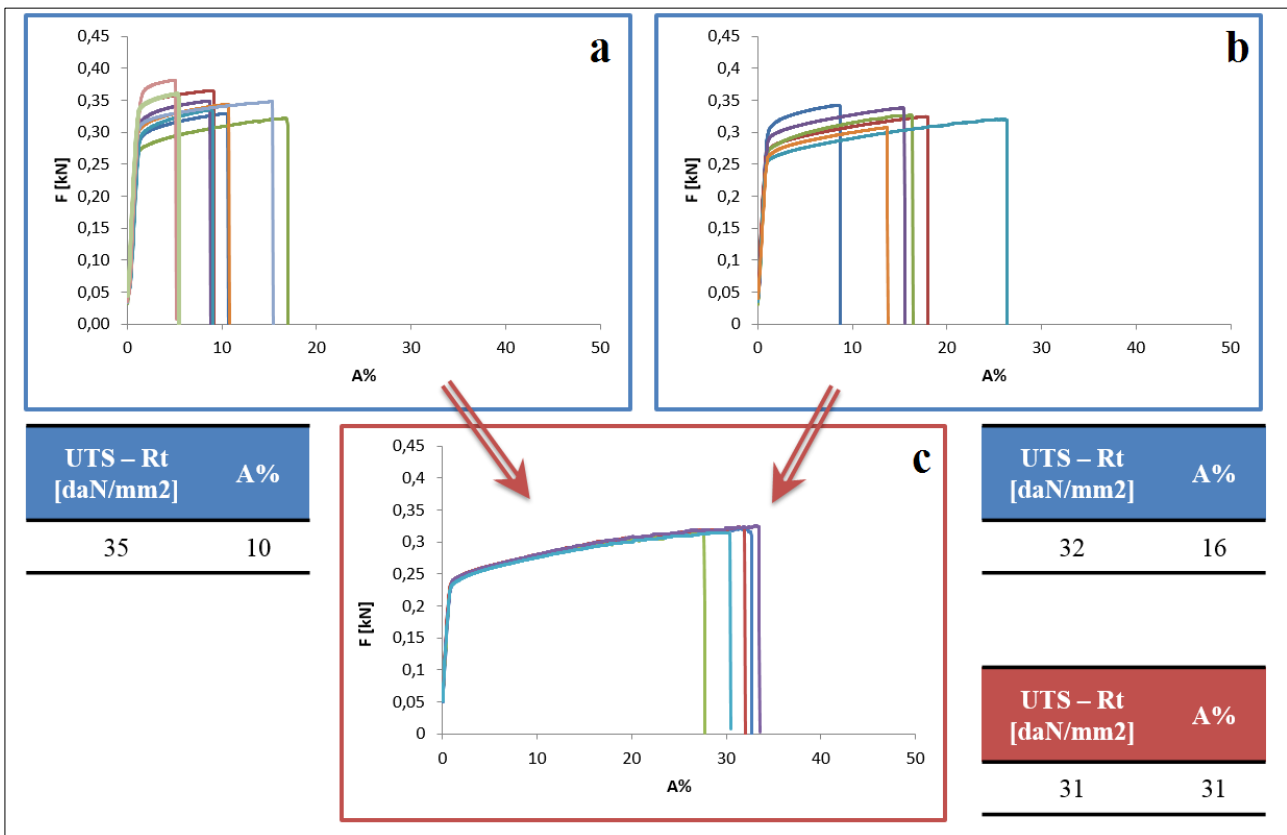


Fig. 6.15 - Tensile curves and the average values of strength and elongation for the final annealed wires obtained with the old process (a), (b) and the new one (c)

Changing several parameters of the process, the fractures, and therefore the wastes, were enormously reduced. Before, they amounted to about 30% of the production.

6.3.5 Residual stresses and corrosion resistance tests

As previously reported, the corrosion of gold alloys starts with a selective dissolution of the less noble species (particularly in welding alloys which are rich in such elements), and ends with the formation of superficial oxides and their decomposition [86]. Mass transport, defined as the volume diffusion from the bulk to the superficial layers of the material, is an important phenomenon as it leads to the exposure of more dissolvable species at the surface. This flow of atoms can be represented by an interior flux of lattice vacancies created by the dissolution of individual atomic sites on the surface of the alloys [87]. Generally gold alloys, near the equiatomic composition, form a face-centered cubic (FCC) lattice rather than a face-centered tetragonal (FCT) lattice. However, above 683K (410 °C), two ordered crystallographic structures (AuCuI and AuCuII) exist. When the AuCuI ordering prevails in the alloy, the arrangement of the atoms passes from FCC to FCT which generates a considerable amount of strain as a result of the distortion of crystal lattice [88]. These stresses lead to a decrease in the corrosion resistance of the material. The transition from the compact cubic structure to the tetragonal one, allows the less noble elements to migrate across the surface easily, which therefore increases the rate of volume diffusion.

In this thesis, the correlation between the residual stresses, resulting from the specific process parameters of the production cycles of gold wires and their corrosion resistance, was analyzed. The correlation between the decrease of the corrosion resistance and the increase of the tensile state can be found in literature for steels and other materials, but not for gold [89, 90]. The residual stresses were calculated using X-ray diffraction. A linear elastic distortion of the crystal lattice planes was assumed. The penetration depth of the beam depends on the material and on the parameters of the sample. Effectively, the measured strain is the average from depths less than a few microns under the surface of the specimens. Considering a crystalline material, the planes of atoms can cause

interference diffraction patterns; this interference is dependent on the spacing between the planes and the wavelength of the incident beam. A free strain material is characterized by a particular diffraction pattern dependent on a determined inter-planar spacing. The elongation and contraction produced during the deformation process of the gold wires generates internal strains in the crystal lattice which changes the spacing between the $\{hkl\}$ lattice planes. This results in a measurable shift and broadening of the diffraction pattern, due to a shift from the “free strain” position. This change in the inter-planar spacing can be evaluated in order to define the residual stress within the material [84]. Figure 6.15 shows the diffraction patterns of the gold alloys that have been studied.

For the 9, 10 and 14 Kt gold alloys, reference angles of 68.61° , 68.16° and 67.35° were used respectively.

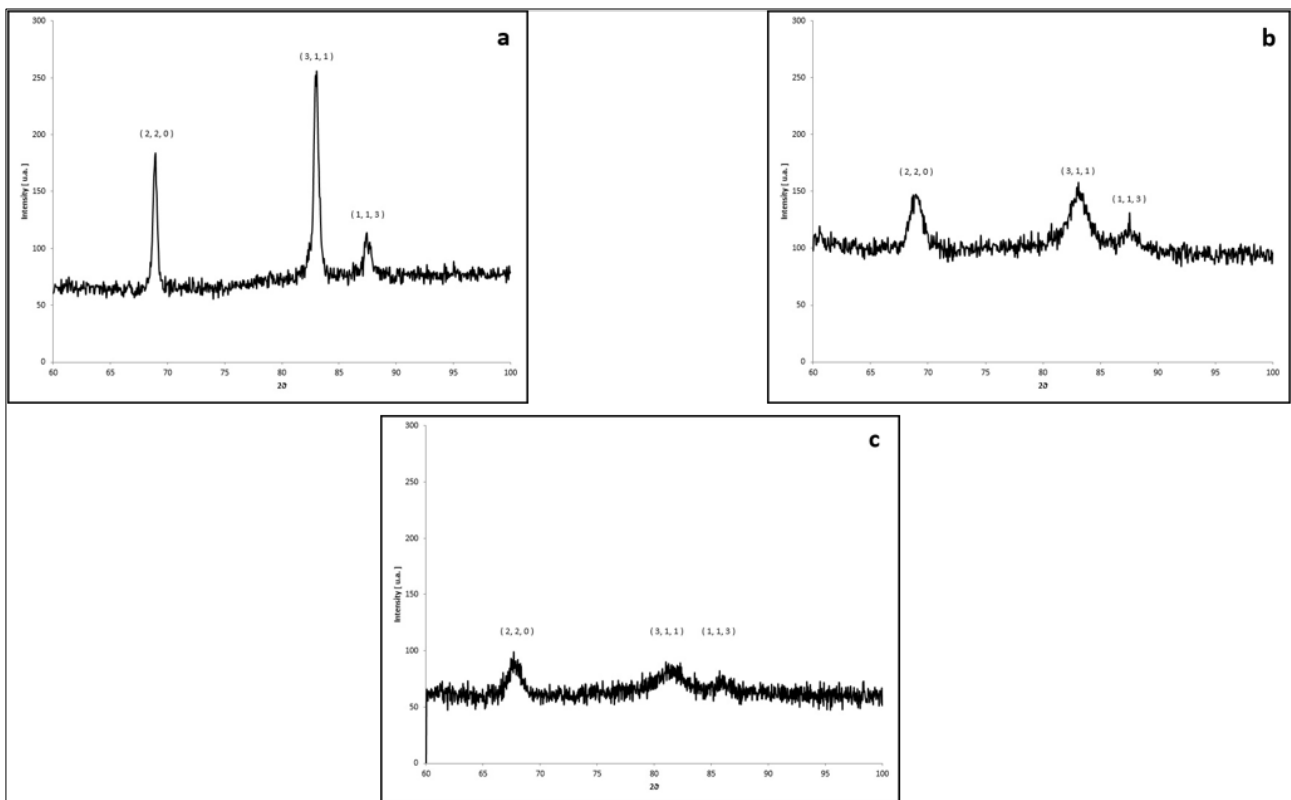


Fig. 6.15 - X-Ray Diffraction patterns for the 10 Kt carat gold alloy (a), for the 9 Kt gold alloy (b) and for the 14 Kt gold alloy (c)

The XRD analysis showed that the corrosion behavior of the gold wires depends not only on the specific process parameters but also on the stress state of the material and, in particular, is connected to the residual stresses. Tab. 6.11 shows the residual stresses obtained by XRD.

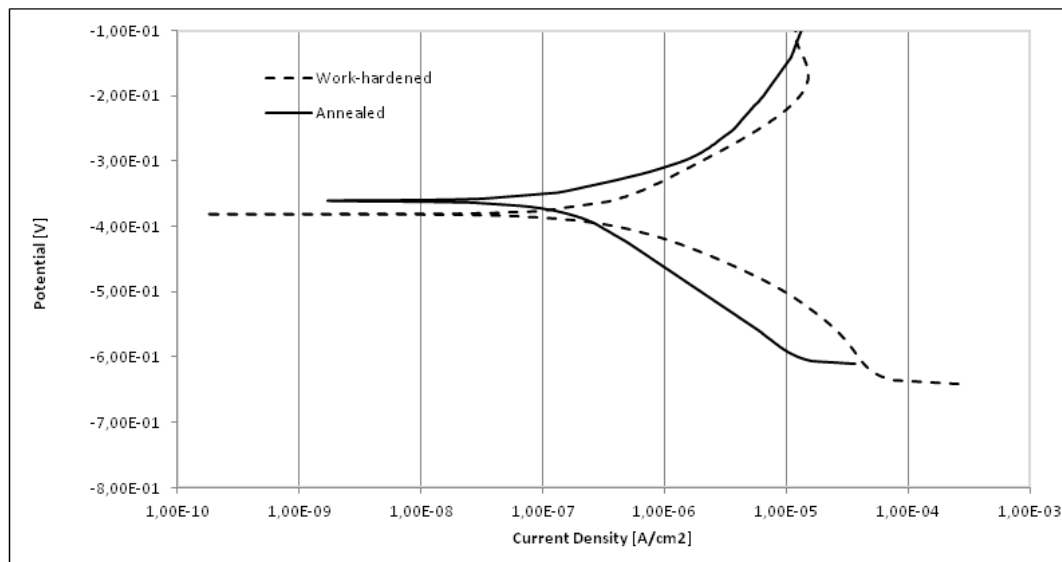
It should be noted that there is a considerable difference in the value of the residual stresses for the 9 Kt gold alloy specimens when obtained by implementing the new process. After the final step of rolling the surface tension of the wire was in a tensile state. The optimization of the annealing treatments changed this to a compression state.

Tab. 6.11 - *Residual stresses of all carat gold alloy samples that were studied*

9 Kt gold alloy deformed (New Process)	$\sigma = 49 \pm 6 \text{ Mpa}$
9 Kt gold alloy annealed (New Process)	$\sigma = - 227 \pm 26 \text{ Mpa}$
10 Kt gold alloy annealed (Old Process)	$\sigma = 158 \pm 66 \text{ Mpa}$
10 Kt gold alloy annealed (New Process)	$\sigma = - 51 \pm 29 \text{ Mpa}$
14 Kt gold alloy deformed (New Process)	$\sigma = 229 \pm 97 \text{ Mpa}$
14 Kt gold alloy annealed (New Process)	$\sigma = 120 \pm 29 \text{ Mpa}$

The greater homogeneity of the annealed material and the compressive strength of the wire resulted in a better corrosion resistance, as this study will demonstrate. To evaluate the difference between the first process and the optimized one for the 10 Kt gold-welding alloy, the final annealed microstructures of the specimens obtained with the two processes were tested. It is possible to analyze the different stress states generated by the different optimizations in the final step of wire production cycle. The change of the internal stress from a tensile superficial stress, achieved with the old process, to a compressive stress, obtained with the new process, resulted in an improvement of material's properties. The considerations regarding the 14 Kt gold alloy are the same as the 9 Kt gold-welding alloy. The greater homogeneity of the microstructure and the crystallization phenomena allowed to reduce the residual stresses.

In order to obtain information on the corrosion resistance of the different samples, anodic polarization tests in the solution that simulates human sweat were performed. Regarding the 9 Kt samples, work-hardened and annealed samples were compared and the results are reported in fig. 6.16, corrosion potentials and corrosion current densities (I_{corr}) were also evaluated and reported.

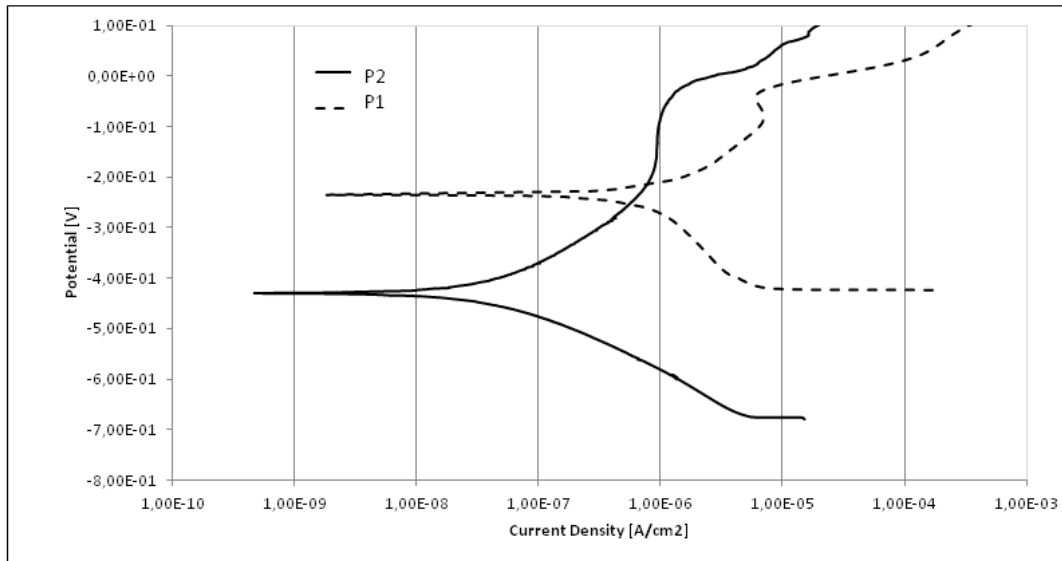


	Work - hardened	Annealed
I_{corr} [A/cm ²]	1×10^{-6}	1×10^{-7}
E_{corr} [V]	-0,38	-0,36

Fig. 6.16 - Potentiodynamic polarization test on the final work-hardened and the annealed wires obtained with the new optimize process for the 9 Kt gold alloy samples

It has been observed that the two samples have the same corrosion potential but the corrosion current density of the annealed sample, which is directly linked with the corrosion rate by Faraday's law, is one order of magnitude lower. This observation can be connected to the decrease of the internal residual stresses during the annealing process, as previously discussed. For the 10 Kt alloy, samples were compared between the old and new production processes. The results of this comparison are presented in fig. 6.17. A significant increase in the corrosion resistance can be observed with the new process, as the samples are characterized by a value of I_{corr} which is

approximately one order of magnitude lower, even though the corrosion potential is 0.2 V higher in the samples obtained with the old process.

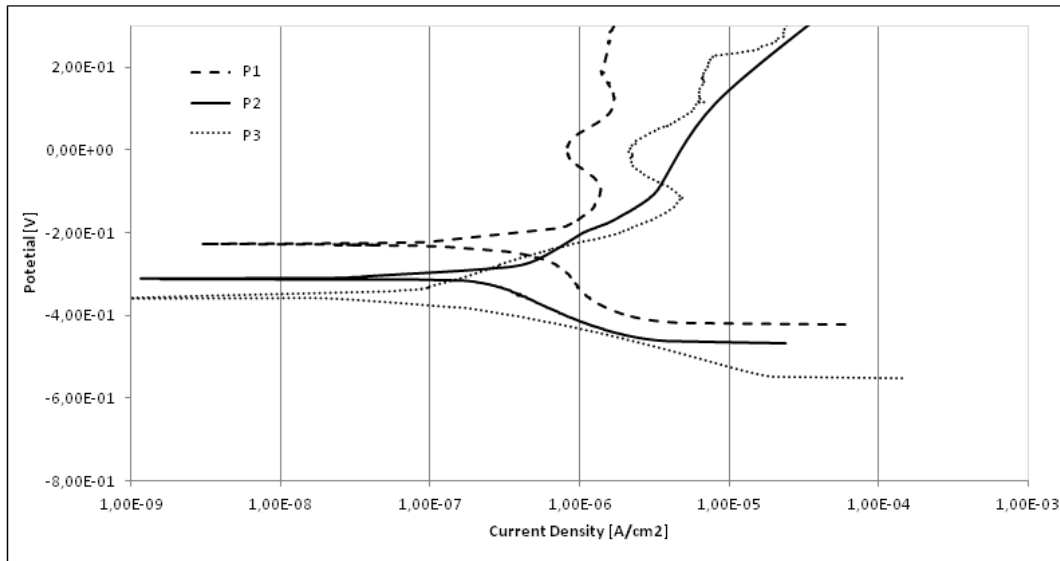


	Old Process (P1)	Optimized Process (P2)
I_{corr} [A/cm ²]	8×10^{-7}	7×10^{-8}
E_{corr} [V]	-0,23	-0,41

Fig. 6.17 - Potentiodynamic polarization test on the final annealed wires obtained with the two different processes performed for the 10 Kt gold alloy samples

In the case of the 10 Kt sample, the improved corrosion performances can be correlated with the decrease of the residual stresses in the samples obtained with the optimized process as previously discussed.

Samples of 14 Kt gold alloy obtained with the old and the new process were tested, and the results are reported in fig. 6.18. In the case of 14 Kt samples, the samples obtained with the new process are characterized by a higher corrosion resistance due to the lower residual stresses previously reported, so that the corrosion current density decreases by one order of magnitude.



	Old Process (P1)	Modified Process (P2)	Optimized Process (P3)
I_{corr} [A/cm ²]	6×10^{-7}	2×10^{-7}	1×10^{-7}
E_{corr} [V]	-0,23	-0,30	-0,36

Fig. 6.18 - Potentiodynamic polarization test on the final annealed wires obtained with the three different processes for the 14 Kt gold alloy samples

For all of the analyzed alloys, the corrosion tests performed on the different samples give evidence for an increase in the corrosion resistance (observed with the decrease of the corrosion current density) that can be correlated with the decrease of the internal residual stresses as shown by XRD analysis [91].

6.3.6 Concluding Remarks

The presented optimization of the production steps of gold-welding alloys allows one to have a consistent reproducibility of the material properties. A greater control of time and temperatures, during the melting and annealing processes, demonstrated the relevance of a proper control in the process parameters in order to obtain the desired results in term of hardness. With an immediate cooling out of the furnace there is insufficient time to create an orderly distribution of atoms in the microstructure, therefore the annealing process generates a decrease in hardness. The gold wire can be further deformed because the recrystallization process restored the initial workability. The

optimization of the whole process had not only an influence on the hardness but, also, produced an increase in the ductility of the gold alloys and in the microstructural homogeneity. The final grain size was also reduced. The tensile tests, performed on the final annealed wires, showed a smaller range of variability of the tensile curve, which is indicative of improved uniformity of properties along the skein of yarn produced. The optimization of the melting, rolling and annealing processes for gold-welding alloys wires allows for the reduction the residual stresses on the wires at the end of the production cycle, with improvements in mechanical properties, machinability, corrosion resistance during the emptying process, and a better finishing surface. The potentiodynamic polarization tests performed on the samples showed the importance of minimizing the residual stresses. It was shown that, independently of the carat of the gold alloys, the annealed microstructures, characterized by a lower level of residual stresses, have a better corrosion resistance. The corrosion current densities increased by one order of magnitude in the deformed samples, which implies an increase in the corrosion rate. Considering the same annealed state on samples produced either with the old process or with the optimized process, it is possible to say that the grain size and the homogeneity of the microstructure strongly influence the corrosion susceptibility of the gold alloys. Smaller grain size and greater homogeneity, obtained with the optimized process, are preferred because these characteristics cause an increase in the corrosion resistance of the material.

Chapter 7

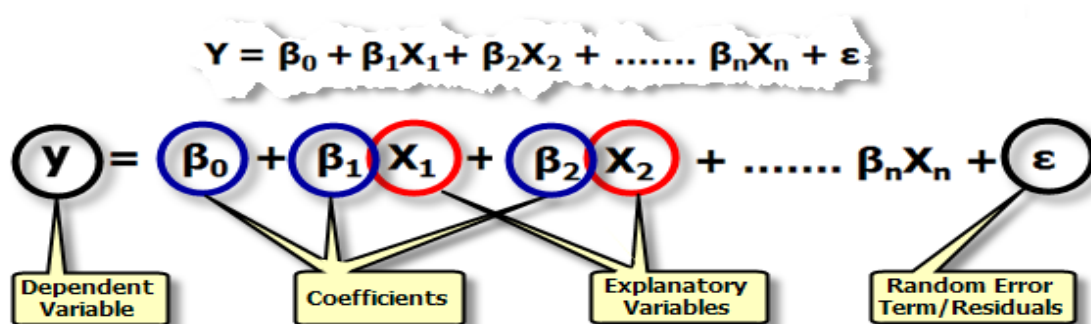
Statistical Analysis on a Mechanical Tests Dataset of Gold Alloy Wires

In this chapter, different mechanical and compositional characteristics of gold alloy wires will be studied with the purpose of approximating the possible existing influences and relationships between these and the energy absorbed during deformation.

The use of some general statistical models, such as the linear or general regression model, and the analysis of the residuals obtained from the study (histograms, scatterplots, normal probability plots...) has allowed us to draw some important conclusions.

Compositional variant has a marginal influence on the dependent variable while mechanicals play an important role.

The aim of this statistical model is to possibly identify a linear relationship between a dependent variable (or response) Y and several independent variables (regressor variables) x



It tried to define these relationships by analyzing the influence of some mechanical and compositional properties (elongation, Young modulus, ultimate strength, concentration of gold) on the energy absorbed by the material during the deformation. This type of study is necessary because the company does not possess an historical database of its alloys, and in literature, only scanty information is available about metallographic and mechanical characterization of gold alloys.

The dataset is obtained from tensile tests on 100 gold wires of different carat weights, the final diameter of 1,00 mm is the result of a series of deformations and subsequent annealing.

For this statistical computing and graphics the free software environment R has been employed, a fully planned and coherent system designed around a computer language. Minitab is the other software used for the graphic part.

Being a random sample, it is possible to generalize the behavior of this dataset to a large number of samples.

The variables measured are showed in Tab. 7.1:

Tab. 7.1 – Variables obtained from the tensile tests performed and used in the statistical analysis

Absorbed Energy [J]	UTS - R_t [daN/mm ²]	A% - Elongation	E – Young Modulus [daN/mm ²]	Gold Concentration ‰
14.3	37.17	28.8	3453	750
10.4	36.19	20.3	3529	750
13.7	38.30	25.8	3244	750
10.6	35.09	21.8	2800	750
13.7	38.35	25.3	3700	750
21.9	45.87	35.1	3665	417
21.0	45.48	34.2	3087	417
20.9	45.03	34.3	3487	417
18.9	43.98	31.3	4017	417
20.9	44.70	33.9	3522	417
21.7	44.27	35.9	2916	417
9.8	38.01	18.4	2935	750
11.9	40.71	20.9	3229	750
10.6	38.95	19.5	3262	750
9.9	39.95	17.7	3491	750
9.9	39.55	18.3	3543	750
15.4	35.71	31.5	2828	750
14.7	36.44	29.2	2957	750
13.7	36.63	26.6	2787	750
14.8	38.66	27.6	2858	750
17.4	42.79	29.5	3349	417
19.1	45.59	30.6	3299	417
18.8	44.98	30.4	4144	417
21.5	54.99	29.0	2282	585
23.7	55.88	31.2	4033	585
22.8	55.18	30.2	4137	585
19.7	45.72	31.6	3186	417
22.4	46.98	35.4	3196	417
22.3	46.69	35.4	3453	417
19.6	46.40	31.5	3291	417
20.3	45.87	33.1	3094	417
22.1	46.27	35.6	2367	417
22.9	46.35	36.3	3492	417
20.3	45.39	33.4	3208	417
22.7	46.54	35.8	3001	417
12.3	36.83	24.0	2897	750
15.7	36.95	30.8	2904	750
12.5	36.95	24.3	3366	750
11.4	37.65	21.9	3248	750

4.4	41.06	7.9	3197	750
9.1	38.36	18.0	3355	750
10.7	38.52	19.8	2806	750
4.1	43.53	7.4	3940	750
21.8	45.80	35.0	3277	417
22.2	45.73	36.2	3422	417
23.4	45.30	38.3	3332	417
13.4	37.98	25.1	3485	750
12.3	36.15	24.6	3049	750
11.4	36.10	22.7	3274	750
14.2	39.56	25.4	3192	750
12.6	39.50	23.1	2898	750
14.5	39.30	26.0	3760	750
15.1	37.75	28.6	3117	750
12.7	38.18	23.8	3379	750
13.0	36.95	25.4	2529	750
15.0	38.45	27.8	3302	750
11.1	36.91	21.7	3281	750
11.8	37.04	22.8	2801	750
15.5	37.40	30.1	2868	750
11.9	40.64	20.9	3238	750
17.3	39.06	32.5	2390	750
12.8	41.30	21.9	3470	750
16.0	38.21	31.0	2954	750
12.0	38.20	22.8	3268	750
21.1	46.97	32.5	4020	375
21.6	47.54	32.7	3830	375
17.6	45.77	29.0	3977	375
22.8	44.98	38.5	3529	375
21.2	45.49	35.4	3585	375
24.2	46.10	39.7	3934	375
21.9	47.14	33.6	4008	375
23.7	47.28	36.0	4004	375
21.4	45.12	34.7	3848	375
20.9	45.58	33.5	3928	375
21.4	45.02	35.5	3664	375
23.3	44.79	38.7	4125	375
23.3	45.72	37.0	3944	375
20.7	45.07	33.9	3757	375
21.5	45.45	34.7	4047	375
13.7	38.29	25.9	3061	750
11.1	40.74	19.5	3818	750
13.7	35.69	27.9	2661	750
8.1	40.99	13.9	4070	750
13.4	41.58	23.1	4128	750
13.1	40.74	22.9	3764	750
11.6	40.93	20.1	3499	750
18.4	38.60	34.6	3828	750
12.3	41.41	21.1	4065	750
19.9	46.49	31.0	3810	417
18.8	46.40	29.2	3842	417
19.2	46.75	29.7	4157	417
19.3	50.78	27.6	3523	585
21.7	50.73	31.2	3827	585
22.8	51.48	32.4	3650	585

16.5	38.69	31.7	3611	750
12.0	41.51	20.6	3845	750
17.6	39.90	31.8	3682	750
14.7	41.93	24.7	3905	750
13.8	41.00	23.8	3511	750
18.7	39.95	33.4	3600	750

A preliminary analysis of data distributions shows that it is possible to define a relationship between the energy absorbed by the system during deformation and, for example, the elongation, but not exactly the gold concentration, figures 7.1 and 7.2.

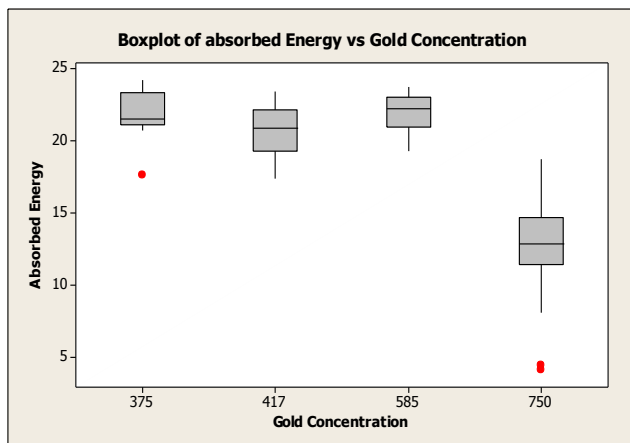


Fig. 7.1

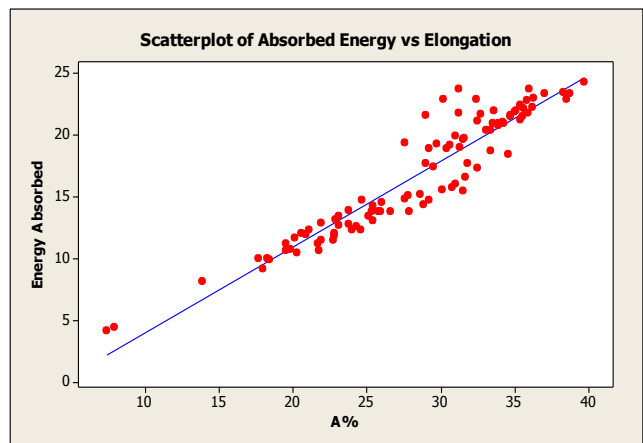


Fig. 7.2

Although the Young Modulus presents a normal distribution of value, it is characterized by a random pattern in the scatterplot, graphs are showed in figures 7.3 and 7.4.

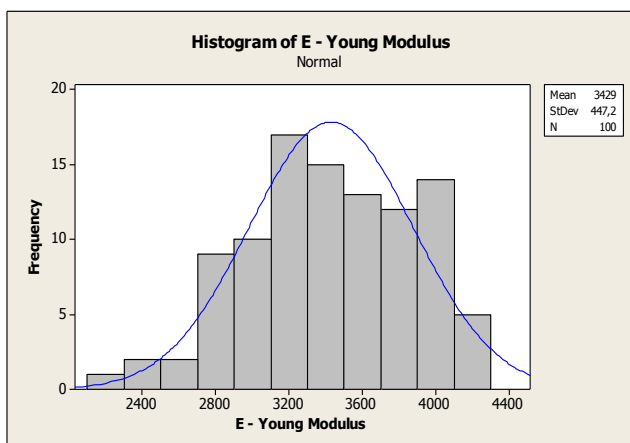


Fig. 7.3

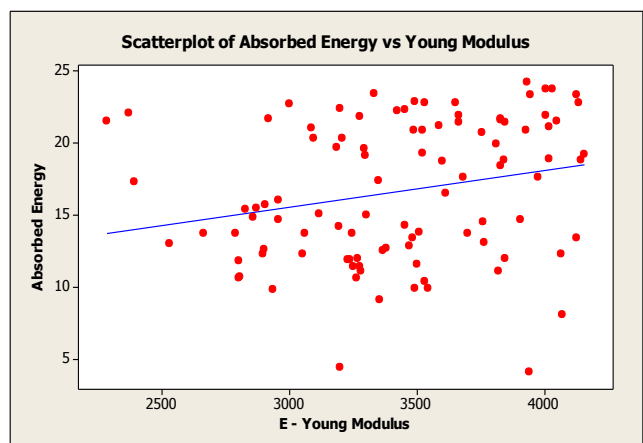


Fig. 7.4

However, a two sample t-test, which results are showed in table 7.2, confirms the hypothesis of a possible relationship between absorbed energy and gold concentration; in fact, the p -value < 0.05

(confidence level 95%) and the great difference of means are indicative that the gold content in alloy influences the material deformation.

Tab. 7.2 – Results of the two samples t-test performed

t	df	p-value	Gold Concentration	
			K mean Gold 18K [J]	K mean Gold 9K [J]
-15.9166	40.53	< 2.2e-16	12.81636	21.77333

The resistance seems related to the energy absorbed by the system too. Its chart's observation is similar to the elongation one, figure 7.5.

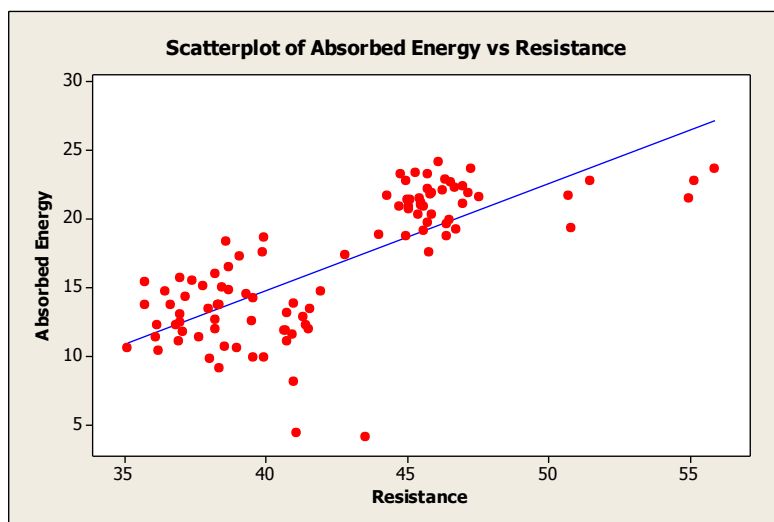


Fig. 7.5

The goal is to understand the variation in the response that can be partially explained by predictors. For this purpose a linear regression model will be used because the response variable is continuous, Tab. 7.3.

Tab. 7.3 – Parameters of the statistic model used

Predictors	Estimates	Standard error	t value	P-value
Rt	0.3818	0.0105	36.392	<2e-16
A%	0.5612	0.00734	76.471	<2e-16
E	0.000116	0.000079	1.462	0.147
Conc. Gold	0.000126	0.000368	0.343	0.733

The regression equation is:

$$G = -15.9 (\text{constant}) + 0.382 Rt + 0.561 A\% + 0.000116 E + 0.000126 \text{ Conc. Gold} \quad (7.1)$$

Tab. 7.4 – Output of the linear regression model

Multiple R-squared	0.996	This model explains about 99.58% variation in absorbed energy, and the F-test gives a very small p-value, indicating the full model is useful, as it is showed in table 7.4.
Adjusted R-squared	0.9958	
Residual std. error	0.3138	
p-value	< 2.2e-16	

However, the concentration of gold in this model is not significant although in the first analysis it seems to be quite the opposite. Probably in the full predictors model the concentration of gold has a marginal influence on the energy absorbed as compared with other covariates.

As shown in the graphs of residuals analysis (figures 7.6, 7.7, 7.8 and 7.9), this model may be good because it fits the data well.

Values of residuals are distributed around the zero line without a clear pattern, and the normality assumption is appropriate; in fact, the points in the Normal Probability Plot are roughly close to a straight line. The histogram of the residuals shows a trend of value similar to a Gaussian curve, so it is possible to consider the sample sufficiently large [92].

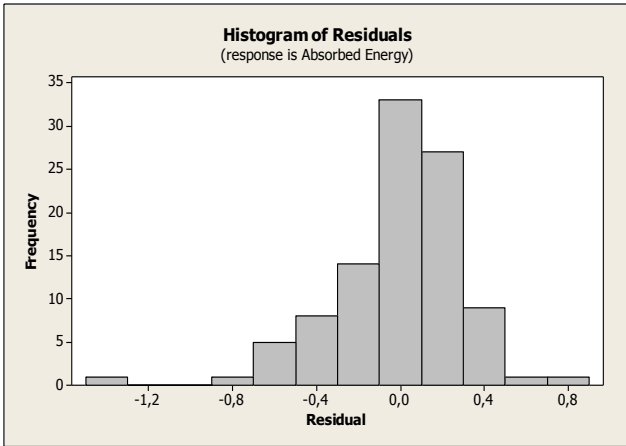


Fig. 7.6

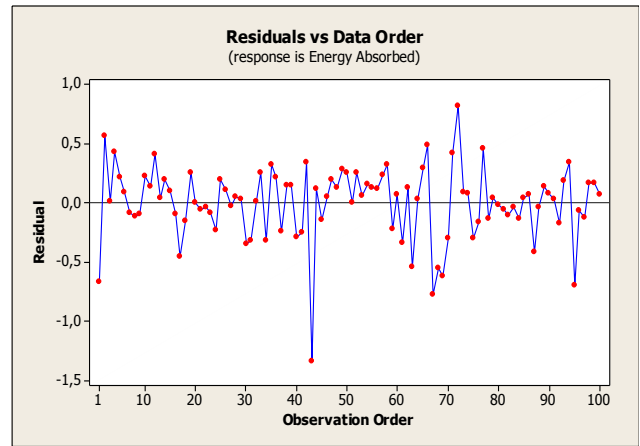


Fig. 7.7

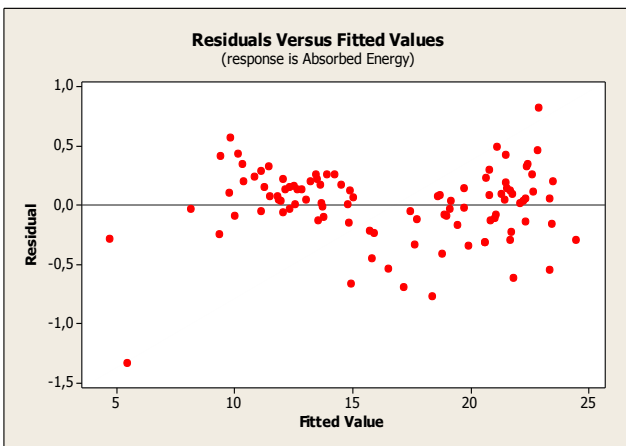


Fig.7.8

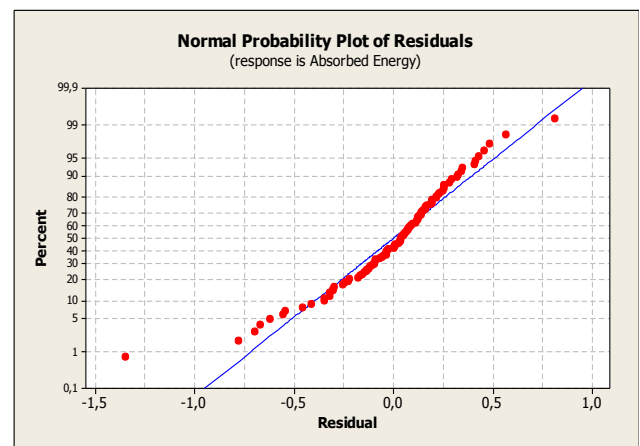


Fig. 7.9

Analyzing the data with another statistics model, for example a logistic regression model, it is possible to compare the new results with the previous.

Deviance Residuals:

<i>Min</i>	<i>1Q</i>	<i>Median</i>	<i>3Q</i>	<i>Max</i>
-0.25174	-0.10969	-0.01430	0.03837	0.71998

Coefficients:

	<i>Estimate</i>	<i>Std. Error</i>	<i>t value</i>	<i>Pr(> t)</i>
<i>(Intercept)</i>	-1.605e+00	6.348e-01	2.529	0.01313 *
<i>Resistance</i>	2.925e-02	1.321e-02	2.215	0.02923 *
<i>Elongation</i>	2.839e-02	4.530e-03	6.266	1.14e-08 ***
<i>Young Modulus</i>	6.943e-05	5.214e-05	1.332	0.18623
<i>Gold 10K</i>	8.482e-02	6.621e-02	1.281	0.20338
<i>Gold 14K</i>	-5.739e-02	1.346e-01	-0.426	0.67084
<i>Gold 18K</i>	-3.457e-01	1.265e-01	-2.733	0.00752 **

*Signif. codes: 0 '***' 0.001 '**' 0.01 '*' 0.05 '.' 0.1 ' ' 1*

The interpretation of the regression coefficient is similar for linear regression and logistic regression.

The influence of the Young Modulus on the absorbed energy is not significant as already seen in the previous model, and only the concentration of 18K gold seems linked to energy. This could explain the hypothesis of the partial influence of this characteristic on the values of the response.

These results indicate that the selected covariates may be related to absorbed energy, whether energy is viewed as a continuous variable or a discrete variable.

Finally, a possible linear relationship between absorbed energy, tensile strength and elongation was defined, with a useful statistical model:

$$\text{Absorbed energy} = -15.9 (\text{constant}) + 0.382 Rt + 0.561 A\% \quad (7.2)$$

These conclusions and results can be generalized to other more general settings because, in this analysis, the most common commercial type of gold alloys have been investigated.

It is important to pay attention to the concentration of gold and its not linear relationship with the energy absorbed during deformation.

The large sample used is quite representative of a bigger population so the statistical analysis, the p-values and the diagnostic analysis of residuals can be considered objectively valid. However, it is not always true, probably because the data may not be strictly independent.

Chapter 8

Study of 10 Kt Gold Alloys Used in Cable Chain Industrial Production Processes

8.1 INTRODUCTION

In this chapter, the production processes parameters of gold alloys plates were investigated to optimize the microstructure and the mechanical properties of the products. These gold alloys plates were successively welded to an iron sheet to create the base for the final hollow chain products.

For this study, two different 10 Kt gold alloys were used: one containing a higher amount of silver and Co as grain refiner, the other one with a lower amount of silver and ruthenium as grain refiner.

The microstructures were analyzed by optical and scanning electron microscopy, whereas the variation of mechanical properties by micro-hardness tests. The changing of the process parameters and of the compositions of the alloys may lead to different levels of residual stresses within the material, which can generate a variation in the mechanical and corrosion behavior of gold sheets. The residual stresses of the samples were evaluated using XRD analysis, whereas the corrosion resistance by potentiodynamic polarization tests. The results showed that with the optimized process and using the alloy with ruthenium a higher homogeneity of the microstructure, with an increase of the quality of semi-finished products, was obtained.

Moreover, to improve the weldability of the final chains, a different gold welding alloy with a lower melting point was developed and optimized.

8.2 EXPERIMENTAL PROCEDURE

Object of this research were gold alloys sheets that are used to be welded to an iron sheet to create the base for the final hollow chain products. In the production of hollow chains, the iron core is necessary to support the gold sheet, during the plastic deformation processes, when the double-layer wire is produced. A solder wire is inserted after the plating of gold and iron sheets to allow the welding process after the chain's formation [72]. This iron core has to be removed by chemical dissolution in HCl solutions [85]. During this step, called "emptying" process, the corrosion phenomena have to be monitored to avoid problem on the final quality of the products.

In the present work, the production parameters process of gold alloys sheets were studied to optimize the whole process. In particular, to avoid rupture during rolling process, the parameters of

continuous casting and of the annealing treatment were modified. The results were correlated to the microstructure and to the mechanical properties of the material. Two different 10 Kt alloys were investigated to improve the machinability and to optimize the final properties of the products.

Moreover, two compositions of the welding alloy, used for the solder wire, were studied and optimized to improve the weldability of the chains produced with the gold sheets.

The composition of the gold alloys studied in this investigation are reported in Tab. 8.1.

Tab. 8.1 - Chemical composition of the 10 carat yellow gold alloy studied

	Kt	Au [%]	Zn [%]	Ag [%]	Cu [%]
Alloy 1 with Co	10	41.7	5.5	17.3	BALANCE
Alloy 2 with Ru	10	41.7	6.3	12.8	BALANCE

The alloy 1 contained a higher amount of Ag (17.3%) and use Co as grain refiner, whereas the alloy 2 contained 12.8% of Ag and as grain refiner was used Ru. The study about the optimization of the continuous casting and of annealing treatment parameters was performed with the alloy 1. The microstructural analysis and hardness tests were performed in order to analyze the effect of the variation of process parameters on the structure and the mechanical properties of the alloys. A mapping of the temperature over time during the annealing process was also performed. The heating conditions and the temperatures in the annealing furnace were modified in order to ensure a suitable recrystallization process.

The optimized parameters obtained in the first part of the study, were applied also to the alloy 2 and the results were compared with the results of the alloy 1.

To evaluate the mechanical properties of the samples, hardness tests were performed. Optical microscopy (OM) observation was performed with the aim to evaluate the microstructure of the sample. The samples were prepared with the standard metallographic technique of polishing and the electrolytic etching was performed using a low concentrate HCl solution, a platinum wire as cathode and a voltage of 1.5 V. Other etching processes, using different solution of cyanide, are optimized and performed at the laboratory of Progold S.p.A.

SEM microscopy observation and several residual stresses tests were performed to evaluate the structure and the properties of the material. The corrosion resistance of the gold alloys employed for the production of gold sheets was evaluated with potentiodynamic polarization tests in a solution of 10% HCl. In fact, this solution simulates the environment of the emptying process when the semi-finished products are transformed in hollow chains. Anodic polarization tests were performed using a saturated calomel electrode as the reference electrode (SCE) and a platinum electrode as the counter electrode, figure 8.1.

Finally, regarding the study of new welding alloys for the solder wire, a new composition was developed and analysed (Tab. 8.2).

Tab. 8.2 - Chemical composition of the two different 10 carat yellow gold welding alloys

	Kt	Au [%]	Zn [%]	Ag [%]	Ga [%]	Cu [%]
Old alloy	10	41,7	17,1	17,6	-	BALANCE
New alloy	10	41,7	3,9	28,2	3,7	BALANCE

The corrosion resistance of the welding alloys was evaluated with potentiodynamic polarization tests in a solution that simulates human sweat, in order to replicate the environment of final use for the welding wires. The solution consisted of 0.5% NaCl, 0.1% lactic acid and 0.1% urea. NaOH was used to guarantee a pH of 6.5.



Fig. 8.1 - Anodic polarization tests system

8.3 RESULTS AND DISCUSSION

The different steps of the process can be observed in Tab. 8.3 and Tab. 8.4.

Tab. 8.3 - Continuous casting parameters for the old production path for the 10 carat gold alloy

MELTING PROCESS	T crucible [°C]	T mould [°C]	Melting velocity [mm/s]	Working t [s]	Pause t [s]	T before quenching [s]
	1120	710	3	1	1	0

Tab. 8.4 - Deformation and annealing process parameters for the old production path for the 10 carat gold alloy

PROCESS	T Annealing [°C]			t Annealing [min]
ROLLING	1° STEP			
ANNEALING	660	660	660	45
ROLLING	2° STEP			
ANNEALING	660	660	660	45
ROLLING	3° STEP			
ANNEALING	660	660	660	45
PLATING				
ANNEALING	660	660	660	45

In particular, the production cycle of the final sheet started with the continuous casting process, passing through the deformation and annealing steps, and finished with the plating process. The first production problem, considered in this part of research, was about the ruptures under the train rollers (showed in Fig. 8.2).

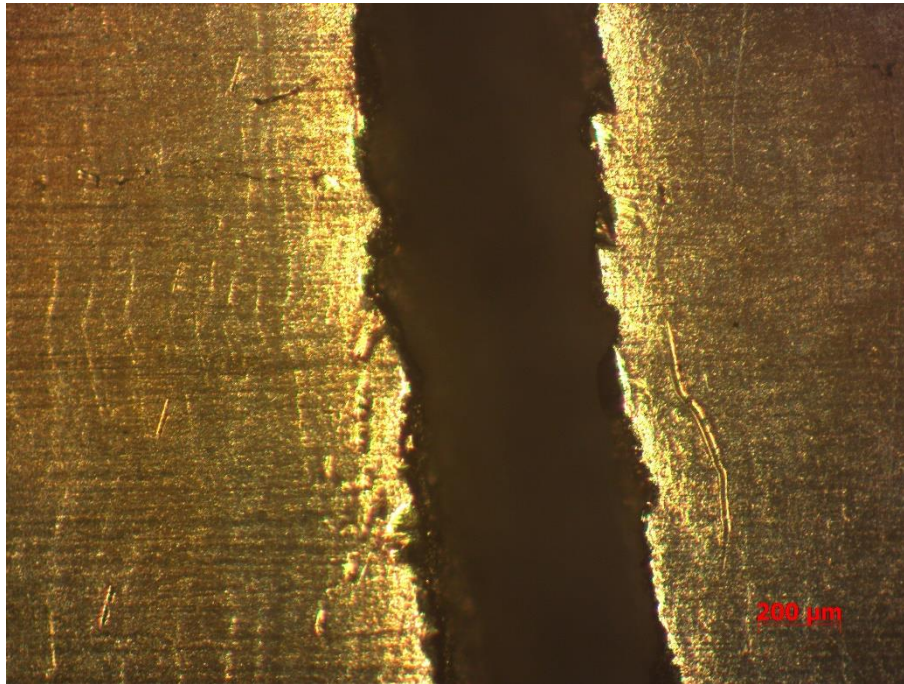


Fig. 8.2 - Gold sheet surface particular, ruptures during deformation steps

Several micro-hardness and residual stresses tests were performed on the gold alloy sheets in order to investigate the problem. The aim was to verify whether the continuous casting parameters could affect the material's susceptibility to rupture. Moreover, a mapping of the annealing temperature was performed to control its trend during the progress of the semi-finished products charges into the static step furnace. A thermocouple linked to the gold sheets was used. Analyzing the results, showed in Tab. 8.5, the measures of the graphite mould was modified, Fig. 8.3.

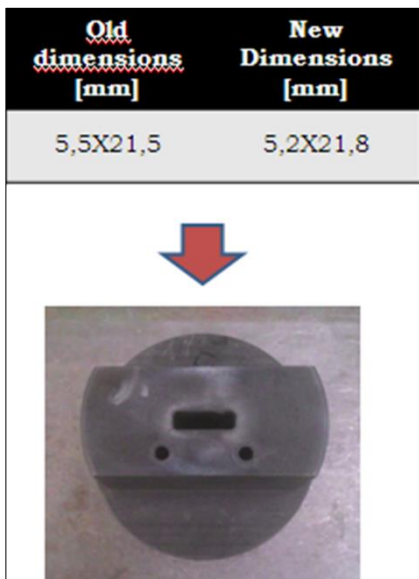


Fig. 8.3 - Change of the melting mould's dimensions and its representation

The thickness of the sheet was reduced and the width was increased, with a small reduction of the total area of the mould size. The aim was to reduce the stresses generated during the first steps of rolling and to increase the velocity of solidification after the melting process, with an improvement of the workability of the material. The rolling steps remained the same while the temperatures of the annealing treatments were modified. As it is possible to observe in Fig. 8.4, which shows the results of the temperatures mapping, the initial configuration of the annealing furnace did not allow to maintain the material over the recrystallization temperature for a suitable time into the furnace, figure 8.5. The optimization of the process involved the increase of the temperature in the first and in the second zone of the

furnace in order to rise the velocity of heating of the gold sheet charged.

Tab. 8.5 - Micro-vickers hardness and residual stresses values obtained with the standard production process and the optimized production path for the 10 carat gold alloy (alloy 1)

PROCESS	Hardness tests (Standard Process) [HV]	Hardness tests (Optimized Process) [HV]		Residual stresses – σ (Standard Process) [MPa]	Residual stresses – σ (Optimized Process) [MPa]
AS-CAST	160 ± 10	160 ± 5		- 55 ± 5	- 63 ± 10
1° ROLLING STEP	270 ± 5	250 ± 5		58 ± 10	30 ± 2
ANNEALING	170 ± 5	160 ± 5		- 28 ± 3	- 69 ± 7
2° ROLLING STEP	265 ± 10	215 ± 10		95 ± 8	70 ± 7
ANNEALING	170 ± 5	165 ± 5		- 48 ± 6	- 62 ± 13
3° ROLLING STEP	255 ± 5	240 ± 5		83 ± 5	30 ± 5
ANNEALING	170 ± 5	160 ± 5		57 ± 12	- 55 ± 8
PLATING	170 ± 5	160 ± 5		-29 ± 9	- 32 ± 8
ANNEALING	165 ± 5	150 ± 5		-51 ± 8	- 81 ± 7

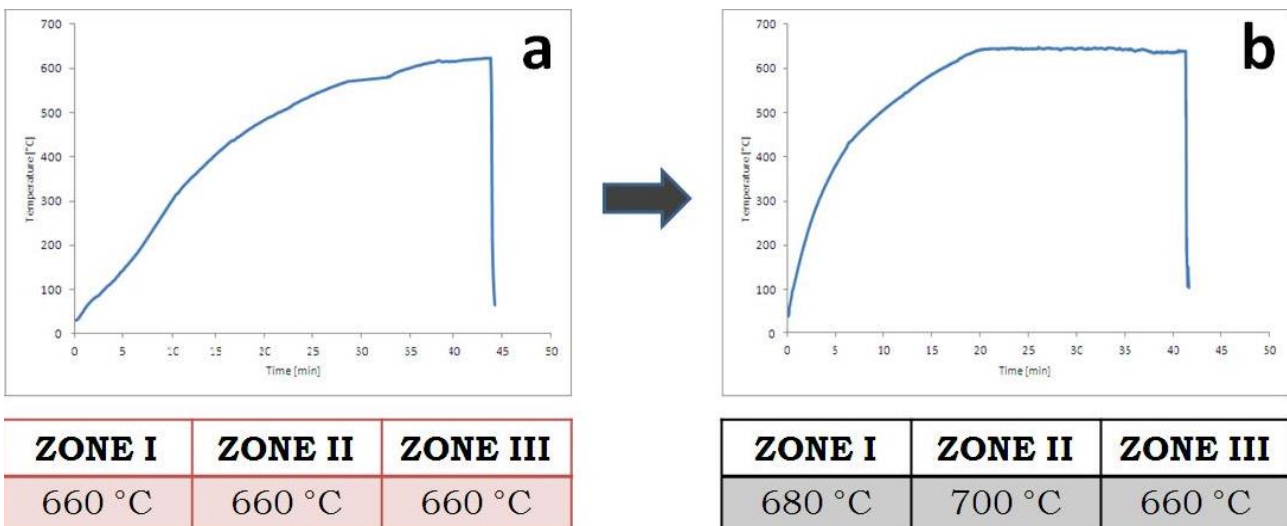


Fig. 8.4 - Temperatures mapping of the three different zone of the annealing furnace, obtained with the old process (a) and the new optimized one (b)



Fig. 8.5 - *Static step annealing furnace used in the process*

The process was modified in order to hold the samples for 15-20 min, over the characteristic temperature required by the recrystallization (about 600°C). From OM analysis it resulted that the section's reduction of the gold sheets, adopted during the continuous casting process, allowed to obtain a greater microstructure homogeneity of the material (Fig. 8.6).

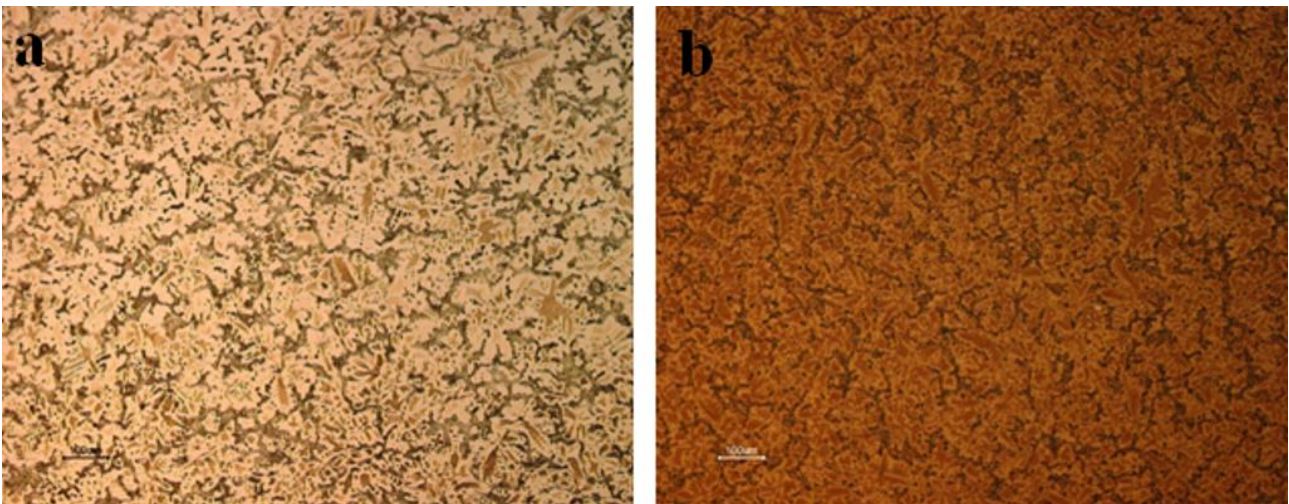


Fig. 8.6 - *Microstructure of the gold alloy sheet obtained with the standard process (a) and after the modify to the mould dimensions (b). OM images*

Moreover, modifying the temperatures of the annealing treatment, an increase of the grain dimensions was observed, as is shown in Fig. 8.7.

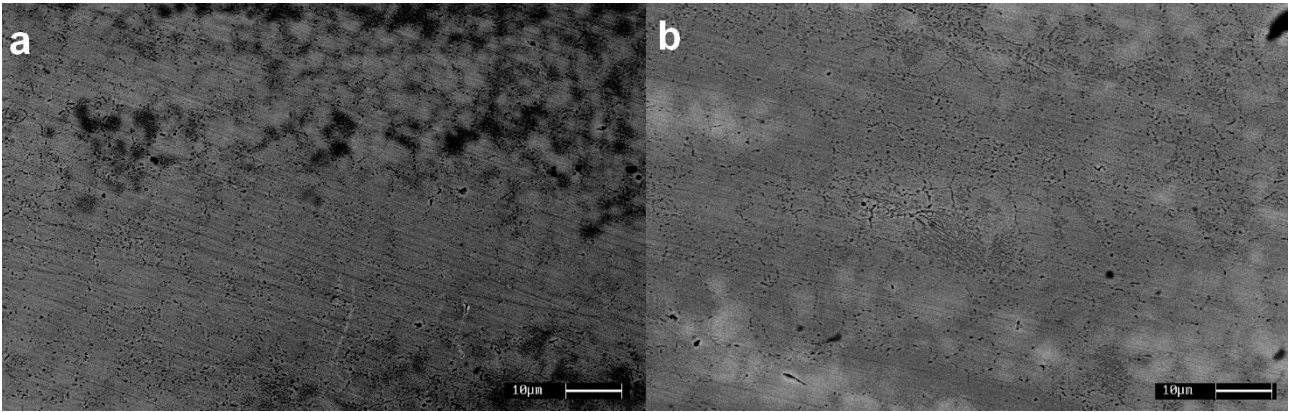


Fig. 8.7 - Microstructure of the gold alloy sheet obtained with the standard process (a) and with the new optimized process (b). SEM images

This is an index of the quality of the semi-finished products. In this work of thesis, the correlation between the residual stresses, resulting from the specific process parameters of the production cycles of gold sheets and their tendency to ruptures during deformation processes, was analyzed. The modification of the process parameters changed the material structure and its behavior. In fact, as previously showed in Tab. 8.5, passing from the old production process to the new optimized one, it was possible to observe a decrease in hardness for the samples taken at the end of the production process. Moreover, after each optimized deformation and the annealing step, the samples obtained were characterized by a decrease of the hardness value with an improvement of the machinability of the material.

The residual stresses were evaluated using X-ray diffraction. The strain in the crystal lattice was measured and the combined residual stresses were defined from the elastic constants. Table 8.5 shows also the residual stresses obtained by XRD analysis. A significant difference in the values of the residual stresses passing from the old to the new optimized process was observed. The tensile superficial stresses, obtained after the rolling steps, decreased whereas the compressive stresses, resulted after the melting and the annealing processes, increased. The greater homogeneity of the microstructure and the crystallization phenomena, obtained with the new process, allowed to reduce the residual stresses and to improve the material's properties. From the industrial point of view, with the new process, the ruptures under the rollers train during deformation steps were avoided, thus increasing the constancy of the process and reducing the production of metal waste.

The second part of this chapter was focused on the possibility to improve the workability of the gold sheets and on the elimination of the undesired magnetic behavior of the final gold chains by changing the composition of the gold alloy. A new 10 carat yellow gold alloy, named alloy 2, was introduced, and the composition is reported in Tab. 8.1.

The percentage of Ag was reduced and a different grain refiner was used, replacing cobalt with ruthenium. Also for this new alloy, hardness and residual stresses tests were performed. The results are shown in Tab. 8.6.

Tab. 8.6 - *Micro-vickers hardness and residual stresses values obtained with the optimized production path for the new 10 carat gold alloy (alloy 2)*

PROCESS	Hardness tests (Optimized Process) [HV]	Residual stresses – σ (Optimized Process) [MPa]
AS-CAST	130 ± 5	- 54 ± 10
1° ROLLING STEP	235 ± 10	29 ± 3
ANNEALING	150 ± 5	- 83 ± 8
2° ROLLING STEP	210 ± 5	43 ± 4
ANNEALING	140 ± 5	- 48 ± 7
3° ROLLING STEP	205 ± 5	14 ± 3
PLATING	140 ± 5	- 48 ± 10
ANNEALING	140 ± 5	- 90 ± 9

The reduction of the silver content in the composition decreased the precipitation hardening phenomena. In fact, a decrease in the hardness of the samples, after the production process steps, was measured, with an improvement of the semi-finished product's machinability. Moreover, the new composition of the alloy made it possible to move the products directly from the final third rolling step to the plating process without any annealing treatments, which were instead necessary with the old composition. The residual stresses, measured after the annealing and melting process, remained substantially the same of the one obtained with the old composition, whereas the superficial tensile stress after the rolling process decreased. The change of the gold alloy composition influenced not only the first part of the production process but, also, the creation of the double-layer sheet welded during the plating process.

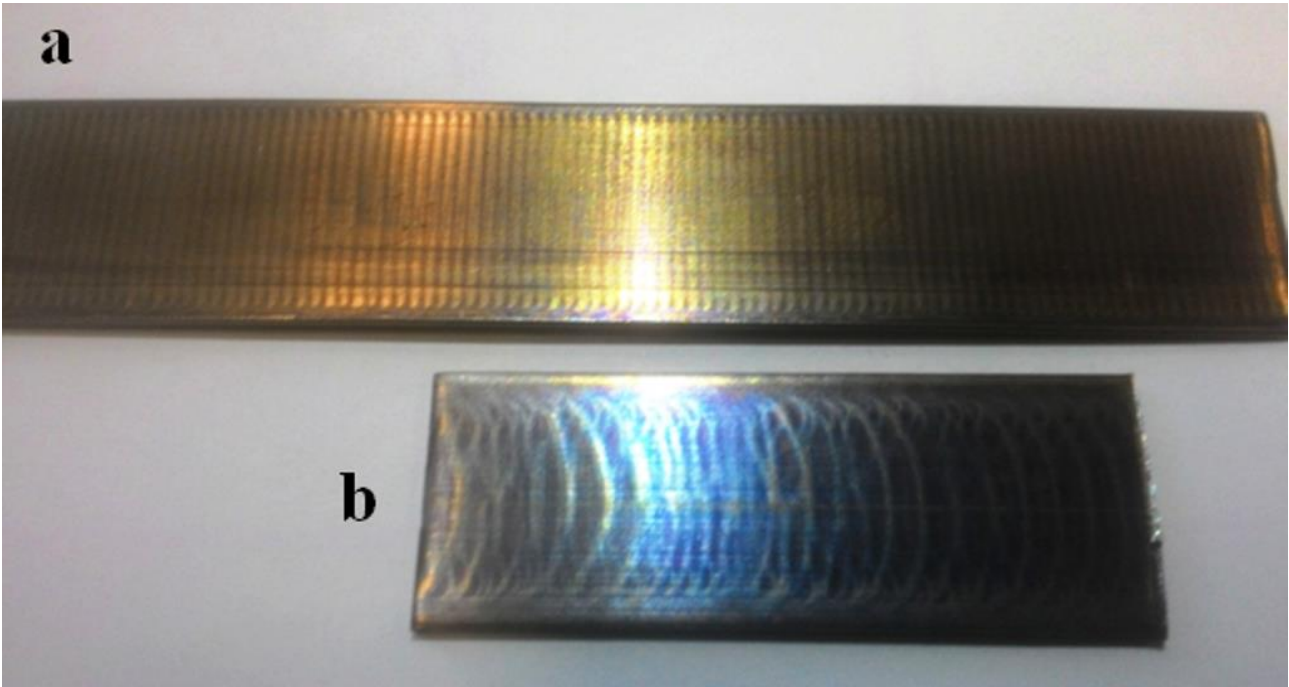


Fig. 8.8 - *Welding lines observable on the iron layer surface of the gold alloy containing Ru (a) in comparison with the other containing Co (b), obtained both with the new optimized process*

As shown in Fig. 8.8, the welding lines, identifiable on the iron surface, were more regular and symmetric in the product obtained with the gold alloy containing Ru (Fig. 8.8a) in comparison with the one containing Co (Fig. 8.8b). Probably, the different magnetic behavior of the two elements affected the process and the quality of the gold plated sheets. The improved behavior of the Ru containing sheet was attributable to a different microstructure, in comparison with the one of the alloy 1, containing Co. In fact, the gold sheet containing Ru (Fig. 8.9a) was characterized by a higher homogeneity in the dimension and distribution of the grains than the one containing Co (Fig. 8.9b).

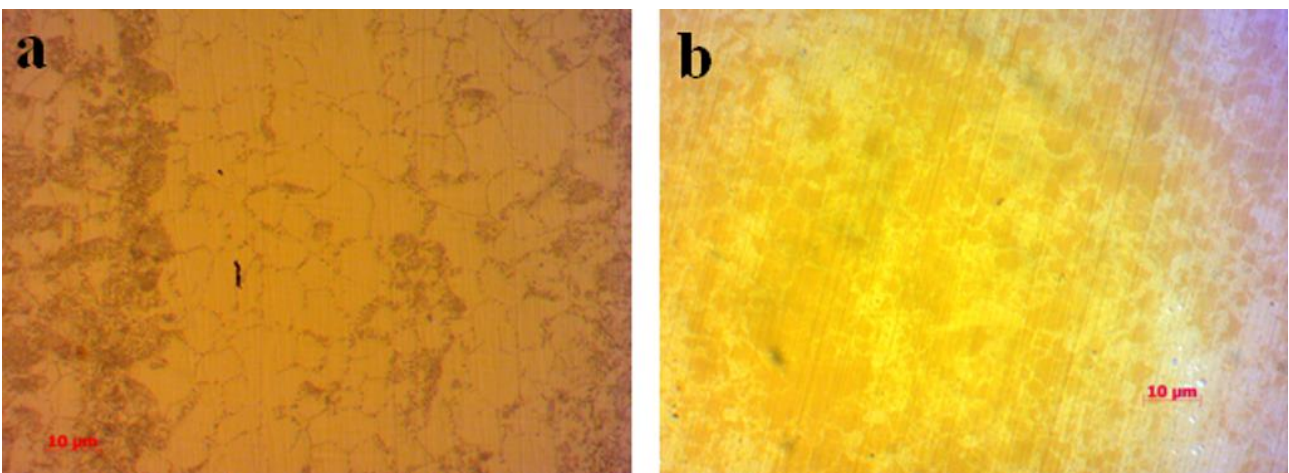
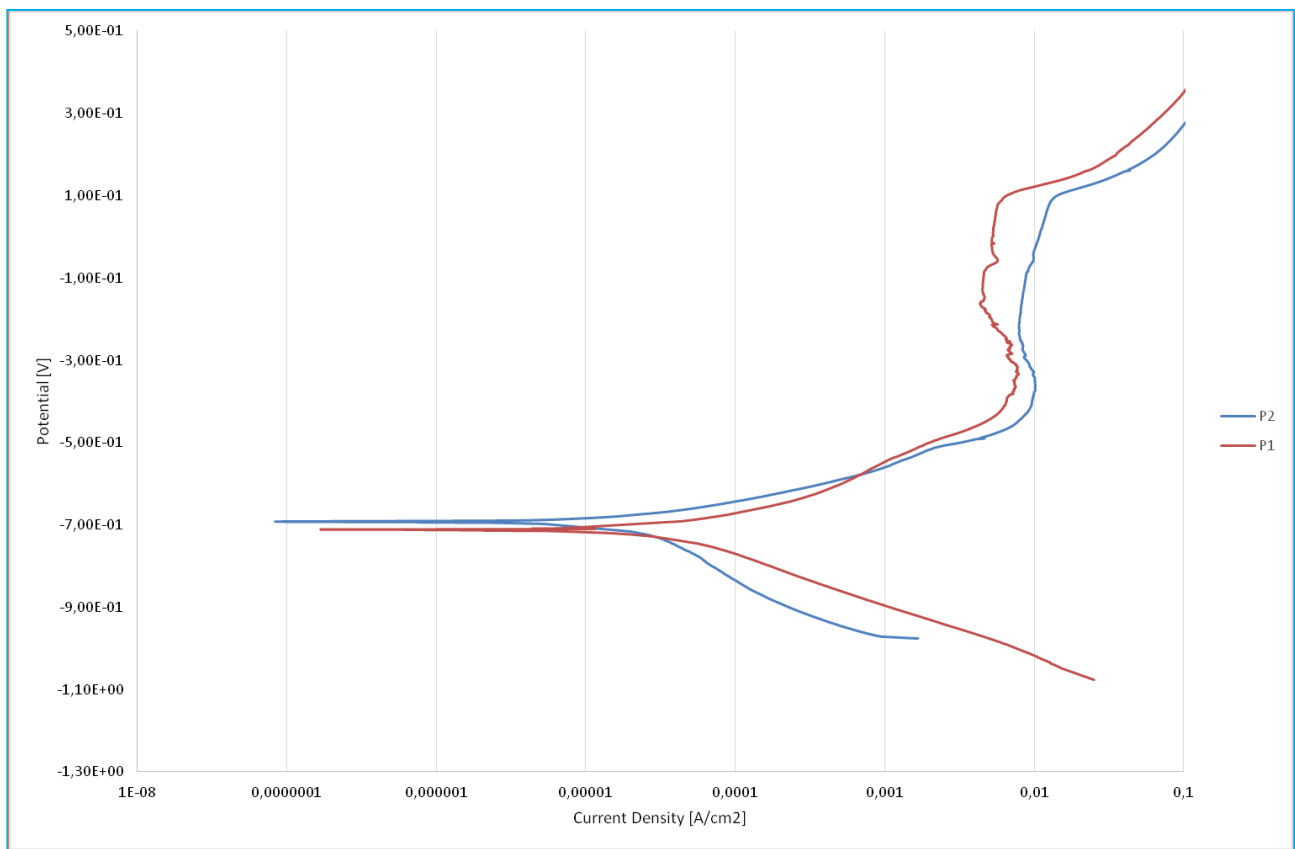


Fig. 8.9 - *Microstructure of the gold alloy sheet, obtained with the new optimized process, for the gold alloy with Ru (a) and the one with Co (b). OM images*

Another aspect of the work was to characterize the corrosion resistance of the two alloys of gold sheets, in a 10% HCl solution that simulates the environment of industrial emptying process.

Regarding the alloy 1, containing Co, both the samples produced with the standard process and with the new optimized process were analyzed and the results were compared (Fig. 8.10).

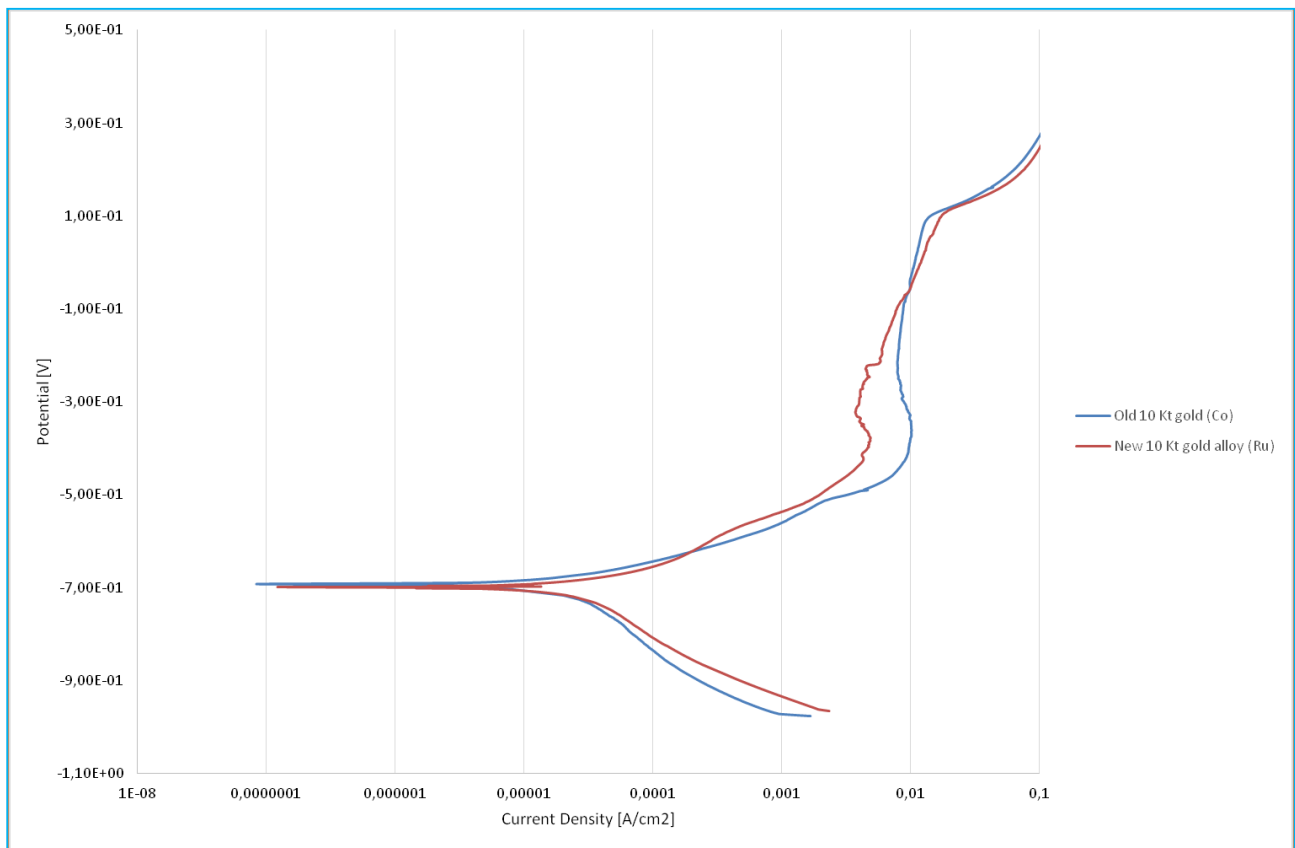
It can be observed that the two samples had the same corrosion potential and substantially, the same corrosion current density. The change in the process parameters did not influence the corrosion behavior of the material, and the decrease of the residual stresses increased the workability of the gold sheets but it was too low to induce relevant differences in the corrosion resistance.



	Standard Process (P1)	Optimized Process (P2)
I_{corr} [A/cm ²]	4×10^{-5}	2×10^{-5}
E_{corr} [V]	-0,70	-0,70

Fig. 8.10 - Potentiodynamic polarization tests on the final annealed sheet after plating process, obtained with the two different production path

Considering the two different alloys, with different grain refiners, it is possible to observe that both the corrosion potential and the corrosion current density remained the same, as reported in Fig. 8.11. The change in the grain refiner did not influence the corrosion resistance of the gold sheets ensuring the maintenance of the quality of the semi-finished product after the emptying process.



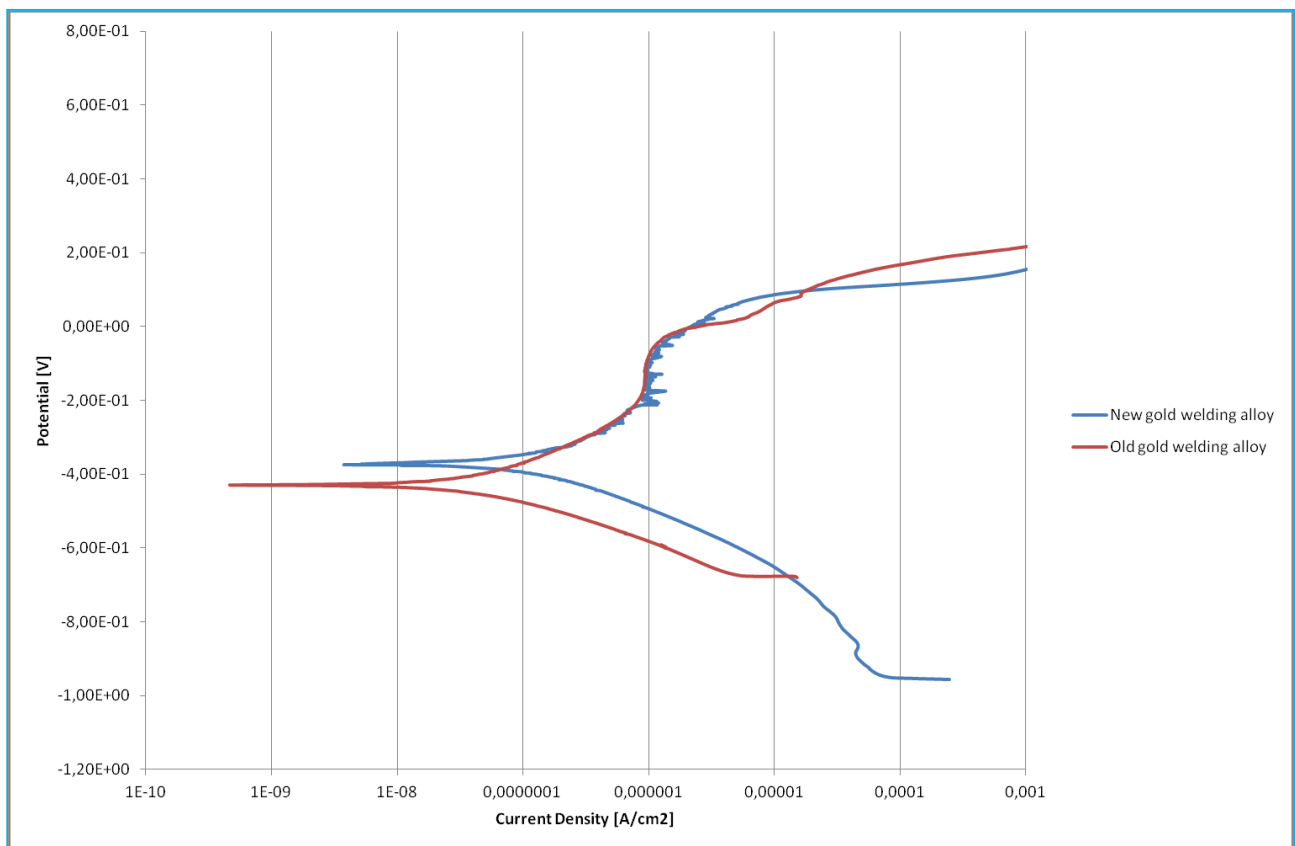
	Old 10 Kt gold alloy (Co)	New 10 Kt gold alloy (Ru)
i_{corr} [A/cm ²]	2×10^{-5}	2×10^{-5}
E_{corr} [V]	-0,70	-0,70

Fig. 8.11 - Potentiodynamic polarization tests on the final annealed sheet after plating process, obtained with the new optimized production process for the two different gold alloy compositions

Finally, the last objective of this part of thesis was the study of the final hollow gold chain's welding process. A new 10 Kt gold welding alloy for the solder wire was developed (Tab. 8.2), and optimized in order to reduce the temperatures used to melt the welding alloy wire within the hollow chain, to improve the wettability and to make easier the thermal insulation of the chains during the welding process. The use of gallium into the new alloy composition allowed to decrease the melting

point and, simultaneously, to improve the wettability of the gold welding alloy in comparison with the old welding based on zinc. The temperatures used in the belt furnace were decreased with a reduction of the orange-peel effect and an improvement of the quality surface. The reduction of about 40 °C in the treatments allowed to make easier and faster the critical insulation of the chains. Moreover, the number of preparation steps and the quantity of talc used to insulate the products were reduced.

To evaluate the corrosion resistance of the two welding alloys, anodic polarization tests in a solution that simulates human sweat were performed and the results are reported in Fig. 8.12.



	Old gold welding alloy	New gold welding alloy
I_{corr} [A/cm²]	2x10 ⁻⁸	7x10 ⁻⁸
E_{corr} [V]	-0,43	-0,37

Fig. 8.12 - Potentiodynamic polarization tests on the final annealed welding wires, obtained with the two different gold alloy compositions

The gold welding alloy containing gallium showed a nobler corrosion potential but a slightly increase in corrosion current densities, suggesting a slightly decrease in the corrosion resistance due to the presence of gallium.

8.4 CONCLUDING REMARKS

The optimization of the whole process parameters and the modification of compositions allowed a remarkable improvement in the industrial production. The optimization of the whole process had not only an influence on the hardness but, also, produced an increase in the ductility of the gold alloys and in the microstructural homogeneity. The final grain size, index of suitable recrystallization treatments, was also increased. The optimization of the melting, rolling and annealing processes for gold alloy sheets allowed the reduction of the residual stresses on the sheet during the whole production cycle, with an increase in machinability and a decrease in fragility. In addition, the corrosion resistance during the emptying process was maintained at good levels. The introduction of the new composition containing ruthenium allowed to avoid the magnetic behavior of the final chain produced, to decrease the hardness and to increase the workability of the gold sheets. The homogeneity of the microstructure was improved, thus producing a greater maintenance of the properties during plating process. Moreover, the corrosion resistance in solution that simulate the industrial environment, during the emptying process, was not influenced by the change of the grain refiner. The reduction of the temperatures used during the welding process for the production of hollow chains, due to the introduction of a new 10 Kt gold welding alloy optimized with gallium, allowed to guarantee a suitable final surface of the semi-finished product and an easier thermal insulation step before the process [93].

Study of Plating Process and Ageing Treatments for the Production of Hollow Gold Chains

9.1 PLATING PROCESS

9.1.1 Introduction

In this chapter, the final plating process was analysed. The creation of the multilayer base (iron sheet – gold sheet), used to make hollow chains, is a critical step. The gold sheets arrive at this step

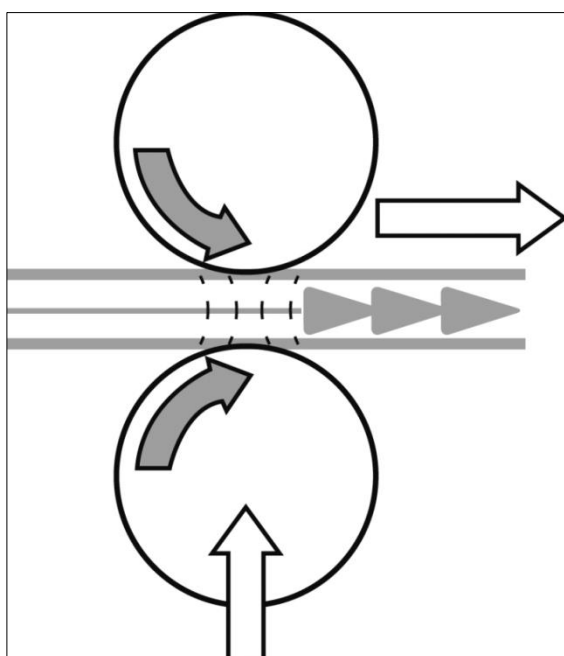


Fig. 9.1 - Scheme of the plating process system

of the production process after several deformation and annealing steps. The study of the microstructure resulted from the process and the variation, caused by the production parameters, on it, is important to define the subsequent behaviour of the material. Spot welding, in this case known as “plating process”, is one of the most widely used welding processes of resistance welding, figure 9.1. To obtain a good welding is necessary to use rather high current values. The current is closely linked to the Joule's law where the energy, in form of heat, is proportional to the square of the product of the delivery current with the resistance, which, in this case, is represented by the

superimposition of the two basis materials. The time is another parameter to consider, in fact, for the same energy, to a decrease of the time should match an increase of the current. The current is still linked to the pressure, because with higher pressures, there is less resistance in the contact areas, and this resistance is concentrated between the two materials increasing the current intensity. During the welding phase, the current intensity can remain constant or vary depending on the operational requirements. During the initial phases of welding, the current remains constant, but in reality, this undergoes changes as it increases the pressure. Increasing the pressure on the two electrodes, the contact resistance on the same decreased, in this way the current will find a lower contact resistance, while it will encounter a higher resistance at the interface of the two materials.

The system used by the company consists in two electrodes made by different copper alloys, depending on the type of material with which they enter in contact (gold or iron). The pressures used during the plating process on the sheets surfaces are between 3 kN and 6 kN. The continuous current is about 20.000 A. The study involved the 10 Kt gold alloy used by the company, which covers the bigger part of the chains production, the composition is reported in table 9.1.

Tab. 9.1 – *Composition of the 10 Kt gold alloy studied*

Kt	Au [%]	Ag [%]	Zn [%]	Cu [%]
10	41.7	17.3	5.5	BALANCE

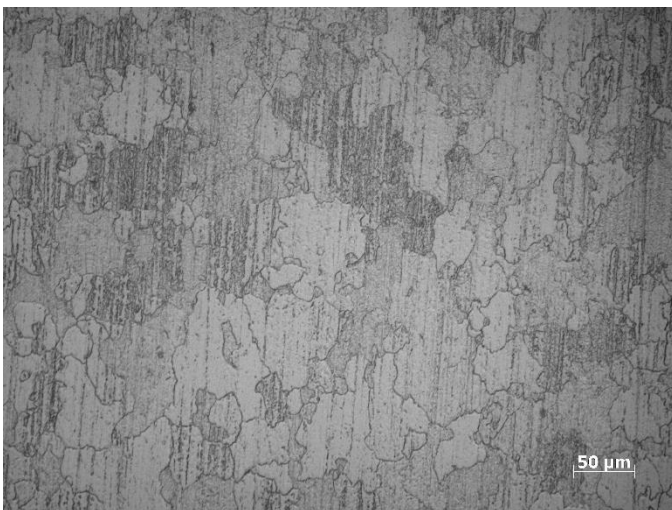


Fig. 9.2 - *OM observation of the microstructure of iron sheet before the plating process*

In figure 9.2, the microstructure of the iron sheet before the plating process is showed. The grain size of the gold sheet coupled is comparable, and in tab. 9.2 the hardness of the two sheets, after the annealing treatment and before the spot welding process are reported.

Tab. 9.2 - *Values of hardness for the gold and iron sheets before plating process*

	Hardness
Iron sheet	140 HV
Gold sheet	145 HV

The influence of different parameters like the current density, the velocity of the process, the pressure and the shape of the copper alloy rollers was studied, and some hardness tests to evaluate the change in mechanical properties were performed.

9.1.2 Results and Discussion

The pressure of rollers, was the first parameter investigated, it was increased equally for both copper electrodes.

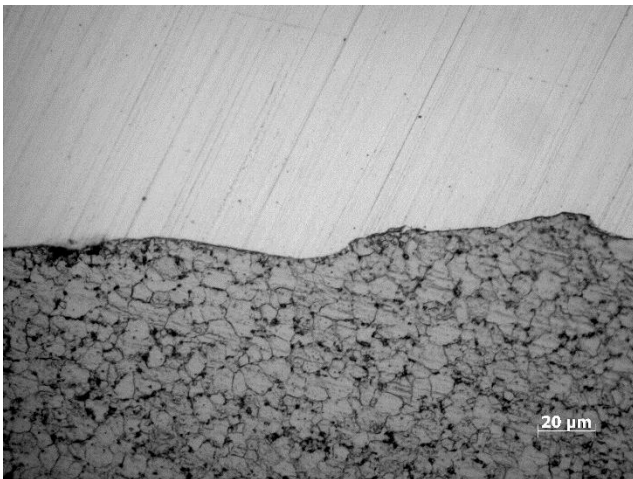


Fig. 9.3 - OM observation of the interface obtained with standard parameters (iron sheet chemically etched)

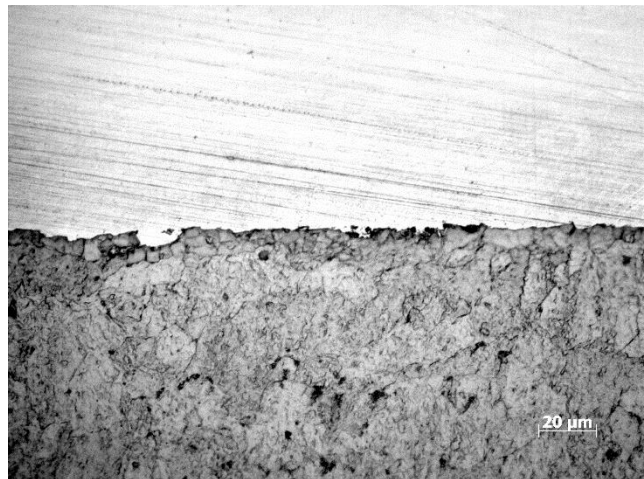


Fig. 9.4 - OM observation of the interface obtained with higher pressure of rollers (iron sheet chemically etched)

Tab. 9.3 - Hardness tests results

		Hardness
Standard rollers pressure	Fe sheet	148 HV
	Au alloy sheet	145 HV
Higher rollers pressure	Fe sheet	150 HV
	Au alloy sheet	160 HV

With the increase of the pressure of rollers, the welding interface between the two sheets remains well defined but starts a disruption of iron grain. In figures, 9.3 and 9.4, the interface between gold and iron is represented. The hardness tests showed a small increase in hardness, probably due to the small increase of superficial deformation caused by the rollers pressure, tab. 9.3.

The convexity of rollers was the second parameter investigated. The shape of the upper roller, in contact with the iron sheet, was modified.

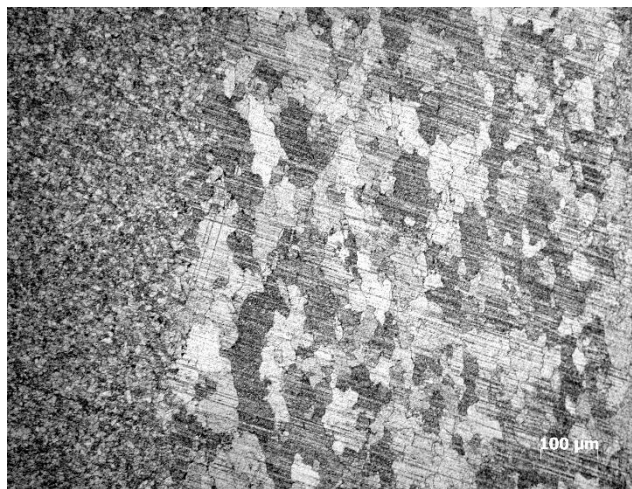
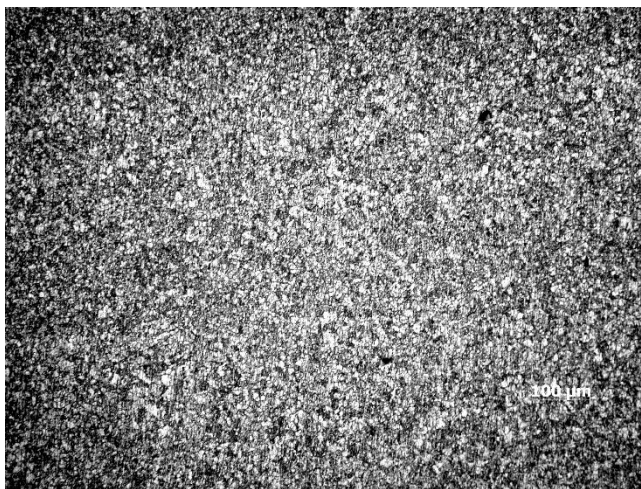


Fig. 9.5 - OM observation of the iron surface near the edge of the sheet obtained with standard parameters

Fig. 9.6 - OM observation of the iron surface near the edge of the sheet obtained with change in the convexity of roller

The change in the roller convexity, resulted in an increase of the hardness of iron sheet (tab. 9.4), and a partially welding due to the lack of current penetration in the edge of the sheets. In figure 9.5 is reported the microstructure of the iron near the edge sheet produced with the standard parameters, while in figure 9.6 is reported the microstructure obtained after the change in roller convexity. The higher difference in the grain size between the two situations is due to the change in the interaction with the current and the contact resistance.

Tab. 9.4 - Hardness tests results

		Hardness
Standard rollers convexity	Fe sheet	148 HV
	Au alloy sheet	145 HV
Change rollers convexity	Fe sheet	160 HV
	Au alloy sheet	148 HV

The velocity of plating process was the third parameter investigated. During welding, the time is closely related to the intensity of the current:

- Considering the pressure constant, increasing the current, the welding time decreases,
- Considering the current constant, increasing the pressure, decreases the contact resistance and consequently must be increased the welding time

These factors are closely linked to productivity, with pressures and high currents, the welding times are reduced allowing a lower heating of the welded parts and an increase in productivity. In order to perform a rapid welding, it is necessary to monitor the surfaces of the materials to be bonded and welded, they must be clean and free of oxides.

Regarding the goldsmith company's production process, the change in the velocity of plating process influences the aspect of the interface, passing from a regular one to another characterized by a not negligible interdiffusion between the iron and the gold alloy.

The results are reported in figures 9.7 and 9.8.

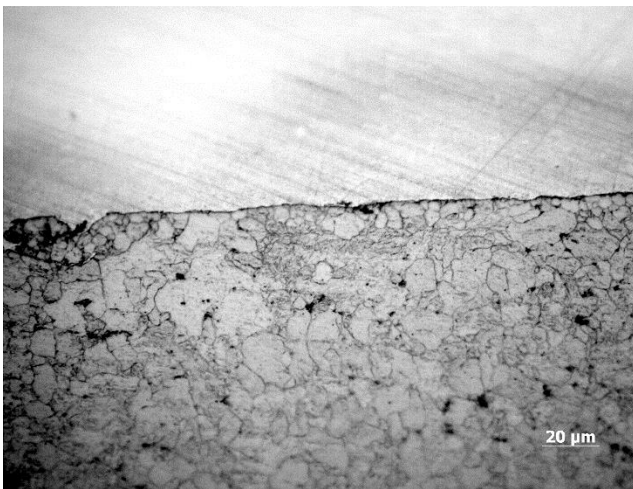


Fig. 9.7 - OM observation of the interface obtained with standard parameters (iron sheet chemically etched)

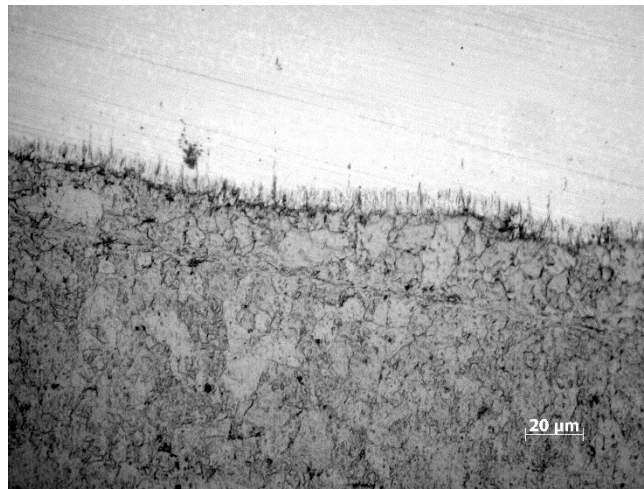


Fig. 9.8 - OM observation of the interface obtained by changing the velocity of the process (iron sheet chemically etched)

In Table 9.5 are showed the hardness values obtained after the tests.

Tab. 9.5 - *Hardness tests results*

		Hardness
Standard process velocity	Fe sheet	148 HV
	Au alloy sheet	145 HV
Change in process velocity	Fe sheet	155 HV
	Au alloy sheet	150 HV

The increase of the current, instead, hadn't a considerable influence on the properties and the aspect of the semi-finished plated, probably due to the already high currents.

9.1.3 Concluding Remarks



Fig. 9.9 - *Particular of the iron sheet surface. OM observation*

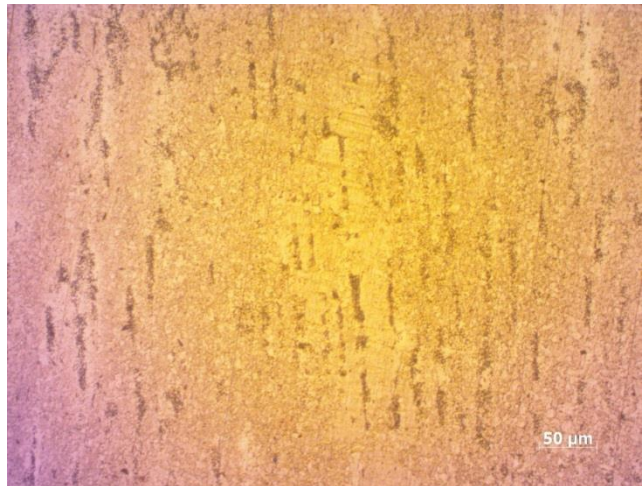


Fig. 9.10 - *Particular of the gold sheet surface. OM observation*

In all the samples, in correspondence of the welding lines generated by the process, the microstructure of the two materials (gold and iron) changes, as it possible to see in figures 9.9 and 9.10. The grain size was reduced with an increase of the mechanical properties, whereas in the other remaining areas the structures remain substantially the same of the annealed state.

High current density could enhance the atomic flux that accelerated diffusion, and increased the temperature. The thermal effect of the process is strengthened. With the increase of the number of atoms (characterized by an energy higher than energy barriers) and of their vibration intensity, the diffusion rate increased when the temperature rises. The temperature influences the recrystallization process and the final dimension of grain size. Combining the effect of high temperature localized and the large atomic flux, recrystallization can take place in a short time [94].

The recrystallization process, during the plating process, is also influenced by a typical athermal effect. Increasing the temperature, due to the pass of the current, increase the mobility of the electrons causing a more severe interaction between electrons and atoms. Under the high current used in the plating process, grains have tendency to form equiaxed shape. With the alteration of the grains, the energy barriers were overcome.

Therefore, if the energy obtained in the plating process was sufficiently high, there is the possibility to generate the recrystallization within the material. Probably, the reason is due to the subsequent precipitations dissolved and then recrystallized, when a high amount of electrical energy has overcome the energy barriers. The structure defects were reduced [95]. The production deformation processes of the sheet and the pressure generated by rollers, during the plating process, affect the properties of the material's structure. The stored energy of the residual dislocation density is the major driving force for the growth of new grains, the recrystallization occurs due to the presence of the driving force, of the high current and the high mobility of dislocation [96].

9.2 AGE-HARDENING TREATMENTS

9.2.1 Introduction

The production of hollow and small thicknesses jewelry, obtained by plastic deformation processes and subsequent hardening by particular heat treatments, occupies a relevant place into the production of goldsmith companies. However, the used alloys have to maintain a good workability to guarantee the possibility of high reduction of section during the deformation process. In this work different hardening processes were tested with the aim to improve the hardness of the gold alloy used to make hollow chains. Different compositions of 18 Kt, 14 Kt, 10 Kt and 9 Kt yellow gold alloys were investigated. The influence of the hardening mechanisms, the compositions and process parameters on microstructure and mechanical properties was evaluated.

All the different samples of gold alloys, coming from the production process, were considered in the annealed state. Hardening treatments were performed in a static furnace with an inert atmosphere. The samples were treated for different time (2h or 2h30') and temperatures, from 200 °C to 300 °C, in order to analyze the effect of these parameters on the mechanical properties and on the microstructure. Mechanical properties were evaluated with micro-hardness tests. The micro structural analysis was performed by optical microscope observation and X-ray diffraction analysis.

9.2.2 Results and Discussion

18 Kt thermosetting gold alloy

Regarding the 18 Kt gold yellow alloys, two different composition, reported in Tab. 9.6, were tested.

Tab. 9.6 - *Compositions of the two gold thermosetting alloy tested*

	Au [%]	Ag [%]	Zn [%]	Cu [%]
Alloy 1	75.0	4.5	1.5	19.0
Alloy 2	75.0	7.5	2.5	15.0

The alloy 1, with the higher percentage of copper in mass, presented the highest values of hardness, Tab. 9.7.

Tab. 9.7 - Hardness tests results

ALLOY 1			ALLOY 2		
T [°C]	t	Hardness [HV]	T [°C]	t	Hardness [HV]
Annealed		255	Annealed		215
200	2h	293	200	2h	232
200	2h30'	303	200	2h30'	245
225	2h	318	225	2h	264
225	2h30'	325	225	2h30'	268
250	2h	365	250	2h	280
250	2h30'	355	250	2h30'	292
275	2h	340	275	2h	302
275	2h30'	310	275	2h30'	300
300	2h	330	300	2h	302
300	2h30'	325	300	2h30'	295

With the higher content of copper, the results showed that the highest hardness values were achieved for time and temperature lower than alloy 2. In figure 9.11 is shown the microstructure of the alloy 1 in the annealed state (a) and treated for 2h at 250 °C (b). While the process proceeds, the growth phenomenon occurs, with an increase in the grain dimension.

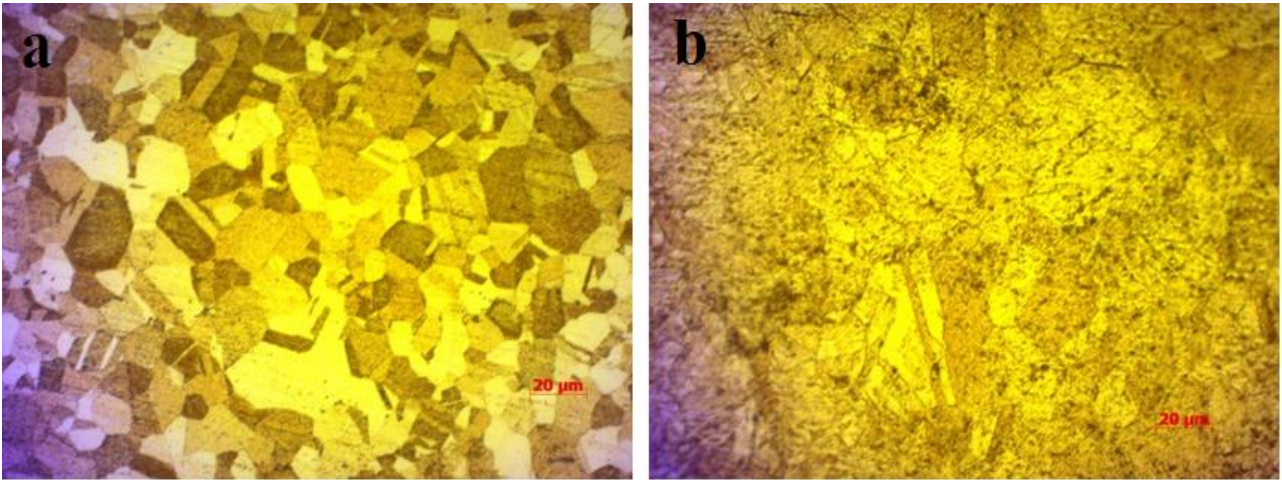


Fig. 9.11 - Microstructure of the alloy 1 in the annealed state (a) and treated for 2h at 250 °C (b). OM observation

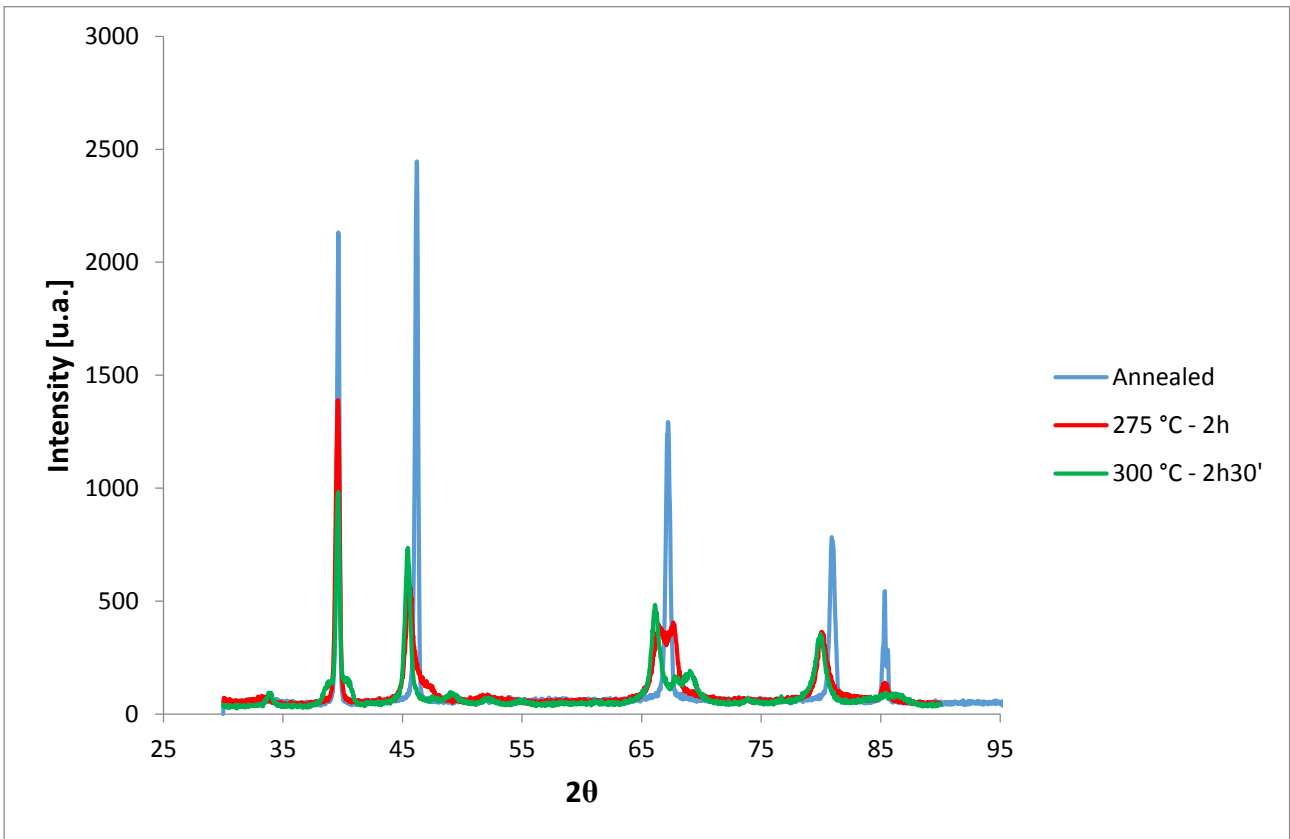


Fig. 9.12 - XRD results performed on the annealed and two treated samples for the 18 Kt gold alloy 1

The X-ray diffraction, figure 9.12, showed a shift and broadening of the diffraction pattern, index of the re-ordering of the crystal structure and of the grain growth. Time and temperature influence the

ordering structure phenomena and the precipitation of secondary phases. The hardness achieved depends on the chosen combination of these parameters.

14 Kt thermosetting gold alloy

In table 9.8 is reported the composition of the gold alloy investigated.

Tab. 9.8 - *Compositions of the 14 Kt thermosetting gold alloy tested*

	Au [%]	Ag [%]	Zn [%]	Cu [%]
14 Kt gold alloy	58.5	13.0	7.0	21.5

The micro-hardness tests performed on the 14 Kt gold samples showed, substantially, the same values from 250 °C to 300 °C, showed in table 9.9.

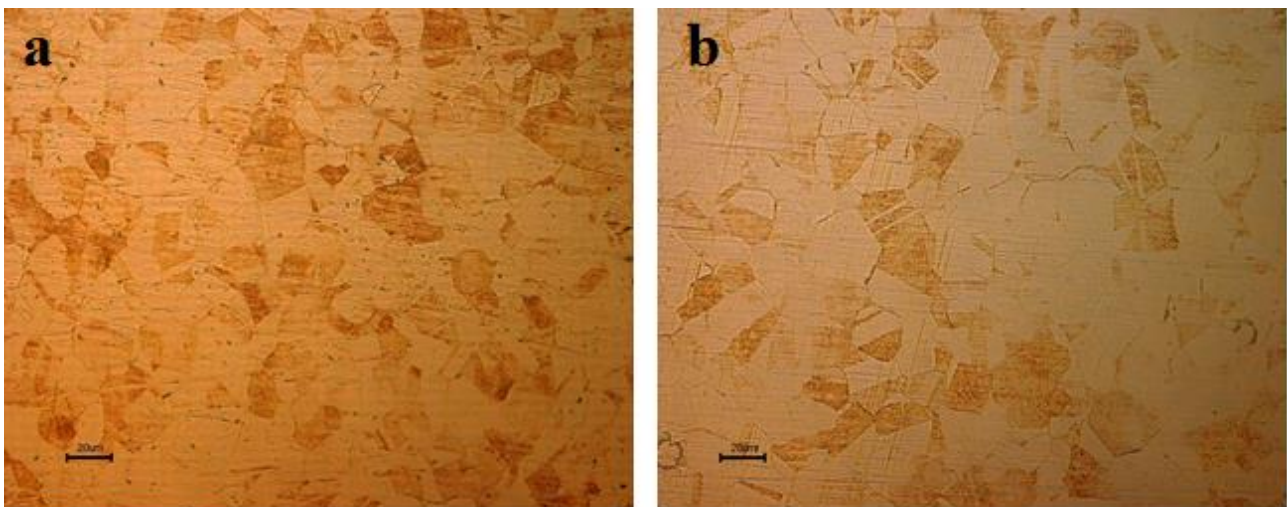


Fig. 9.13 - *Microstructure of the 14 Kt gold samples in the annealed state (a) and treated for 2h30' at 300 °C (b). OM observation*

In figure 9.13 are showed the microstructure of the samples annealed (a) and treated for 2h30' at 300 °C, also in this case, it is possible to notice the growth of the grain dimension with the maintaining of the sample at relatively high temperature.

Tab. 9.9 - *Hardness tests results*

14 Kt GOLD ALLOY

T [°C]	t	Hardness [HV]
Annealed		180
200	2h	223
200	2h30'	220
225	2h	243
225	2h30'	244
250	2h	251
250	2h30'	260
275	2h	258
275	2h30'	257
300	2h	259
300	2h30'	260

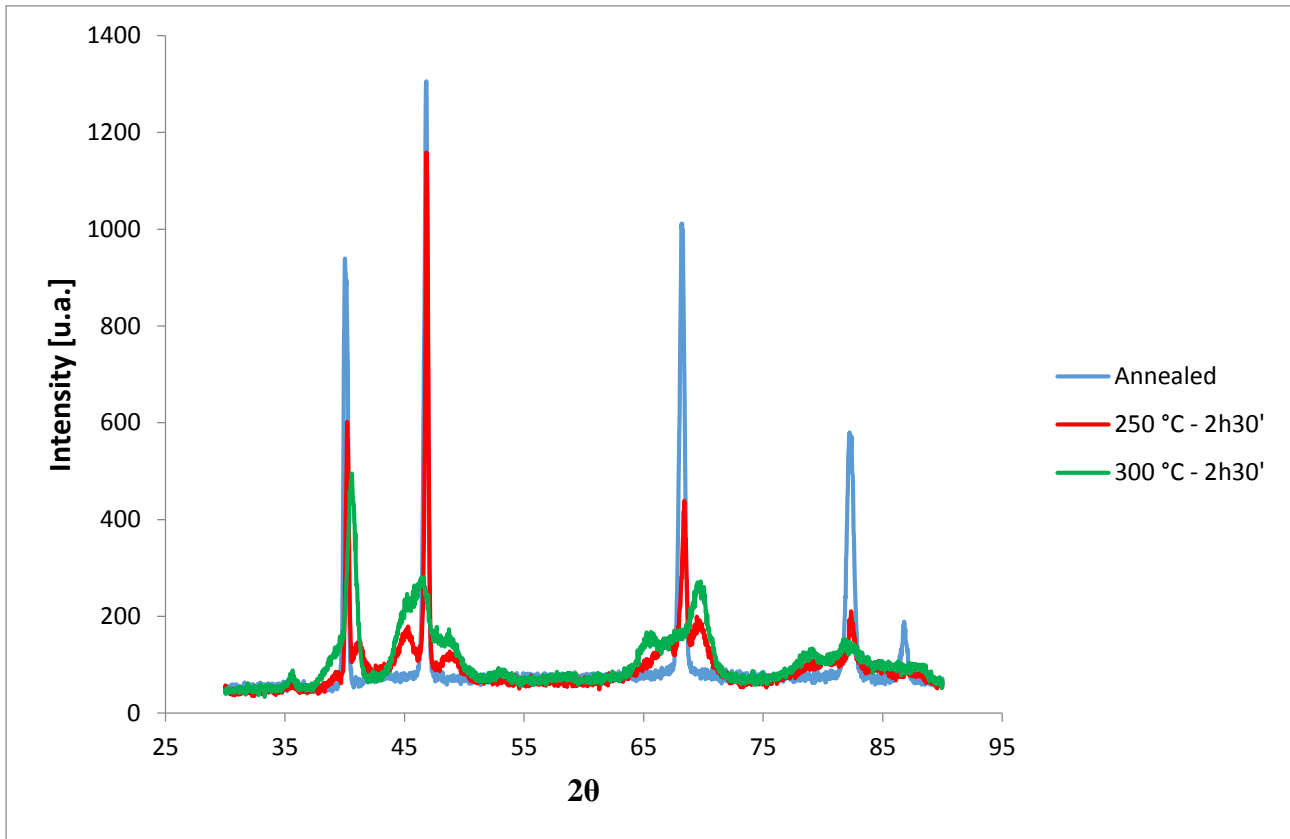


Fig. 9.14 - XRD results performed on the annealed and two treated samples for the 14 Kt gold alloy

Analyzing the results obtained from the XRD tests performed (figure 9.14), the formation of new phase can be observed especially for the sample treated at 250 °C. While for the sample treated at 300 °C, the peaks of the new phase are more pronounced. Further investigations should be carried out to define the nature of this phase.

10 Kt thermosetting gold alloy

Regarding the 10 Kt gold yellow alloys, two different composition, reported in Tab. 9.10, were tested.

Tab. 9.10 - *Compositions of the two gold thermosetting alloy tested*

	Au [%]	Ag [%]	Zn [%]	Cu [%]
Alloy 1	41.7	17.3	5.5	35.5
Alloy 2	41.7	12.8	6.3	39.2

The hardness tests, reported in table 9.11, showed that, the hardness values increased with the content of silver and not with the copper as previously for the 18 Kt gold alloys.

Tab. 9.11 – *Hardness tests results*

ALLOY 1			ALLOY 2		
T [°C]	t	Hardness [HV]	T [°C]	t	Hardness [HV]
Annealed		182	Annealed		177
200	2h	195	200	2h	187
200	2h30'	205	200	2h30'	185
225	2h	220	225	2h	190
225	2h30'	223	225	2h30'	190
250	2h	230	250	2h	220
250	2h30'	225	250	2h30'	216

275	2h	212	275	2h	216
275	2h30'	213	275	2h30'	210
300	2h	219	300	2h	210
300	2h30'	216	300	2h30'	200

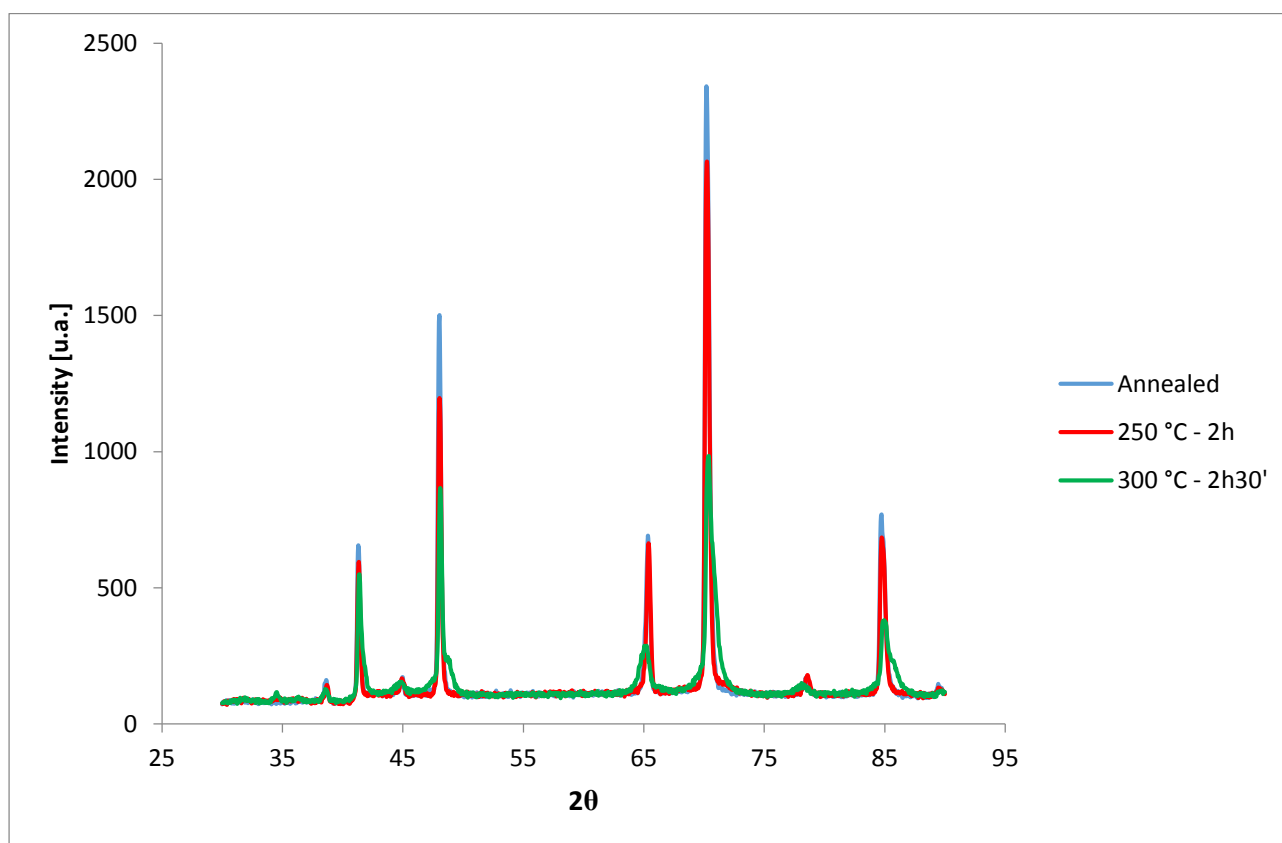


Fig. 9.15 - XRD results performed on the annealed and two treated samples for the 10 Kt gold alloy 1

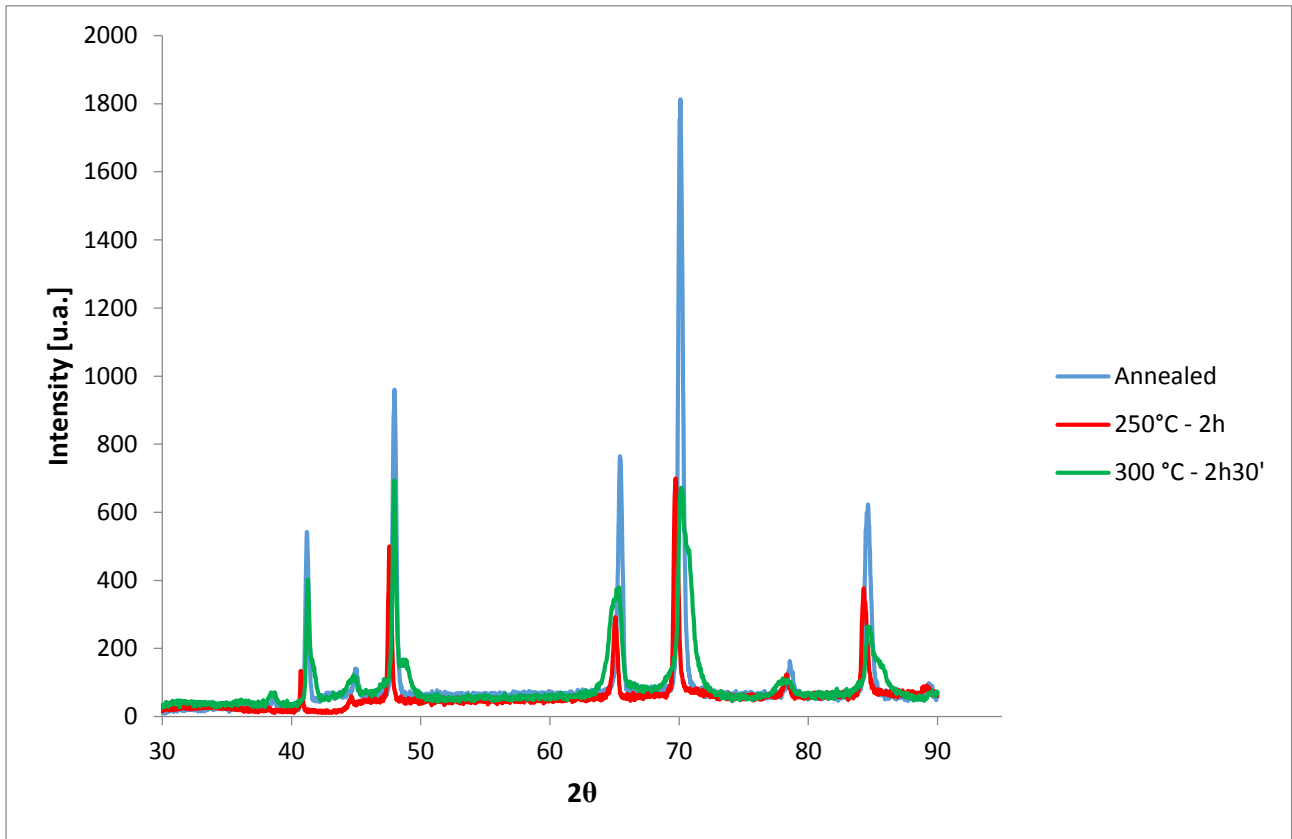


Fig. 9.16 - XRD results performed on the annealed and two treated samples for the 10 Kt gold alloy 2

The diffraction pattern obtained from the XRD analyses, reported in figures 9.15 and 9.16, showed did not present any shift of the peaks, in comparison with the 18 Kt gold alloys. Only for the specimen treated at 300 °C, it is possible to observe a slight broadening on the base of the peaks.

9 Kt thermosetting gold alloy

In table 9.12 is reported the composition of the gold alloy investigated.

Tab. 9.12 - Compositions of the 9 Kt thermosetting gold alloy tested

	Au [%]	Ag [%]	Zn [%]	Cu [%]
9 Kt gold alloy	37.5	14.1	5.2	43.2

Tab. 9.13 - *Hardness tests results*

9 Kt GOLD ALLOY

T [°C]	t	Hardness [HV]
Annealed		157
200	2h	167
200	2h30'	180
225	2h	165
225	2h30'	180
250	2h	180
250	2h30'	191
275	2h	190
275	2h30'	186
300	2h	200
300	2h30'	199

The hardness tests, performed on the 9 Kt gold samples, showed an increase of ca. 50 HV in the hardness values for the highest times and temperatures used in the treatments (table 9.13).

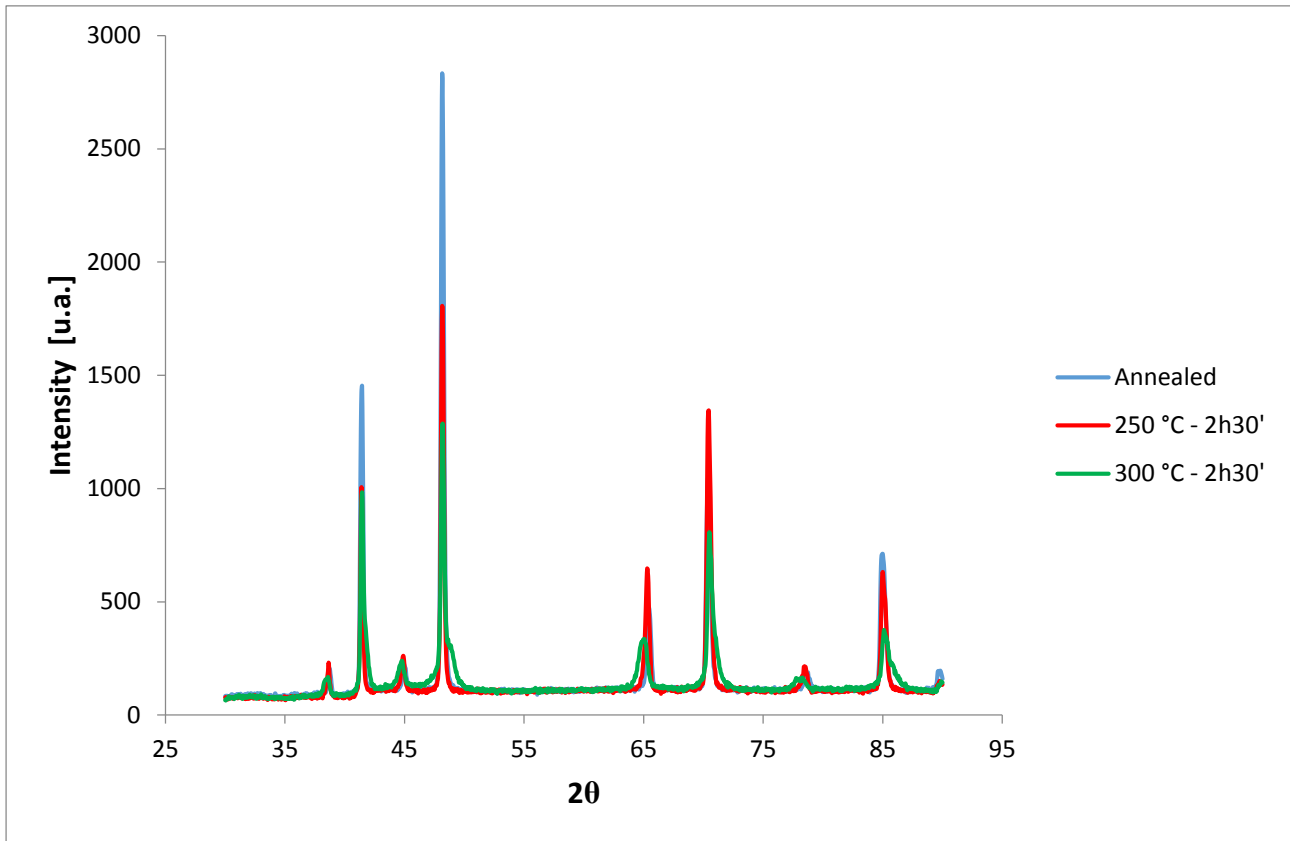


Fig. 9.17 - XRD results performed on the annealed and two treated samples for the 9 Kt gold alloy

In figure 9.17 is reported the diffraction pattern of the 9 Kt gold alloy studied, with the increase of temperature and time of treatments there aren't changes in the position and in the shape of the peaks.

9.2.3 Concluding Remarks

Time and temperature influence the ordering structure phenomena and, also, the formation of secondary phases.

It is possible to observe the influence of the percentage of copper and the disorder-to-order solid transformation as the major hardening mechanism for the 18 Kt gold alloys. The diffraction pattern showed a change in the microstructure, a remarkable increase in the micro-strain can be observed passing from the samples annealed to the samples age-hardened. The AuCuI ordered phase generated after the treatment is characterized by a higher internal micro-strain [97]. The highest value of hardness were achieved with intermediate times and temperatures of treatment, index of a stronger hardening effect due to a partially ordered state if compared to a fully ordered state.

Regarding the 14 Kt thermosetting gold alloy studied, the analysis showed that exist a cooperation between the disorder-to-order solid transformation and the precipitation of secondary phases. In this case, other analyses are necessary to explain better the hardening phenomena.

With the lowest carat gold alloys (10 Kt, 9 Kt), instead, the hardening mechanism that overcomes is the precipitation hardening and not the re-ordering, which increases with the percentage of silver and other elements (like grain refiners).

A suitable control of the grain size and of the heat treatments allows achieving the necessary properties to guarantee machinability and quality to the product.

CONCLUSIONS

In this thesis work, after a short introduction on the state of art of jewelry production, the industrial production processes of gold chains were studied, in order to optimize the parameters used in the production cycle, the compositions of gold alloys and the mechanical properties of the semi-finished products. In the last years, the scientific approach to the traditional jewelry industries has been adopted more and more often. The aim is to reduce the production wastes, to improve the characteristics of the final artifacts surface and to increase the constancy of results.

All the sampling was carried out at Filk S.p.A., the goldsmith company partner of the research, the characterization was performed at the Department of Industrial Engineering of the Padua University and at Progold S.p.A.

In the first experimental part of the thesis were described the results obtained by the analyses of the production process of gold welding wires. After a primary investigation, the temperatures of crucible and mould, the time and temperatures of the annealing steps and the quenching system after melting and annealing processes were modified. The velocity of the rollers, during the deformation process, was decreased. The results showed, using the new optimized process, a reduction of the hardness and of the grain size. Furthermore, a greater microstructural homogeneity and the increase of ductility allowed to improve the workability of the material. The tensile tests performed on the final annealed samples, showed a smaller range of variability and a better uniformity of the tensile curves, demonstrating the suitable control of the parameters during all the production cycle. Another important aspect analyzed is the influence of the production parameters on the tensile state presents within the material. Through the annealing treatments, it was possible to restore a positive compressive state in comparison with the undesired tensile state obtained after the deformation processes. This is an important aspect considering the emptying process with acids used by the company. The greater homogeneity of the microstructure, a smaller grain size and a reduction of the residual stresses, obtained with the new optimized process, are preferred because these characteristics cause an increase in the corrosion resistance of the material.

Adopting these changes in the production cycle of the company, it was possible to improve the quality of the semi-finished products, increase the machinability of the welding wires and the industrial scraps were, almost completely, eliminated.

Another part of the experimental study was focused on the analysis and optimization of the compositions and production processes for the realization of gold alloy sheets.

The objectives are the study of some critical problems that affect the production cycle. With the aim to avoid the ruptures under the rollers, during deformation steps, the dimension of the mould in the melting process and the temperatures in the annealing treatment were modified with a reduction of the quenching time and a decrease in hardness. The increase in the workability and the reduction of the residual stresses allowed to avoid brittle fractures.

The development of another 10 Kt gold alloy, with a different grain refiner (Ru) and a lower content of Ag, allowed eliminating the undesired magnetic behavior of the final chain produced. This new gold alloys showed a further reduction of hardness and of residual stresses, obtained with the new optimized process. The homogeneity of properties under plating process increased, and the change in composition did not affect the corrosion properties of the material, ensuring, substantially, the same behavior during emptying process. Subsequently, the welding process was analyzed, a different composition of the 10 Kt gold alloy used by the company was developed. The reduction of the melting point range and the increase of wettability, obtained with the new composition based on gallium, allowed to decrease the temperature of the process and made easier the preparation of the gold chain through the preparation steps. The quality of semi-finished welded products increases with the reduction of the orange-peel effect.

In the last experimental part of this thesis, the study of the plating process (with the formation of the double-layer sheet gold-iron), and of several age-hardening treatments was performed.

The knowledge of the influence that the process parameters have on the microstructure and properties of the materials is very important. A good choice of the pressure and the velocity of welding is necessary to guarantee a suitable interface between the two material, without an excessive interdiffusion, and the convexity of the rollers is an important parameter to consider for the uniform superficial contact between the sheets. The local increase of temperatures, generated by the current, lead to a recrystallization of the material in correspondence of the welding line. Structures completely different from the other areas where the grains remain the same of the annealed state before the plating process.

With this analysis, the influence of parameters like the velocity of the process, the convexity and pressure of rollers on the quality of the semi-finished product was studied in order to better understand the mechanisms that occur and where it is appropriate intervening to adapt the process to the needs of single cases.

Finally, the age-hardening treatments were investigated. In the production of hollow chains, the hardness and other mechanical properties are critical variable. A relevant place in the company's production is occupied by production of hollow chains, and their behavior during plastic deformation steps is important. Several hardening treatments were performed for different caratage

of gold alloys. The hardness and XRD tests showed that for 18 Kt gold alloy the hardening mechanism that overcome is the solid disorder-to-order transformation, controlled by the percentage of copper present in the composition. Instead, for the lower carat gold alloy the hardening phenomenon is controlled by the Ag content into the gold alloy, because, in this case, is the generation of secondary phases mechanism that overcome. A suitable control of composition, time and temperatures of treatments is suggested to guarantee an increase of hardness adequate for the mechanical deformation to which the material undergoes. The tests performed allowed to optimize this parameter for the thermosetting alloy used by the company, improving the resistance and the quality of the semi-finished product.

Concluding this thesis work was devoted to optimize the production parameters from the melting process to the final production of the semi-finished welded. The experimental work showed that the modification of the process parameters and the formulation of different compositions of gold alloys, can improve the properties of the semi-finished and final products, and can, also, reduce the amount of industrial scraps, with a reduction of the overall cost of the process. So the results reported, permit to extend the knowledge regarding the gold chain production processes and the possible usefulness of a scientific approach also in the handcrafted jewelry world.

REFERENCES

- [1] *Gold Survey 2008*, Published by GFMS Ltd. London, 2008.
- [2] *CRC Handbook of Chemistry and Physics*, D. R. Lide (ed.) (Taylor & Francis, London, 2008).
- [3] *Impact of gold nanoparticles combined to x-ray irradiation on bacteria*, A. Simon-Deckers, E. Brun, B. Gouget, M. Carriere, and C. Sicard-Roselli, *Gold Bull.*, 2008, 41, 187.
- [4] *The fascinating implications of new results in gold chemistry*, H. Schmidbaur, *Gold Bull.*, 1990, 23, 11.
- [5] *Relativity and the periodic system of elements*, P. Pyykko and J.-P. Desclaux, *Acc. Chem. Res.*, 1979, 12, 276.
- [6] *Relativistic effects in gold chemistry. I. Diatomic gold compounds*, P. Schwerdtfeger, M. Dolg, W. H. E. Schwarz, G. A. Bowmaker, and P. D. W. Boyd, *J. Chem. Phys.*, 1989, 91, 1762.
- [7] *Relativistic effects in inorganic and organometallic chemistry*, N. Kaltsoyannis, *J. Chem. Soc. Dalton Trans.*, 1997, 1, 1.
- [8] *Wetting and surface tension measurements on gold alloys*, E. Ricci, R. Novakovic, *Gold Bull.*, 2001, 34, 41.
- [9] *Size and temperature-dependent structural transitions in gold nanoparticles*, K. Koga, T. Ikeshoji, K. Sugawara, *Phys. Rev. Lett.*, 2004, 92, 115507.
- [10] *The chemistry of gold as an anion*, M. Jansen, *Chem. Soc. Rev.*, 2008, 37, 1826.
- [11] *Optical properties of the intermetallic compounds AuAl₂, AuGa₂ and AuIn₂*, S. S. Vishnubhatla, J. P. Jan, *Philos. Mag.*, 1967, 16, 45.
- [12] *Solid State Physics*, N. W. Ashcroft, N. D. Mermin (ed.) (Harcourt College Publishers, New York, 1976).
- [13] *Optical properties of selected elements*, J. H. Weaver, H. P. R. Frederikse, *CRC Handbook of Chemistry and Physics*, D. R. Lide (ed.) (CRC Press, Boca Raton, 2001) 133.
- [14] *Colour Res. and Appl.*, K. Nassau, 1987, 12, 4
- [15] *Precious Metals Science and Technology*, K. Yonemitsu, eds. L.S. Benner, T. Suzuki, K. Meguro, S. Tanaka, International Precious Metals Institute, Allentown, 1991, p.13
- [16] *Coloured gold alloys*, C. Cretu, E. van der Lingen, *Gold Bulletin*, December 1999, Volume 32, Issue 4, pp 115-126
- [17] *The Santa Fe Symposium on Jewelry Manufacturing Technology 1988*, D.P. Agarwal, G. Raykhtsaum, ed. D. Schneller, Santa Fe, 1988, p. 229
- [18] *American Jewelry Manufacturer*, M. Plotnick, Jan. 1991, 20

- [19] *Light and Color*, R.D. Overheim, D.L. Wagner, John Wiley & Sons Inc., New York, 1982, 63, 253
- [20] *American Jewelry Manufacturer*, G. Raykhtsaum, D.P. Agarwal, February 1990, 116
- [21] *Selected properties of gold*, J. G. Cohn, Gold Bulletin, 1979, 12, 21.
- [22] *The malleability of gold. An explanation of its unique mode of deformation*, J. Nutting, J. L. Nuttall, Gold Bulletin, 1977, 10, 2.
- [23] *Melting in small gold clusters: a Density Functional molecular dynamics study*, B. Soule de Bas, M. J. Ford, and M. B. Cortie, J. Phys: Condensed Matter, 2006, 18, 55.
- [24] *Direct observation of ferromagnetic spin polarization in gold nanoparticles*, Y. Yamamoto, T. Miura, M. Suzuki, N. Kawamura, H. Miyagawa, T. Nakamura, K. Kobayashi, T. Teranishi, and H. Hori, Phys. Rev. Lett., 2004, 93, 116801.
- [25] *Phase Diagrams of Binary Gold Alloys*, eds. H. Okamoto, T. B. Massalski, ASM International, Metals Park, Ohio, 1987.
- [26] *Ternary Alloy Systems, Subvolume B: Noble Metal Systems*, eds. G. Effenberg, S. Ilyenko, Landolt-Bornstein New Series Group IV Volume 11, Springer-Verlag, Berlin, Germany, 2006.
- [27] *The Structures of Binary Compounds. Cohesion and Structure*, P. Villars, K. Mathis, F. Hulliger, F.R. De Boer, D.G. Pettifor (Eds.), vol. 2, North Holland, Amsterdam, 1989.
- [28] *A survey of gold intermetallic chemistry*, R. Ferro, A. Saccone, D. Maccio, and S. Delfino, Gold Bulletin, 2003, 36(2), 39.
- [29] *Gold in dentistry: alloys, uses and performance*, H. Knosp, R. J. Holliday, and C. W. Corti, Gold Bulletin, 2003, 36(3), 93.
- [30] *The effects of small additions and impurities on properties of carat golds*, D. Ott, Gold Technology, 1997, 22, 31.
- [31] *Grain size of gold and gold alloys*, D. Ott and Ch. J. Raub, Gold Bulletin, 1981, 14(2), 69.
- [32] *The mobility and migration of boundaries*, in Recrystallization and Related Annealing Phenomena (Second Edition), F. J. Humphreys and M. Hatherly, Elsevier, New York, 2004, 121.
- [33] *Influence of small additions on the properties of gold and gold alloys* (in German), D. Ott and Ch. J. Raub, Part I: Metall, 1980, 34, 629; Part II: Metall, 1981, 35, 543; Part III: Metall, 1981, 35, 1005; Part IV: Metall, 1982, 36, 150.
- [34] *Gold-silver-copper alloys*, A. S. McDonald, G. H. Sistare, in Metals Handbook, American Society for Metals, Materials Park, OH, 1979, 2, 681.
- [35] *Hardening of gold-based dental casting alloys: Influence of minor additions and thermal ageing*, J. J. Laberge, D. Treheux, P. Guiraldeng, Gold Bulletin, 1979, 12(2), 45.
- [36] *Palladium Recovery, Properties and Uses*, E. M. Wise, Academic Press, New York, 1968.

- [37] *The development of 990 gold-titanium: Its production, use and properties*, G. Gafner, Gold Bulletin, 1989, 22, 112.
- [38] *Stable strengthening of 990 gold*, D. M. Jacobson, M. R. Harrison, S. P. S. Sangha, Gold Bulletin, 1996, 29(3), 95.
- [39] *The development of a novel gold alloy with 995 fineness and increased hardness*, M. du Toit, E. van der Lingen, L. Glaner, and R. Suss, Gold Bulletin, 2002, 35(2), 46.
- [40] *Alloying and strengthening of gold via rare earth metal additions*, Y. Ning, Gold Bulletin, 2001, 34(3), 77.
- [41] *Thermodynamic modelling of precious metals alloys*, B. Kempf, S. Schmauder, Gold Bulletin, 1998, 31(2), 51.
- [42] *Hardening of low-alloyed gold*, J. Fischer-Buhner, Gold Bulletin, 2005, 38(3), 120–131.
- [43] *Dispersion hardened gold: A new material of improved strength at high temperatures*, M. Poniatowski, M. Clasing, Gold Bulletin, 1972, 5, 34.
- [44] *Z. Metallkde.*, L. Nowack, 1930, 22, 94-103.
- [45] *Acta Met.*, M. Hirabayashi, S. Weissmann, 1962, 10, 25-36.
- [46] *Age-hardening and related phase transformations in dental gold alloys*, K. Yasuda, Gold Bulletin, 1987, 20(4), 90.
- [47] *A plain man's guide to alloy phase diagrams: their use in jewellery manufacture – Part 2*, M. Grimwade, Gold Technology, 2000, 30, 8.
- [48] *Gold: Science and Application*, C. Corti, R. Holliday, Taylor & Francis Group, 2009.
- [49] *The colour of Au-Ag-Cu alloys: Quantitative mapping of the ternary diagram*, R. M. German, M. M. Guzowski, D. C. Wright, Gold Bulletin, 1980, 13, 113.
- [50] *Don't let nickel get under your skin – the European experience!*, R. Rushforth, Gold Technology, 2000, 28, 2.
- [51] *Development of 18ct white gold alloys without Ni and Pd*, A. Basso, J. Fischer-Buehner, M. Poliero, in Proceedings of The Santa Fe Symposium on Jewelry Manufacturing Technology 2008, ed. E. Bell, Met-Chem Research, Albuquerque, NM, 2008, 31.
- [52] *Production and characterisation of 18 carat white gold alloys conforming to European Directive 94/27 CE*, M. Dabala, M. Magrini, M. Poliero, and R. Galvani, Gold Technology, 1999, 25, 29.
- [53] *Blue black and purple! The special colours of gold*, C. W. Corti, in Proceedings of The Santa Fe Symposium on Jewelry Manufacturing Technology 2004, ed. E. Bell, Met-Chem Research, Albuquerque, NM, 2004, 121.

- [54] S. Hori, K. Kurokawa, T. Shimizo, M. Steel, M. Tsuboi, K. Yanagase, in *Precious Metals Science And Technology*, eds. L.S. Benner, T. Suzuki, K. Meguro, S. Tanaka, International Precious Metals Institute, Allentown, 1991, p. 430
- [55] *Microstructure of Au-Al systems manipulated by rapid solidification techniques*, K. Wongpreedee and P. Ruethaithananon, paper presented at Gold 2009, 5th International Conference on Gold Science, Technology and its Applications, Heidelberg, 2009.
- [56] *Determination of the 76 wt% Au section of the Al-Au-Cu phase diagram*, F. C. Levey, M. B. Cortie, L. A. Cornish, *Journal of Alloys and Compounds*, 2003, 354, 171.
- [57] *On the compounds of Sodium and Potassium with Gold* (in German), U. Quadt, F. Weibke, W. Blitz, *Zeitschrift für anorganische und allgemeine Chemie*, 1937, 232, 298.
- [58] *Phase width and valence electron concentration of the ternary cubic Zintl phases of the NaTl type* (in German), H. Pauly, A. Weiss, H. Witte, *Zeitschrift für Metallkunde*, 1968, 59(7), 554.
- [59] *Gold casting alloys: The effect of Zinc additions on their behaviour*, Ch. Raub, D. Ott, *Gold Bulletin*, 1983, 16, 2.
- [60] *The bonding of gold and gold alloys to non-metallic materials*, W. S. Rapson, *Gold Bulletin*, 1979, 12(3), 108.
- [61] *Alloys by Design: Knowing the answer before spending the money*, B. Lohwongwatana, E. Nisaratanaporn, in *Proceedings of The Santa Fe Symposium on Jewelry Manufacturing Technology 2008*, ed. E. Bell, Met-Chem Research, Albuquerque, NM, 2008, 201.
- [62] *Production of gold findings by stamping*, F. Klotz, *Gold Technology*, No. 33, 2001, 13–16.
- [63] *Bi-metal solder flush products and their use for high productivity manufacture*, In *Proceedings of the Santa Fe Symposium on Jewelry Manufacturing Technology*, G. Normandeau, ed. D. Schneller, 1991, 149–170, Albuquerque, NM: Met-Chem Research.
- [64] *The shape of the future – recent developments in electroforming*, C. W. Corti, *AJM Magazine*, Issue 3/03, March 2003, 51–59.
- [65] *Electroforming in gold jewelry production*, F. Simon, *Gold Technology*, No. 4, May 1991, 10–15.
- [66] *Recent developments in the field of electroforming, a production process for hallmarkable hollow jewelry*, F. Simon, *Gold Technology*, No. 16, July 1995, 22–29.
- [67] *Back to basics: Investment casting, Part I*, C. W. Corti, *Gold Technology*, 2000, No. 28, 27–32.
- [68] *Handbook on Casting and Other Defects*, D. Ott, 1997, London: World Gold Council.
- [69] *Vibration technology for the solidification process of investment casting*, P. Hofmann, In *Proc. 3rd Jewellery Technology Forum*, May 2006, 189–199. Vicenza, Italy: Legor Group.

- [70] *Stone-in-place casting for high-end jewelry*, H. Schuster, In Proceedings of the Santa Fe Symposium on Jewelry Manufacturing Technology, 2008, ed. E. Bell, 283–294. Albuquerque, NM: Met Chem Research.
- [71] *Advances in the prevention of investment casting defects by computer simulation*, J. Fischer-Buhner, In Proceedings of the Santa Fe Symposium on Jewelry Manufacturing Technology, 2007, ed. E. Bell, 149–172. Albuquerque, NM: Met-Chem Research.
- [72] *Hollow karat gold jewelry from strip and tube*, P. Raw, Gold Technology, No. 35, Summer 2002, 3–10.
- [73] *The production of karat gold chain wire*, P. Taimsalu, Aurum, No. 14, 1983, 49–55.
- [74] *Overview: Joining technology in chain manufacture*, A. Canaglia, Gold Technology, No. 17, October 1995, 20–25.
- [75] *Evaluation of strength and quality of chains*, D. P. Agarwal, Gold Technology, No. 24, September 1998, 2–5.
- [76] *Health, safety and environmental pollution in gold jewelry manufacture*, M. F. Grimwade, Gold Technology, No. 18, April 1996, 4–10.
- [77] *Sintering technology for jewelry and multicolor rings*, In Proceedings of the Santa Fe Symposium on Jewelry Manufacturing Technology, K. Weisner, 2005, ed. E. Bell, 501–519. Albuquerque, NM: Met-Chem Research.
- [78] *Comparative study on metal finishing techniques on standard sample of cast gold*, In Proceedings of the Santa Fe Symposium on Jewelry Manufacturing Technology, M. Dreher, 1991, ed. D. Schneller, 27–44. Albuquerque, NM: Met-Chem Research.
- [79] *Gold wedding rings from powder – tomorrow’s technology today*, P. Raw, Gold Technology, No. 27, November 1999, 2–8.
- [80] *Laser applications in gold jewellery production*, S. Valenti, Gold Technology, No. 34, Spring 2002, 14–20.
- [81] *Metal injection molding (MIM) for gold jewelry production*, J. T. Strauss, Gold Technology, No. 20, November 1996, 17–29.
- [82] *The role of CAD/CAM in the modern jewelry business*, L. C. Molinari, M. C. Megazzini, E. Bemporad, Gold Technology, No. 23, April 1998, 3–7.
- [83] *CAD-CAM technology: transforming the goldsmith’s workshop*, M. G. Malagoli, Gold Technology, No. 34, Spring 2002, 31–35.
- [84] *Residual Stress – Measurement by Diffraction and Interpretation*, I.C. Noyan, J.B. Cohen, 1987, Materials Research and Engineering, Springer-Verlag, New York Inc.

- [85] *Micromorphological Studies of the Corrosion of Gold Alloy*, A. J. Forty, Gold Bulletin, March, 1981, Volume 14, Issue 1, pp 25-35.
- [86] *J. Electrochem. Soc.*, H. W. Pickering, C. Wagner, 1967, 114, 698-706.
- [87] *Fundamental Aspects of Stress Corrosion Cracking*, H. W. Pickering, edited by R. W. Staehle, A. J. Forty, D. van Rooyen. N.A.C.E., 1967, Houston, TX, pp. 159-174.
- [88] *J. Dent. Res.*, K. F. Leinfelder, D. F. Taylor, 1977, 56, (3), 335-345.
- [89] *Werkstoffe und Korrosion.*, A. Randak, F. W. Trautes, 1970, Vol 21, no. 2, page 97.
- [90] *Corrosion*, K. Elayaperumal, P. K. De, J. Balachandra, 1972, Vol 28, no. 7, page 269.
- [91] *Effect of microstructure and residual stresses, generated from different annealing and deformation processes, on the corrosion and mechanical properties of gold welding alloy wires*, C. Cason, L. Pezzato, M. Breda, F. Furlan, M. Dabalà, Gold Bulletin, December 2015, Volume 48, Issue 3-4, pp 135-145.
- [92] *Design and Analysis of Experiments (8th Edition)*, Douglas C. Montgomery, John Wiley and Sons. ISBN: 978-1118-14692-7.
- [93] *Effect of the composition and production parameters on the microstructure, residual stresses, mechanical and corrosion properties of gold alloys used in industrial jewelry processes*, (in press), C. Cason, L. Pezzato, K. Brunelli, F. Furlan, M. Dabalà, Advanced in Materials Science, ISSN: 2398-6883
- [94] *The electroplastic effect in metals*, H. Conrad, Strength of Materials, Vol. 16, No. 2, pp 103-106, February 1984.
- [95] *Effects of electric current on solid state phase transformations in metals*, H. Conrad, in Materials Science and Engineering A287 (2000) 227-237.
- [96] *Nanocrystallization of amorphous Fe-Si-B alloys using high current density electropulsing*, Z.H. Lai, H. Conrad, G.Q. Teng, Y.S. Chao, Materials Science & Engineering, 2000
- [97] *Microstructure and mechanical properties of a 18Kt 5N gold alloy after different heat treatments*, L. Pezzato, G. Magnabosco, K. Brunelli, M. Breda, M. Dabalà, Metallogr. Microstruct. Anal., DOI 10.1007/s13632-016-0262-4, 2016.

LIST OF PUBLICATIONS

Published Papers

- CASON C., Pezzato L, Breda M, Furlan F, Dabalà M *Effect of microstructure and residual stresses, generated from different annealing and deformation processes, on the corrosion and mechanical properties of gold-welding alloy wires*. GOLD BULLETIN, December 2015, Volume 48, Issue 3, pp 135–145

Submitted and accepted

- CASON C., Pezzato L, Brunelli K, Furlan F, Dabalà M *Effect of the composition and production parameters on the microstructure, residual stresses, mechanical and corrosion properties of gold alloys used in industrial jewelry process*. ADVANCED MATERIAL SCIENCE (AMS), Volume 1, Issue 2

Conference Proceedings

- CASON C., Pezzato L, Dabalà M (in press) *Gold alloys hardening: effect of composition and heat treatment on mechanical properties of gold alloys*. JOURNAL OF APPLIED BIOMATERIALS & FUNCTIONAL MATERIALS, ISSN: 2280-8000
- CASON C., Pezzato L, Breda M, Dabalà M *Effect of microstructure and residual stresses, generated from different annealing and deformation processes, on the corrosion and mechanical properties of gold welding alloy wires*. Conference Proceedings. Warsaw, Poland, 21-25 September 2015
- CASON C., Pezzato L, Brunelli K, Dabalà M *Effect of the composition and production process parameters on the microstructure, residual stresses, mechanical and corrosion properties of gold alloys used in industrial processes*. Journal of Material Sciences & Engineering, June 2016, Volume 5, Issue 3, pp 68

- CASON C., Pezzato L, Brunelli K, Dabalà M *Effetto della composizione e dei parametri di produzione sulle caratteristiche di leghe d'oro in 10 Kt usate in processi industriali.* Conference Proceedings. Parma, Italy. 36° Convegno Nazionale AIM, 21-23 September 2016

ACKNOWLEDGMENTS

The realization of this work was made possible by the collaboration between the Department of Industrial Engineering of Padua and Filk S.p.A.

First of all, I want to thank the management of Filk S.p.A., in particular Pietro Cremasco and Elisa Cremasco who believed in this project, I thank also Mario and Carlo Cremasco for the helpful discussions. Special thanks goes to Ing. Fabrizio Furlan for the help, the advices and the trust shown.

I want to thank my supervisor prof. Manuele Dabalà for the support and the constant presence. Thanks also to the other members of the metallurgy group: Katya, Giulia, Massimiliano for the patience and the important help.

I thank also Luca, Pierre, Totò, Marco and Claudio for the collaboration and for all they have given me during these three years.

Returning to the company that has taken me over these years and allowed me to grow professionally; thanks to Emiliano, Cristopher, Lisa, Marco, Luca C., Ernesto, Giampietro, Elena, Mauro, Luca Z., Alfredo, Andrea and Nicola. Special thanks goes to my first two mentors, Mirco and Luciano, the greater part of my training was done under your supervision. I began to learn the ropes from you.

Important was also the support and help given by the laboratories of Progold S.p.A., thanks to Ing. Daniele Maggian, to Dr. Valerio Doppio and to the “chemical etching magician” Dr. Patrizio Sbornicchia for the collaboration and the advices given.

Finally, I want to thank my family for always believing in me. Special thanks to Anna, to be always present, always willing to listen me, to support my professional choices and, very important, to bear me.

RINGRAZIAMENTI

È stato possibile portare a compimento questo lavoro di ricerca grazie alla collaborazione tra il Dipartimento di Ingegneria Industriale dell'Università di Padova e dell'azienda orafa Filk.

Prima di tutto voglio ringraziare la direzione aziendale, in particolare il presidente Pietro Cremasco ed Elisa Cremasco che hanno creduto in questo progetto, ringrazio inoltre Mario e Carlo Cremasco per le utili discussioni e il loro contributo nelle fasi produttive. Un ringraziamento speciale va al direttore di produzione Ing. Fabrizio Furlan per l'aiuto, i consigli e la fiducia dimostratami.

Voglio ringraziare il mio supervisore prof. Manuele Dabalà per il supporto e la presenza costante. Un grazie a tutti gli altri membri del gruppo metallurgico di Padova: Katya, Giulia e Massimiliano per la pazienza e il grande aiuto.

Ringrazio inoltre Luca, Pierre, Totò, Marco e Claudio per la collaborazione e tutto quello che mi hanno dato durante questi tre anni. Anche se suddivisi tra già *dottorati* e ancora *dottorandi*, il gruppo, come pure l'esperienza lavorativa al vostro fianco, rimarranno unici.

Ritornando all'azienda che mi ha accolto in questi ultimi anni e mi ha permesso di crescere professionalmente; vorrei ringraziare Emiliano, Cristopher, Lisa, Marco, Luca C., Ernesto, Giampietro, Elena, Mauro, Luca Z., Alfredo, Andrea e Nicola. Un ringraziamento speciale va ai miei primi due mentori, Mirco e Luciano, gran parte del mio addestramento è stato compiuto sotto la vostra attenta supervisione. Con voi, posso dire di "essermi fatto le ossa" professionalmente parlando, e sono contento che siate stati per me guide prima ancora che colleghi.

Molto importante è stato inoltre il supporto e l'aiuto conferito dai laboratori dell'azienda Progold, un grazie doveroso va all'Ing. Daniele Maggian, al Dr. Valerio Doppio e al "mago degli attacchi" Dr. Patrizio Sbornicchia per la collaborazione, i consigli e l'enorme passione per questo mondo di ricerca che ci accomuna.

Infine, come non poter ringraziare la mia famiglia per aver creduto in me e per essersi dimostrati sempre disponibili. Tutto ciò che sono oggi e quello che ho portato a termine lo devo a voi, e non smetterò mai di ripeterlo, i miei traguardi alla fin fine sono i vostri traguardi. Un ringraziamento speciale va ad Anna, per essere sempre presente, sempre disposta ad ascoltarmi, per supportare le mie scelte professionali e, molto importante, per sopportarmi con estrema pazienza.

